Report 3863

THE STRUCTURAL BEHAVIOR OF GLASS PRESSURE HULLS

[redacted] AL SHIP RESEARCH AND DEVELOPMENT CENTER

Bethesda, Md. 20034

THE STRUCTURAL BEHAVIOR OF GLASS PRESSURE HULLS

00		YNC	
01		SKC	
10		GYSGT	
11		YN	
12			

by

K. Nishida

LIBE

APPROVED FOR PUBLIC RELEASE: DISTRIBUTION UNLIMITED

STRUCTURES DEPARTMENT

RESEARCH AND DEVELOPMENT REPORT

June 1972

Report 3863

The Naval Ship Research and Development Center is a U. S. Navy center for laboratory effort directed at achieving improved sea and air vehicles. It was formed in March 1967 by merging the David Taylor Model Basin at Carderock, Maryland with the Marine Engineering Laboratory at Annapolis, Maryland.

Naval Ship Research and Development Center
Bethesda, Md. 20034

MAJOR NSRDC ORGANIZATIONAL COMPONENTS

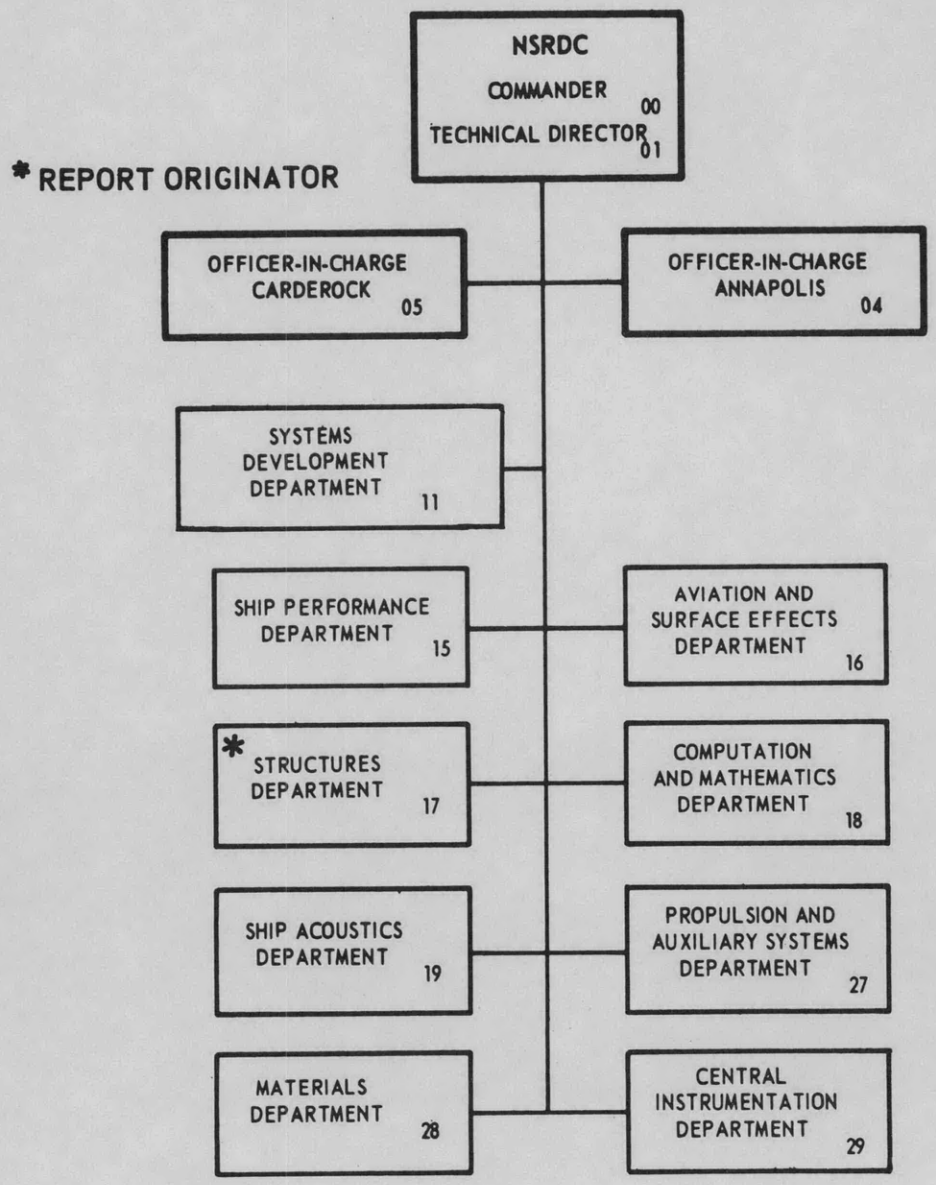

DEPARTMENT OF THE NAVY
NAVAL SHIP RESEARCH AND DEVELOPMENT CENTER
BETHESDA, MD. 20034

THE STRUCTURAL BEHAVIOR OF GLASS PRESSURE HULLS

by

K. Nishida

June 1972 Report 3863

TABLE OF CONTENTS

	Page
ABSTRACT	1
ADMINISTRATIVE INFORMATION	1
INTRODUCTION	1
ANALYSIS OF EARLY GLASS JOINTS	4
PARAMETRIC STUDY OF THE JOINT PROBLEM	6
FINAL JOINT DESIGNS	9
DESCRIPTION OF MODELS	10
TEST PROCEDURE	13
TEST RESULTS AND DISCUSSION	14
SUMMARY	19
ACKNOWLEDGMENTS	21
REFERENCES	104
APPENDIX - BACKGROUND ON GLASS AND CERAMIC SPHERICAL SHELLS	71

LIST OF FIGURES

	Page
Figure 1 - Analysis of Constant Thickness Hemispherical Shell	22
Figure 2 - Grinding Flaws at Beveled Edge	23
Figure 3 - Annealed Glass Hemisphere after Static Test to 17,000 psi	24
Figure 4 - Analysis of Reinforced Joint Design	25
Figure 5 - Surface Compressed Hemisphere with Reinforced Joint after 10 Cycles to 10,000 psi	26
Figure 6 - Joint Geometries for Parametric Study	27
Figure 7 - Stress Contours	28
Figure 8 - Final Joint Designs	37
Figure 9 - Compressive Stress-Strain Curve for 662 Titanium	38
Figure 10 - Analysis of Final Joint Designs	39
Figure 11 - Glass Hemispherical Shell	54

Page

Figure 12 - Assembled Spheres 55

Figure 13 - Model in Test Facility 56

Figure 14 - Inspection Set Up 57

Figure 15 - Fracture on Hemisphere 15 after 100 Cycles to 6500 psi 58

Figure 16 - Inside Edge Chip on Hemisphere 13 after 898 Cycles to 5000 psi 59

Figure 17 - Outside Edge Spall on Hemisphere 13 after 1048 Cycles to 5000 psi 60

Figure 18 - Flaw in Hemisphere 3 61

Figure 19 - Models after Test 64

Figure 20 - Summary of Test Results of 10-Inch-Diameter 0.28 Wall Fusion Sealed Annealed Pyrex Glass Spheres 82

Figure 21 - Examples of Fusion Sealed Seams 83

Figure 22 - Nominal Model Dimensions for Fusion Sealed Spheres with Penetration 84

Figure 23 - 44 Inch Diameter Fusion Sealed Annealed Glass Sphere 85

Figure 24 - Pressure Strain Plots for 44 Inch Glass Sphere 86

Figure 25 - Damage to Model 44-1 after 3500 psi 87

Figure 26 - Gage Locations and Strain Sensitivities for 44 Inch Sphere 88

Figure 27 - Damage to Model C-2 after Cycling to 5000 psi 90

Figure 28 - Nominal Model Dimensions and Test Result of 5 Inch Diameter Pyroceram Hemisphere 91

LIST OF TABLES

Page

Table 1 - Summary of Geometric and Material Properties 67

Table 2 - Test Results of 0.28 in. Wall--10-Inch-Diameter Surface Compressed Glass Hemispheres 68

Table 3 - Test Results of 10-Inch-Diameter 0.36 Wall PPG 1080 K^+ Surface Compressed Glass Hemispheres 69

Table 4 - Test Results of 10-Inch-Diameter Variable Wall PPG 1578 Surface Compressed Glass Hemispheres 70

Page

Table 5 - Effect of Loading Rate and Pressure Medium on Collapse Strength 92

Table 6 - Collapse Strength of 10-Inch-Diameter 0.28 Wall Fusion Sealed Annealed Pyrex Glass Spheres with Modified Seams 93

Table 7 - Cyclic Tests of 10-Inch-Diameter 0.28 Wall Fusion Sealed Annealed Pyrex Glass Spheres 94

Table 8 - Collapse Strength of 10-Inch-Diameter 0.36 Wall Fusion Sealed Annealed Pyrex Glass 95

Table 9 - Summary of Static Tests of 10-Inch-Diameter Fusion-Sealed Annealed Pyrex Glass Spheres with Penetrations 95

Table 10 - State Cyclic Tests of 10-Inch-Diameter 0.18 Wall Monolithic Alumina Spheres 96

Table 11 - Summary of Static Tests of Chemically Strengthened Herculite II (1080 Na^+) Glass Hemispheres 97

Table 12 - Test Results of 10-Inch-Diameter 0.281 Wall Annealed Pyrex Glass Hemispherical Shells without Gaskets 98

Table 13 - Test Results of 10-Inch-Diameter 0.28 Wall Annealed Pyrex Glass Hemispheres with Gaskets 99

Table 14 - Summary of Cyclic Tests of 10-Inch-Diameter 0.28 Wall Annealed Pyrex Glass Hemispheres 100

Table 15 - Summary of Test Results of 10-Inch-Diameter 0.36 Wall PPG 1080 Annealed Glass Hemispherical Shells 101

Table 16 - Summary of Static Tests of Chemcor Hemispheres with Reinforced Bearing Surfaces 102

Table 17 - Summary of Cyclic Tests of Chemcor 0312 Hemispheres with Reinforced Bearing Surfaces 103

ABSTRACT

A report on glass pressure vessels for deep submergence is presented. Emphasis is on the structural response of spherical and hemispherical glass shells under external hydrostatic and cyclic pressure. Results of earlier programs are reviewed. A computerized analysis trading off the variables in the joint problem is presented. Final joint geometries are discussed and data on chemically strengthened glass hemispherical shells with equatorial joint rings under fatigue conditions are presented. The results indicate relatively efficient (W/D = 0.5), small pressure vessels of chemically strengthened glass are practical for unmanned noncritical applications to 20,000 ft. Nine 10-inch diameter chemically strengthened glass hemispherical shells of PPG 1080 glass with overall weight to displacement ratios of 0.5 survived at least 3000 cycles to 20,000 ft. Each hemisphere was then subjected to a proof test to 30,000 ft. Although this data is encouraging, substantial effort is necessary before glass structures can be applied in critical conditions even on the present small scale.

ADMINISTRATIVE INFORMATION

The work described in this report was sponsored by the Deep Ocean Technology (DOT) project and funded under Task Area S 4636, Task 12326.

INTRODUCTION

Glass is a material which exists in large quantities on this earth. Its wide use is prompted largely by economic factors as industrial processing methods have been developed to make its use relatively cheap in such areas as the manufacture of bottle containers, sheet, plate, kitchenware, and fibrous glass products. In general, the present applications require that the glass carry very little to no load. This is only natural because of the brittleness of glass. In the past, whenever a transparent structural material was required designers have favored plastics such as polymethyl methacrylate. The structural plastics, however, are not without their limitations as strength eventually becomes a problem in modern technological applications. Aircraft windshields and pressure vessels for deep sea applications are such examples.

The use of massive glass for deep submergence pressure vessels has been under study by the Navy for several years. Exploratory tests and feasibility studies[1,2] demonstrated the potential superiority of glass over metallic materials. Subsequently, efforts were conducted by several laboratories for various manned and unmanned objectives. The Naval Ordnance Laboratory[3] (NOL) conducted experiments at sea to study the sympathetic implosion problem. They also conducted fatigue tests of annealed and surface strengthened glass hemispherical shells and reported successful results on chemically strengthened models.[4] Stachiw[5] conducted numerous tests on commercially manufactured annealed glass flasks for

---

[1]Kiernan, T.J., "An Exploratory Study of the Feasibility of Glass and Ceramic Pressure Vessels for Naval Applications," NSRDC Report 2243 (Sep 1966).

[2]Coffman, W.B. et al., "Feasibility Study of Plastic-Clad Glass Capsules for Deep Diving Submersibles," NOL TR 65-76 (Jun 1965).

[3]Heathcote, T.B., "The Resistance of Hollow Glass Models to Underwater Explosions at Great Depths III Spheres with Overlays," NOL TR 66-78 (May 1966).

[4]Perry, H.A., "Surface Compression Strengthened Glasses: Some Properties," NOL TR 71-21 (Mar 1971).

[5]Gray, K.O. and J.D. Stachiw, "Light Housings for Deep Submergence Applications--Part III. Glass Pipes with Conical Flanged Ends," NCEL Technical Report R618 (Mar 1969).

adaptation to light housings for deep submergence. Foreman[6] and Murphy[7] in work on the Deep View and Hikino vehicles studied the joint problem on small and large scale annealed glass specimens. NSRDC conducted studies on the impact[8] behavior of brittle hulls, a theoretical study of an imploding spherical bubble,[9] and also the bearing strength of brittle materials.[10]

In 1967 a concerted effort to develop massive glass for deep submergence was established in the U.S. Navy's Deep Ocean Technology Project. One of the long range objectives of the program was the development of a relatively small (7-10 ft diameter), light weight (W/D of 0.5) manned vehicle for operation to 20,000 ft. Glass was one of the candidate materials for this vehicle. Based on work accomplished prior to 1967, the scope of the DOT massive glass effort was established. In essence the guidelines were:

1. The effort would be concentrated on the spherical shell and the hull material would be of a surface strengthened glass.
2. The pressure hull would have an openable girth joint for passage of personnel and equipment.

---

[6]Foreman, W. and R. DeHart, "Submersible Deep View Pioneers Glass/Metal Bonding," Undersea Technology, pp. 24-27 (Dec 1967).

[7]Murphy, D.W., "Development and Testing of a 56-In.-Dia. Jointed Glass Pressure Hull," ASME Paper No. 69-WA/UnT-2 presented at Winter Annual Winter, L.A. Calif (Nov 16-20, 1969).

[8]Zillicaus, S. and H. Hashmall, "Impact Strength and Response of Protected Brittle Models of Deep Submergence Structures," David Taylor Model Basin Report 2314 (Dec 1966).

[9]Lilliston, R.R., "Calculations on the Collapse of a Spherical Gas-Filled Cavity in a Compressible Liquid," David Taylor Model Basin Report 2223 (Aug 1966).

[10]Moreno, D.H. and M.L. Salive, "The Effects of Size and Environment on the Uniaxial Compressive Breaking Strength of Glass, Alumina, and Pyroceram," NSRDC Report 3315 (May 1970).

The structural aspects of the DOT program were assigned to the Naval Ship Research and Development Center (NSRDC) and the material aspects to NOL. After 3 years of effort, a critical review of the massive glass program indicated that the realization of glass in a man rated situation was still a number of years away. Thus, a decision to terminate this phase of the program was made. This report summarizes the analytical and experimental data generated at NSRDC.

ANALYSIS OF EARLY GLASS JOINTS

Prior to the DOT program a number of experiments had been conducted on glass joints. Much of this work was very exploratory in nature and was conducted in many cases mainly to observe mechanical response through simple structures such as a spherical shell formed by butting together two glass hemispherical shells or placing a hemispherical shell on a metal block and loading hydrostatically. A review of some of this work is presented in the appendix. As a general rule the early results indicated that failure in glass hemispherical shells were stress rather than buckle induced. However, an accurate knowledge of the stresses at the joint were not known. The rapid advances made in the field of finite element[11] has made solutions to problems such as joints in glass hemispheres quite routine. In an attempt to explain some of the difficulties experienced in developing reliable mechanical butt joints, two geometries, extensively tested experimentally, were stress analyzed. The finite element computer program utilized was developed by Gifford[12] of the Center. It utilizes triangular ring elements and is applicable to any elastic-plastic axisymmetric structure. It will handle nonlinear effects of the contact problem.

---

[11]Gifford, L.N. and R.F. Jones, "Structural Analysis of Deep Submergence Pressure Hulls," SNAME Paper No. 12 presented at Spring Meeting, Honolulu, Hawaii (May 25-28 1971).

[12]Gifford, L.N., "Finite Element Analysis for Arbitrary Axisymmetric Structures," NSRDC Report 2641 (Mar 1968).

The first geometry analyzed was the glass spherical shell formed by butting together two uniform wall hemispherical shells. The equator represents an axis of symmetry and therefore only one half of the sphere need be analyzed. In the actual hemisphere the edges of the bearing face are beveled or rounded. For this analysis a rounded edge was assumed. A structural idealization of the joint is shown in Figure 1. The mesh was generated by a computer program written by Rockwell and Pincus[13] of the Center. The results of the analysis are also presented graphically in Figure 1. It may be noted that in a spherical shell under hydrostatic pressure the principal directions of stress are meridional, circumferential and radial. Generally, the meridional and circumferential stresses are high in compression and are not believed to be a factor in failure of glass joints. The principal stress with the lowest magnitude is the radial which is shown in Figure 1. Away from local disturbances of the joint, the stress in the radial direction at the outer surface is equal to the hydrostatic pressure and at the inner surface is equal to zero. Note that tensile stresses are present in an area very close to the inner edge of the bearing surface. Thus, flaws in the circumferential direction would be expected to play a role in the fracture process. It is known that flaws of this type exist. Photographs from a typical glass hemispherical shell of Pyrex glass are shown in Figure 2. In this case the edge of the bearing face is beveled at 45 deg. An example of a hydrostatic test of this type of hemispherical shell and the resulting damage is shown in Figure 3. Note the spalling at the inner edge of the hemisphere.

The second geometry analyzed was the reinforced joint design utilized on hemispherical shells of Chemcor 0312 glass. The tests of these models occurred prior to initiation of the DOT project and are summarized in the appendix. Although the results of these tests were quite encouraging, fractures were observed in static tests and catastrophic failure resulted in two fatigue tests after about 100 cycles to 22,500 ft. The average bearing stress at 22,500 ft is about 50,000 psi. The idealized

---

[13]Rockwell, R.D. and D.S. Pincus, "Computer Aided Input/Output for Use with Finite Element Method of Structural Analysis," NSRDC Report 3402 (Aug 1970).

structure used in the analysis is shown in Figure 4a and the results of the analysis are shown in Figures 4b and 4c. Note the tensile stress in the radial direction. This stress is relatively low and would not be expected to cause fracture in Chemcor 0312 glass for the tensile stress (3,000 psi) that was applied during most of the tests. Fractures nevertheless did occur and an example is shown in Figure 5. It is suspected that flaws also played a significant role in these tests.

PARAMETRIC STUDY OF THE JOINT PROBLEM

One of the guidelines established at the initiation of the program was that the glasspressure hull have an openable girth joint. The early results on glass hemispherical shells provided little insight on the optimum joint geometry. Therefore, in an attempt to optimize joint design in glass hemispherical shells a parametric study of the joint problem using the finite element method was conducted. The variables investigated were ring rigidity, glass bearing face geometry and interface layer properties. A summary of the material and geometric parameters is shown in Table 1. The following assumptions were made for this study.

1. The overall weight displacement ratio of the pressure hull would be about 0.5. For a 10 in. diameter shell the corresponding thickness was 0.30 in.
2. The pressure hull would be formed essentially by butting together two hemispherical halves with an equatorial joint.
3. The joint assembly would include a metallic rim into which the glass hemisphere would be potted.
4. The elastic effect of an interface layer between the glass and metallic rim would be considered.
5. The geometry of the edge of the glass hemisphere would be varied.

Sketches showing the nominal model dimensions for the three geometries are shown in Figure 6. The majority of computer runs were with a titanium with a ring 0.58 in. wide. This thickness was obtained by equating the deflection of a 10 inch diameter glass sphere with a wall thickness of 0.3 in. to the deflection of the titanium ring. The results of the computer output are presented in the form of contour maps in Figure 7. Only

the principal stress in the direction through the thickness is shown since the stresses in the other two directions are high in compression. The stresses are given in psi/psi. The results of the output are summarized below.

EFFECT OF POISSON'S RATIO OF THE INTERFACE LAYER

In these runs the following parameters were held constant

Thickness of interface layer, h_i	0.01 in.
Young's modulus of the interface, E_i	5×10^6 psi
Width of ring ω	0.58 in.
E of titanium ring	15×10^6 psi

The value of Poisson's ratio of the interface layer was varied from 0.1, 0.3, and 0.45. For a flat bearing face, as Poisson's ratio of the interface was increased, the radial compressive stress decreased slightly. For rounded-type joints, increasing Poisson's ratio appeared to slightly increase radial compressive stress.

EFFECT OF YOUNG'S MODULUS OF THE INTERFACE LAYER

This series of test cases was identical to the above except that Poisson's ratio of the interface layer was held constant at 0.3. Young's modulus of the interface layer was then changed from $0.5 \times 10,^6$ $5 \times 10,^6$, and 50×10^6 psi. For the flat bearing face, increasing Young's modulus from 0.5 to 50×10^6 psi did not appear to have a discernible effect for the mesh size used. In the case of the rounded joints, a markedly undesirable effect was caused by increasing Young's modulus of the interface layer. At the low value of 0.5×10^6 psi, the compressive stresses in the radial direction were relatively high for both the semi-rounded and full-rounded configurations. At the high value of $50 \times 10,^6$ the stress approached a value of 0 for the semi-rounded configuration and relatively high tensile stresses were observed for the full-rounded configuration.

EFFECT OF RING RIGIDITY

Two configurations were examined for comparison with the membrane titanium ring (0.58-in. width). In one case the ring width was changed

from 0.58 to 0.40 in. and the material was assumed to be titanium with a Young's modulus of 15×10^6 psi. In the second case, a ring width of 0.40 in. was assumed, and the ring material was steel with a Young's modulus of 30×10^6 psi. Decreasing the thickness of a titanium ring from 0.58 to 0.40 in. appeared to have a slightly undesirable effect. Compressive stresses in the radial direction were decreased for all three geometries (flat, semi-rounded, and full-rounded). However, a steel ring of 0.40-in. width appeared to create a more desirable stress state in the glass than did either the membrane titanium ring or a 0.40-in. titanium ring. Higher radial compressive stresses were apparent for all three geometric configurations. At the operating depth of 20,000 ft, the equivalent HVM stresses are 140,000 and 85,000 psi for the steel and titanium rings, respectively. Assuming a factor of safety of 2 on yielding of the ring, a steel with a proportional limit of 280,000 psi and titanium with 170,000 psi would be required.

EFFECT OF THICKNESS OF THE INTERFACE LAYER

One series of test cases was run to examine the effect of interface layer thickness. Respective thicknesses of 0.03 and 0.04 in. were assumed for the flat bearing face and the rounded joints, results were compared to those for the standard thickness of 0.01 in. used for all other runs. Increasing the interface layer thickness caused a slightly undesirable effect (lower radial stress) for the flat bearing face, very little effect for the semi-rounded case, and a slightly desirable effect for the full-rounded configuration.

In general it appeared that the flat bearing face was the least sensitive to changes in material properties of the interface layer. The rounded geometry was the most sensitive. If an interface layer with a high Poisson's ratio and low Young's modulus could be kept between the glass and the metal then the rounded type joint would be expected to perform satisfactorily. From a practical point of view this was considered to be very unlikely. The limited data suggested that extrusion of soft material was a serious problem. Thus, the rounded geometry was eliminated from the possible joint geometries. The optimum properties for the flat geometry was a high value of Young's modulus and a low value of Poisson's ratio. Again,

it appeared that such a material could cause practical difficulties because of microscopic imperfections in the glass part. For example it is very unlikely that a butt joint of a glass hemisphere on a block of a very rigid material such as alumina or tungsten carbide would perform in a desirable manner because of the local contact stresses. Fortunately, changing E and ν of the interface layer does not have a marked effect on the stresses in the glass. Since it was felt that compliance was important a decision to utilize glass reinforced plastic was made.

FINAL JOINT DESIGNS

In the final design of the glass models a number of dimensional changes were made. The wall thicknesses of 10 inch diameter models were 0.28 and 0.36. The titanium ring was made of an alloy (662) that had a Young's modulus of 17.5×10^6 psi rather than 15×10^6 psi assumed in the parametric study. Finally in the course of the program it was decided that a joint ring which would permit in service inspection was desired.

Two membrane joint designs were selected for the 10 in. diameter 0.28 wall type glass hemispherical shell. These are shown in Figures 8a and 8b. The first designated Mod 1 had an "L" shaped cross section, while the Mod 2 ring had a "U" shaped cross section. The advantage of the Mod 1 ring was that it provided greater visibility for inspections. Both rings were of 662 titanium and were designed for membraned deflections at the equator. Because of the slightly different material and geometric properties of the final designs these joints were also stress analyzed by finite element. In the analysis it was assumed that slipping would take place at the curved surfaces of the shell and that no slipping would take place at the glass gasket boundary. The plastic analysis was utilized and the assumed stress-strain curve for the titanium ring is shown in Figure 9. The results of the finite element analysis is presented graphically in Figure 10. Note from the displaced structures membrane conditions were achieved (no bending). Also, there is no indication of tensile stresses in the glass. First yielding (the first triangular ring element whose Henky von Mises stress exceeds the proportional limit) occurs at a pressure of 9540 psi for the Mod 1 ring while first yielding occurs at a pressure of 8910 psi for the Mod 2 ring.

For a 10 inch diameter 0.06 wall glass hemispherical shell a ring with a "U" shaped cross section similar to the Mod 2 ring for the 0.28 wall hemisphere was chosen. A sketch of the geometry is shown in Figure 8c. A finite element analysis was performed on this joint. However, graphical output capability was not available on the computer program at the time and therefore, the stresses are not shown. The ring was designed to provide membrane conditions at the equator and no tensile stresses were indicated on the computer output.

The fourth design was a reinforced concept shown in Figure 8d. This was an attempt to lower the bearing stress at the joint without increasing the overall weight displacement ratio of the structure. The results of this analysis are shown in Figure 10. No tensile stresses are indicated. Note that first yielding in the titanium ring for this geometry does not occur till a pressure of 13,400 psi.

DESCRIPTION OF MODELS

All of the models tested were of chemically treated, surface compressed glass. Twenty four hemispheres were of PPG Code 1578 glass, fifteen were of PPG 1080, and two were of Corning Chemcor 0313 glass. Most of the models were constant-thickness hemispherical shells with an outside radius of 5 in. The PPG 1578 and Chemcor 0313 models were 0.28-in. thick, and the PPG 1080 models were 0.36 in. thick. The corresponding weight-to-displacement ratios for these thicknesses are 0.36 and 0.46. In addition 6 hemispheres of PPG 1578 which had reinforced joints were tested. The W/D ratio for this model was about 0.4.

The PPG 1578 constant thickness and variable wall glass hemispheres were fabricated by pressing hemispherical shell blanks from 0.375-in. and 0.75 plate material. The blanks were then rough ground at the curved surfaces and bearing face with 120-grit wheel. The flat bearing face and edges were then successively ground with loose abrasive as follows:

Loose Abrasive	Material Removed, in.
120	0.0024
W2	0.0016
W5	0.0014
W8	0.0011
Polish	0.0003

The edges were put on with an orbital sander. After grinding on the flat bearing face was completed using a loose abrasive of a particular size, the rounded edge was finished with the same abrasive. The procedure was followed through the steps shown. The models were then acid treated in a 10 percent HF acid solution to remove 0.001 in. of glass, and the hemispheres were chemically strengthened in a sodium salt bath. Surface flatness was checked by placing the bearing surface on a flat table and passing shim stock between them. This inspection procedure indicated that the surface was flat to within 0.001 in. However, when a flat rod was placed across the bearing surface and a light source positioned directly behind, it could be observed that contact was being made only at the inner corner of the bearing surface. It is estimated that the inner edge was less than a half mil higher than the outer edge. The out of flatness of the bearing face is attributed to the effect of the ion exchange treatment.

PPG 1080 glass hemispherical shells with two different strengthening treatments were tested. Six hemispheres were treated in a sodium salt bath (hereafter referred to as 1080 Na^+ glass) which has an abraded modulus of rupture of about 40 ksi and 15 hemispheres were treated in a potasium salt bath (hereafter referred to as 1080 K^+ glass) which has an abraded modulus of rupture of about 80 ksi. All of the hemispheres were 10 in. diameter in wall. The 1080 Na^+ models were fabricated by grinding the entire surface with 120 grit fixed abrassive. The bearing face was then prepared by grinding with successively finer loose abrasives, starting with 120 grit and finishing with W8 garnet. No attempts were made to refine grind the edges of the bearing face. The bearing surface was then polished and the entire hemisphere etched in a solution of 2 percent solution of hydroflouric acid for 10 minutes. Following this the models were chemically strengthened.

The PPG 1080 K^+ glass hemispheres were fabricated in a manner similar to the PPG 1578 models. However, after rough grinding of the shells, one additional acid treatment step was utilized where 0.002 in. of glass was removed. The same steps were utilized in fine grinding the flat bearing face and corner radius as for the 1578 shells. Seven of the nine 1080 K^+ models were acid treated and chemically strengthened after completing the grinding steps. Two hemispheres were polished after grinding, then acid treated and chemically strengthened. The latter procedure was utilized to achieve transparency. This also reduced the wall thickness by about 0.02 on the 2 polished hemispheres. No flatness measurements were made on the shells although it is suspected that the same degree of flatness was obtained as in the case of the 1578 hemispheres.

The fabrication of the Chemcor 0313 models was quite different. The hemispheres were formed by pressing, and no work was performed on the curved surfaces except for acid treatment. The initial rough grinding step at the bearing face was done with a 90-grit loose abrasive. The hemispheres were then acid etched in a HF acid solution. The flat bearing face was then refinished with W-1 loose abrasive, and the edges were ground manually with a 320-grit stone. Following this, a second acid treatment in HF solution was used. The models were then chemically strengthened in a sodium salt bath. Flatness inspection indicated gaps of 0.001 in. for as much as 3 in. around the circumference.

Two of the spherical assemblies HGS 1 and HGS 2 which had PPG 1080 Na^+ hemispheres were potted into the titanium rings which had been filled with epoxy. The remaining models tested were assembled with glass reinforced plastic as the gasket material. The procedure for the models with glass reinforced plastic was as follows.

The glass hemispheres were assembled by first cleaning the glass and titanium rings with alcohol. A release was then applied to the flat surface. Epoxy (EPON 828 and Vers 125) was then applied to the flat bearing face and unidirectional 12 and fiberglass ribbons were manually layed up on the bearing face so that the fibers were oriented in the radial direction. After completion of the layup around the circumference, epoxy was applied to the glass fibers from the top. The inside of the titanium ring was coated with epoxy and the edge of the glass hemisphere placed in

it. The assembled hemisphere was then placed in the concave down position on a flat plate. A hole was drilled into the plate so that a vacuum could be drawn on the inside of the hemisphere. The procedure minimized the thickness* of the GRP gasket and ensured that all excess epoxy was extruded prior to curing (under a vacuum load, a bearing stress of approximately 100 psi is applied). After curing, the excess GRP was trimmed off. A photograph of a completed 1578 hemisphere is shown in Figure 11, and assembled spheres of 1578 and 1080 glass in Figure 12.

TEST PROCEDURE

The primary objective of the program was to observe the performance of surface compressed glass hemispheres under cyclic loads. The cyclic tests of PPG 1080 Na^+ models were tested at 10,000 psi. In the later tests of the PPG 1578 and 1080 glass models, cyclic testing was started at moderately low levels of pressure to observe fatigue behavior at various levels of applied bearing loads. The cyclic test procedure is shown in Tables 2 and 3.

The titanium bearing surface of each hemisphere was coated with silicone grease. The hemispheres were put together, covered with urethane rubber jackets about 0.125-in. thick and then held together with aeroseal bands. The urethane rubber jackets were used so that the glass would not contact the tank wall during the tests. Tests were conducted in the NSRDC 11.5-in.-diameter, and 15-in.-diameter high-pressure test facilities. Figure 13 shows a model in the test facility. Except for HGS-1 which was tested in oil, all other tests were conducted with fresh water as the pressure medium. Cycling rate varied from 60 to 85 cycles per minute. The lower rate of 60 cycles per minute was associated with higher maximum pressures. The pressure application rate for all tests was relatively

---

*In the early model assemblies gaskets were measured and thicknesses of approximately 0.005 in. were obtained. In later tests gaskets were made by overlapping the fiber ribbons to obtain a more dense packing. This also increased the thickness of gaskets to as much as 0.020 in. The reason for this change is discussed later in the report.

constant. The pressure profile was roughly 15 sec. to load, 15 sec. hold at maximum pressure, 15 sec. to relieve pressure, and 15 sec. at minimum pressure (50 psi). Models were inspected at a predetermined number of cycles. The inspection procedure (developed at NOL) consisted of placing the hemisphere in a fluid (cedar oil) with an index of refraction equal to that of the glass so that the glass bearing face could be viewed from the outside. A setup for inspection is shown in Figure 14.

TEST RESULTS AND DISCUSSION

Test results are summarized in Tables 2 and 3.

PPG 1578 GLASS

Cyclic testing of PPG Code 1578 constant thickness glass hemispherical shells was initiated at a pressure of 6500 psi. The average bearing stress at the joint for this pressure is 59,200 psi. The first model tested (designated HGS-10) survived the predetermined objective of 3000 cycles. However, a large crack about 0.5-in. long was observed on Hemisphere 15 of Model HGS-11 after 100 cycles; see Figure 15. The pretest inspection of this model had not revealed any gross flaws in this area although short scratches (less than 0.025 in.) were noted at the inner edge of the bearing face. Unfortunately no photographs were taken of these flaws. However, examination of the photograph in the fractured area appears to indicate that the crack did not extend to the inner corner. The fracture on this hemisphere resembles those more commonly observed on annealed glass hemispheres although this type of splitting has been observed on surface-compressed hemispheres (for example, in Figure 4).

Subsequent to the fracture observed in HGS-11, the cyclic test pressure was reduced to 5000 psi. The average bearing stress at the joint for this pressure is 45,900 psi. Even at this pressure, fatigue damage was observed in the test of Model HGS-12. After 898 cycles to 5000 psi, a small chip on the inner edge was observed on Hemisphere 13; see Figure 16. The pretest inspection of this model had not revealed gross flaws in this area. After additional 150 cycles to 5000 psi were applied to the model, further damage was observed on Hemisphere 13; light spalling of the inner

edge at the 40-deg orientation, light spalling of the outer edge at the 165-deg orientation, and spalling at the outer edge at the 110-deg orientation. Damage in the first two areas could not be identified with preexisting anomalies, but damage in the third area was identified as originating from a deep grinding flaw on the bearing face (see Figure 17).

After damage had been observed on HGS-12 at 5000 psi, the cyclic test pressure was further reduced to 2500 psi for the remaining four model tests. All four assemblies survived 3000 cycles to 2500 psi and subsequently 3000 cycles to 3750 psi. Although each sphere survived 3000 cycles to 5000 psi, spalling was observed in two areas of Hemisphere 3 of Assembly HGS-16. The light spalling on the outer edge of the bearing face at the 235-deg orientation could not be identified with a preexisting flaw. The heavy damage on the inner edge of the bearing face at the 45-deg orientation is thought to have been caused by an untreated zone on the bearing joint. The pretest inspection of the joint revealed a check in the rounded corner which was so oriented that a piece of glass about 0.125-in. long was about to spall; see Figure 18a. After the visual inspection, a plastic replica was made of the edge and examination indicated that the piece of glass had actually spalled out; see Figure 18b. After 3000 cycles to 5000 psi, rather extensive damage was observed in this area; see Figure 18c. The previous inspection at 1800 cycles had not revealed any fatigue damage. No further tests were attempted on HGS-16 after 3000 cycles to 5000 psi. However, the remaining three assemblies were cycled at 6500 psi. Models HGS-14 and HGS-17 survived 2000 cycles and HGS-15 1500 cycles at this pressure. When the cyclic pressure was raised to 7700 psi (average stress of 70,600 psi), both HGS-14 and HGS-17 failed after application of only 30 cycles. Figure 19 shows photographs of the models after test. No further tests were attempted on HGS-15 after 1500 cycles to 6500 psi, although no damage was apparent in either hemisphere.

Inspections conducted during the earlier tests showed that the GRP gasket (0.005 in. thick) was severely damaged in some of the models. Repeated loads had caused the glass to cut through the fiberglass layer at the inner edge. This was observed at a pressure level of 6500 psi or a membrane stress of 59,200 psi. The cutting in this area is attributable

mainly to high-contact stresses caused by the slightly raised inner edge of the bearing face. Once the deterioration was observed, the model was disassembled and reset with a new gasket. In later tests, an attempt was made to improve the durability of the gaskets by overlapping the fiber ribbons to obtain a more densely packed gasket. This also caused an increase of 0.010 to 0.015 in. in gasket thickness. It appears that some success was achieved since there was no apparent cutting through of the gaskets even after as many as 11,000 cycles of pressure to membrane stress levels between 23,000 and 59,000 psi.

Two types of joint rings were investigated in the tests. The Mod 1 ring had only the inner wall whereas the Mod 2 ring had inner and outer walls. Although the data are limited, one interesting observation can be made regarding the damage that occurred. In all of the tests conducted, the most frequent type of damage observed was at the inner edge of the bearing face. In some instances, it was noted that spalling occurred at the outer edge and in each of these cases (Hemispheres 3, 13, and 18) the models were assembled with Mod 1 type ring. It would appear that the outer wall of the Mod 2 type ring provides better support at the outer radius and may help to prevent the occurrence of spalling. Although the epoxy at the outer radius of a Mod 1 type ring is expected to cause a reaction, it is possible that the less confined condition permits yielding and extruding to occur. If this does take place at the outer edge, the only reaction at the corner that can be expected is that from hydrostatic pressure. Since no spalling was observed at the outer edge of a hemisphere assembled with a Mod 2 type ring, greater confidence can be placed on this geometry.

Six PPG 1578 glass hemispherical shells with reinforced joints were tested. The results are shown in Table 4. Although the first assembly HGS 20 performed extremely well, surviving as many as 15,000 cycles to depths ranging from 14,600 to 30,000 ft, the last 2 assemblies failed catastrophically in the very early stages of the cyclic progression. HGS 21 survived 2000 cycles to 14,600 ft and failed after 300 cycles to 17,200 ft. HGS 22 failed after 1532 cycles to 14,600 ft. For this geometry the average bearing stress at 14,600 ft is 38,000 psi. Based on these results and those obtained on constant thickness PPG 1578 glass hemispherical shells, it appears that bearing loads in excess of about 30,000 ksi should be avoided for this glass, method of treatment and assembly procedure.

CORNING 0313 GLASS

Only one spherical assembly of Corning Chemcor 0313 glass was tested. The model failed catastrophically after 218 cycles to 5000 psi (stress of 46,000 psi). The results of this one test appear to be consistent with results obtained by NOL. They have observed cracks at the inner edge after 675 cycles to 3000 psi. In two other tests, catastrophic failure resulted within 5 cycles when a pressure of 9000 psi was applied. In view of these results, no further attempts were made to continue these tests.

PPG 1080 GLASS

The 3 spherical assemblies of PPG 1080 Na^+ were all tested to a pressure of 10,000 psi in fatigue.

Model HGS 1 survived 106 cycles to 10,000 psi. Inspection of the glass at this level revealed no apparent damage to the model and therefore it was placed back in the test facility. While pressure adjustments were being made in the cyclic system, the model failed at a pressure of 8300 psi.

Model HGS 2 survived 715 cycles to 10,000 psi. The model was inspected after 1, 10, 300, and 700 cycles and gave no indications of damage. After inspection at 700 cycles, the model was put back in the test tank. It failed on the 715th cycle, while pressure was being applied at 9000 psi.

Model HGS 3 survived a total of 2380 cycles to 10,000 psi. The last inspection of the model was after 1100 cycles at which time no damage was apparent except for some pits on the inner and outer surfaces of one hemisphere. The model failed on the 2380th cycle, while pressure was being applied at 9000 psi.

The failure of Models HGS 1, 2, and 3 is believed to have occurred at the joint. In each case the fractured glass in the titanium ring was in the form of very fine white powder that had a considerably finer grain than all other pieces of fractured glass. A photograph is shown in Figure 19. The average bearing stress at 10,000 psi for this geometry is 72,000 psi. Since the residual surface compression on PPG 1080 Na^+ models

is similar to 1578 glass it is not surprising that failure occurred on HGS 1, 2, and 3. None of the PPG 1578 hemispheres survived more than 380 cycles at a stress of 70,000 psi.

Nine hemispherical shells of PPG 1080 K^+ models were tested. The results are shown in Table 3. Each of the hemispheres survived a minimum of 3000 cycles to a depth of 20,000 feet. Seven of the 9 hemispheres were subjected to as many as 12,500 cycles to depths ranging from 24,600 to 27,500 feet. All 9 hemispheres were then proof tested to a depth of 30,000 feet. The results of these tests are some of the most encouraging obtained to date. In view of the repeatability of the tests and the fact that 7 hemispheres survived at least 500 cycles to 27,500 feet (bearing stress of 87,000 psi) it is estimated that reliable performance from PPG 1080 K^+ 10 in. diameter models can be obtained at a stress of 64,000 psi.

The significant difference in performance of PPG 1578 Na^+ and PPG 1080 K^+ models is attributed to the effects of the ion exchange treatment. The average modulus of rupture for unabraded 1578 Na^+ glass based on concentric ring tests of 21 samples of 3/8 in. plate was 70,800 psi. These plate specimens were ion exchanged with the hemispherical shell models. The average modulus of rupture for unabraded 1080 K^+ glass based on concentric ring tests of 15 samples of 0.115 in. plate was 90,300 psi. Probably as important as the difference in strengths is the fact that 1578 Na^+ glass is more susceptible to strength degradation from mechanical abrasion than is 1080 K^+ glass. Although only 2 abraded (sand blasted) specimens of 1578 Na^+ glass were tested there is strong indication that the abraded strength may be more than 30 percent less than the unabraded strength. NOL, in independent tests, reports an average modulus of rupture of 37,000 psi for the abraded condition. By comparison, the 1080 K^+ glass shows very little effect from mechanical abrasion. The 14 abraded 1080 K^+ specimens had an average modulus of rupture of 84,000 psi or only about 7 percent less than the unabraded strength. Under bearing loads as in the case of hemispherical shells, it would be suspected that mechanical abrasion plays a role in the fracture process.

PAGES (S) MISSING FROM ORIGINAL

PAGES (S) MISSING FROM ORIGINAL

considered practical for unmanned noncritical conditions to 20,000 ft. Some effort is necessary to study effect of exposure to marine environment, design details to ensure watertight integrity and effects of thermal shock and dynamic loads.

5. Although some encouraging data was obtained in this program a considerable effort is necessary before surface strengthened glasses can be considered practical for critical applications, even for the size tested.

ACKNOWLEDGMENTS

The author expresses his appreciation to Messrs. T.J. Kiernan and M.A. Krenzke of the Center for their contributions in this project. Thanks also go to Mr. R. Provencher of NAVSEC for his interest in this program and to Mr. J. Freund of NAVSHIPS for support of the program. Finally, appreciation is expressed to Mr. C.R. Frownfelter of PPG Industries for his cooperativeness throughout the entire project.

CONTOURS OF PRINCIPAL STRESS FOR A 0.28 WALL GLASS HEMISPHERE
WITH ROUNDED EDGES P 1 PSI
CONTOUR INTERVAL IS 0.20

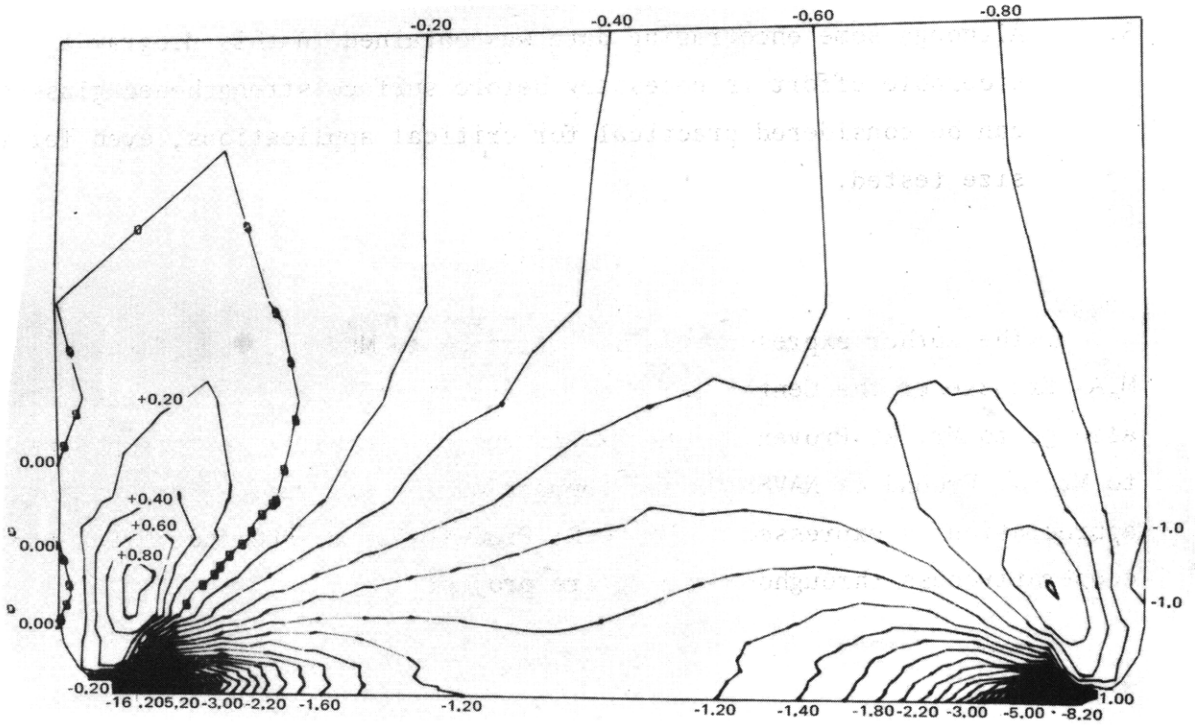

STRUCTURAL IDEALIZATION

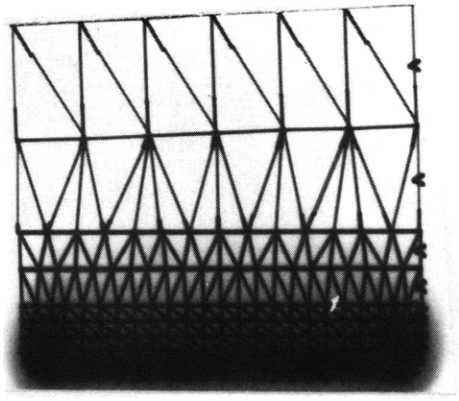

Figure 1 - Analysis of Constant Thickness Hemispherical Shell

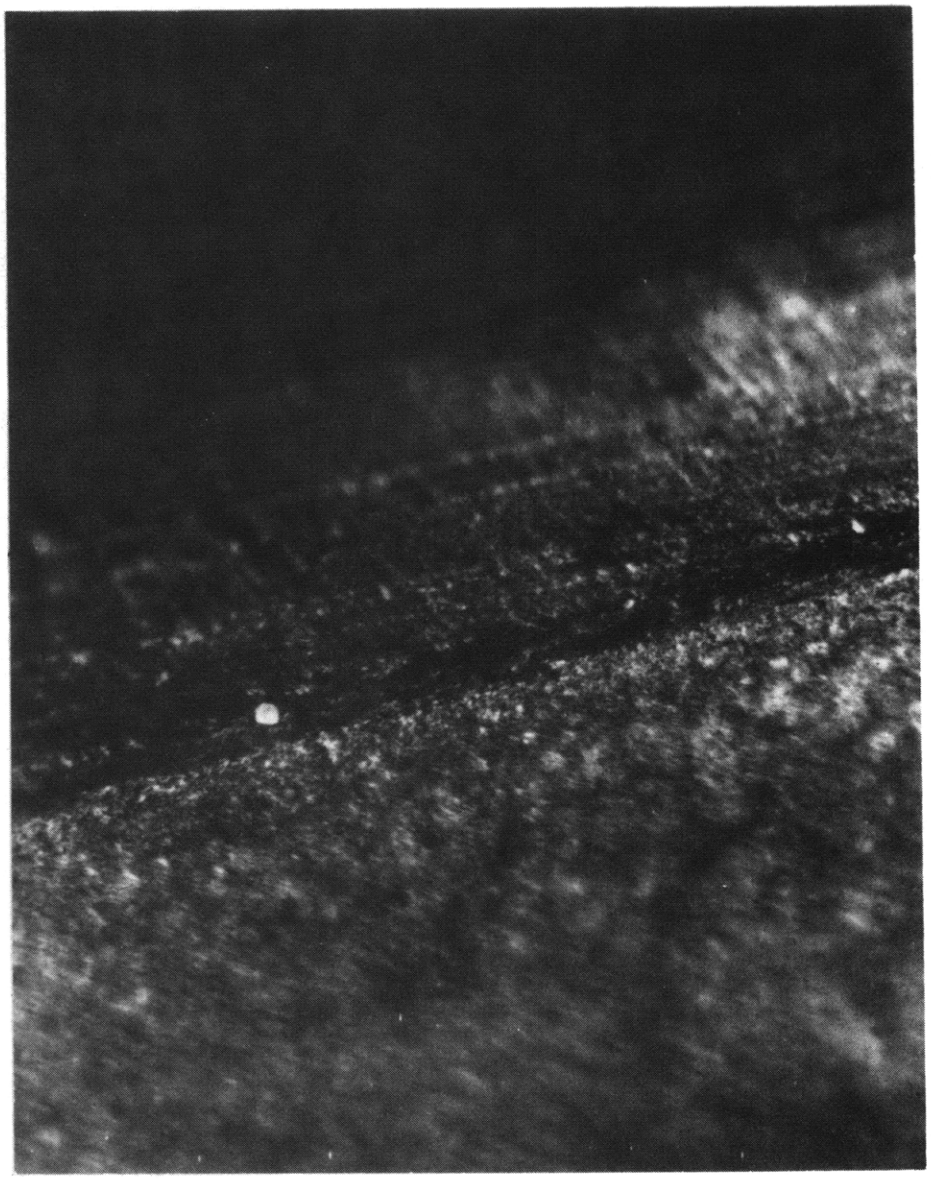

Figure 2 - Grinding Flaws at Beveled Edge

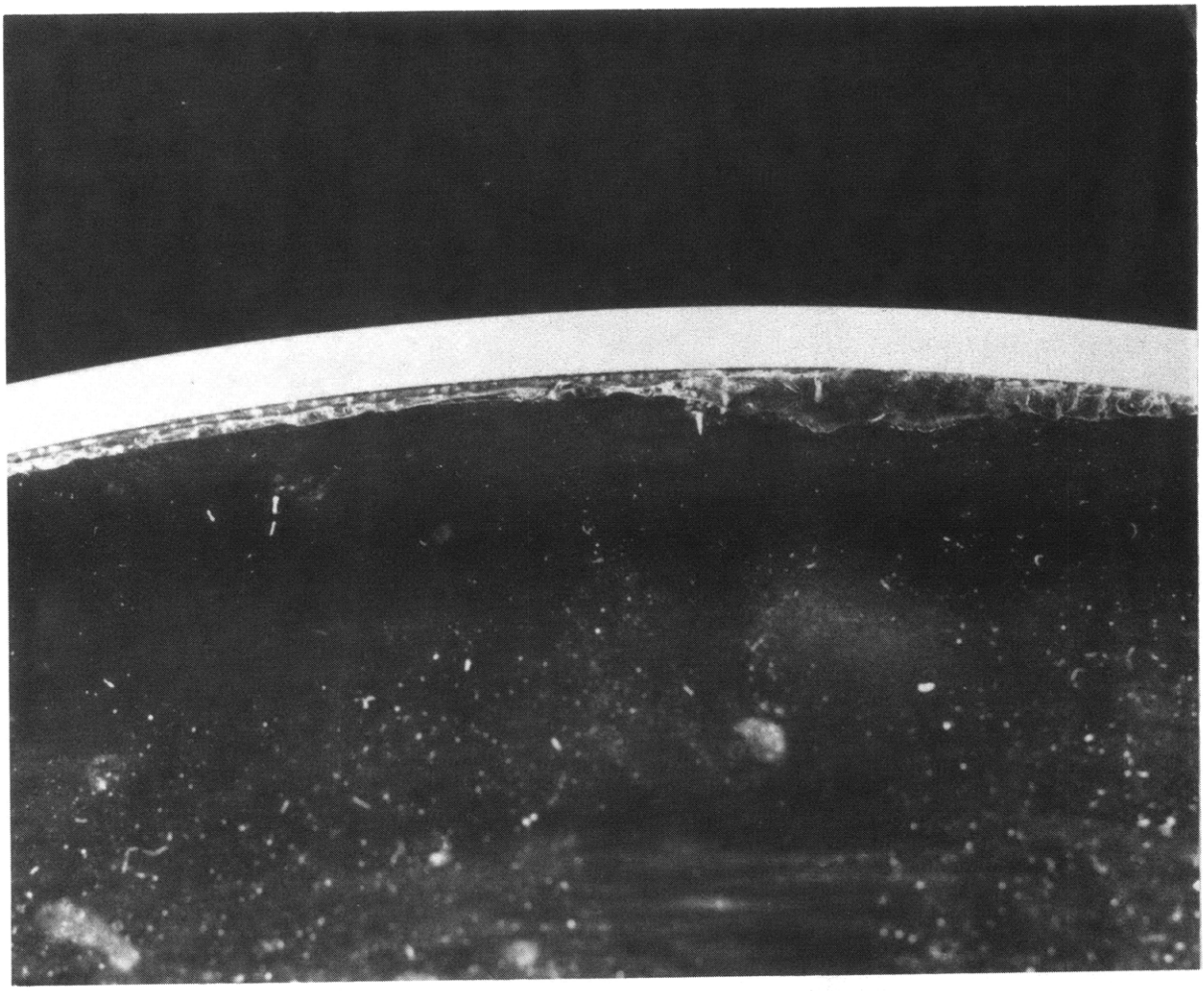

Figure 3 - Annealed Glass Hemisphere after Static Test to 17,000 psi

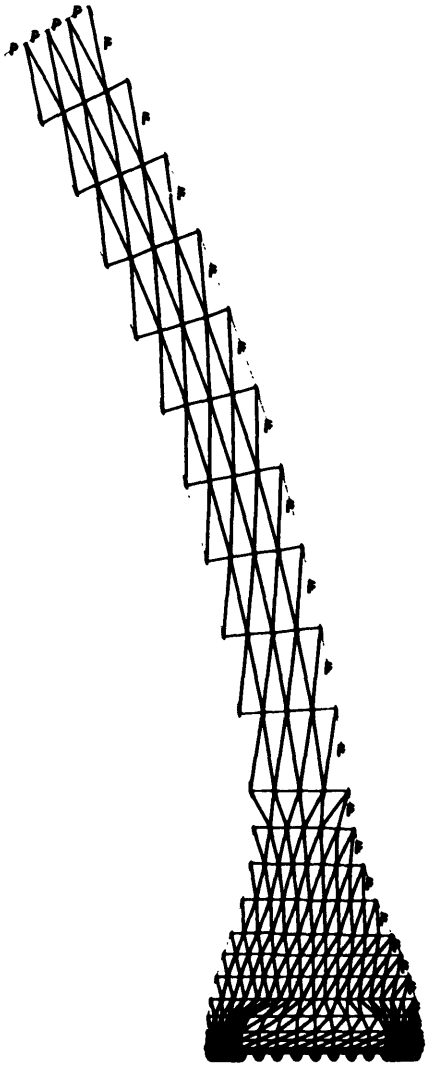

Figure 4a - Structure Idealization

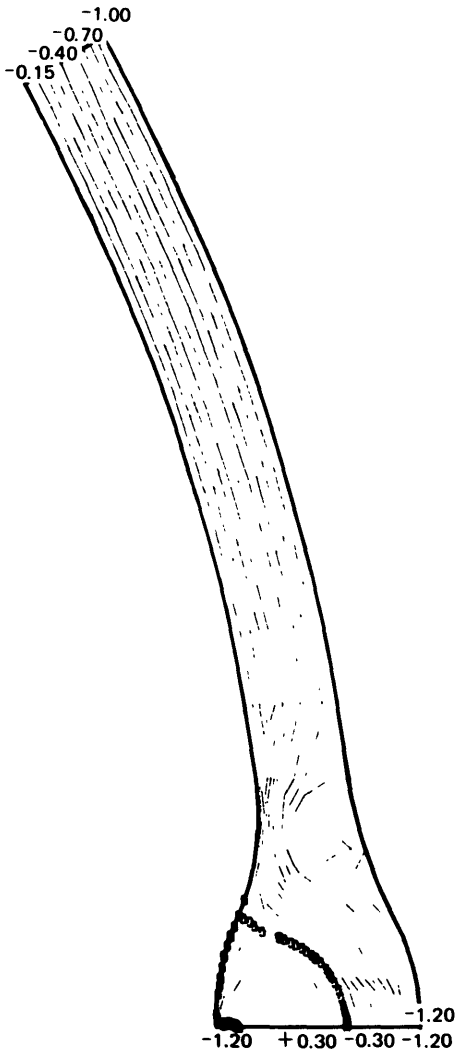

Figure 4b - Radial Stress

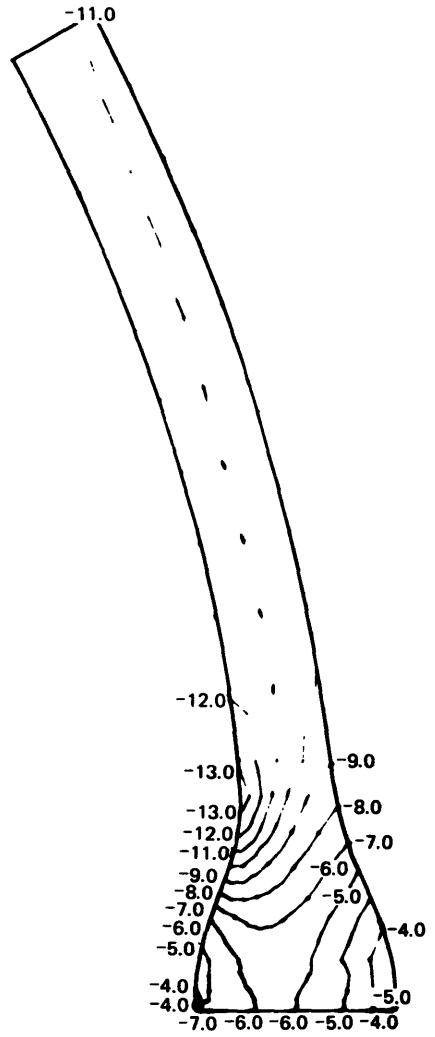

Figure 4c - Meridional Stress

Figure 4 - Analysis of Reinforced Joint Design

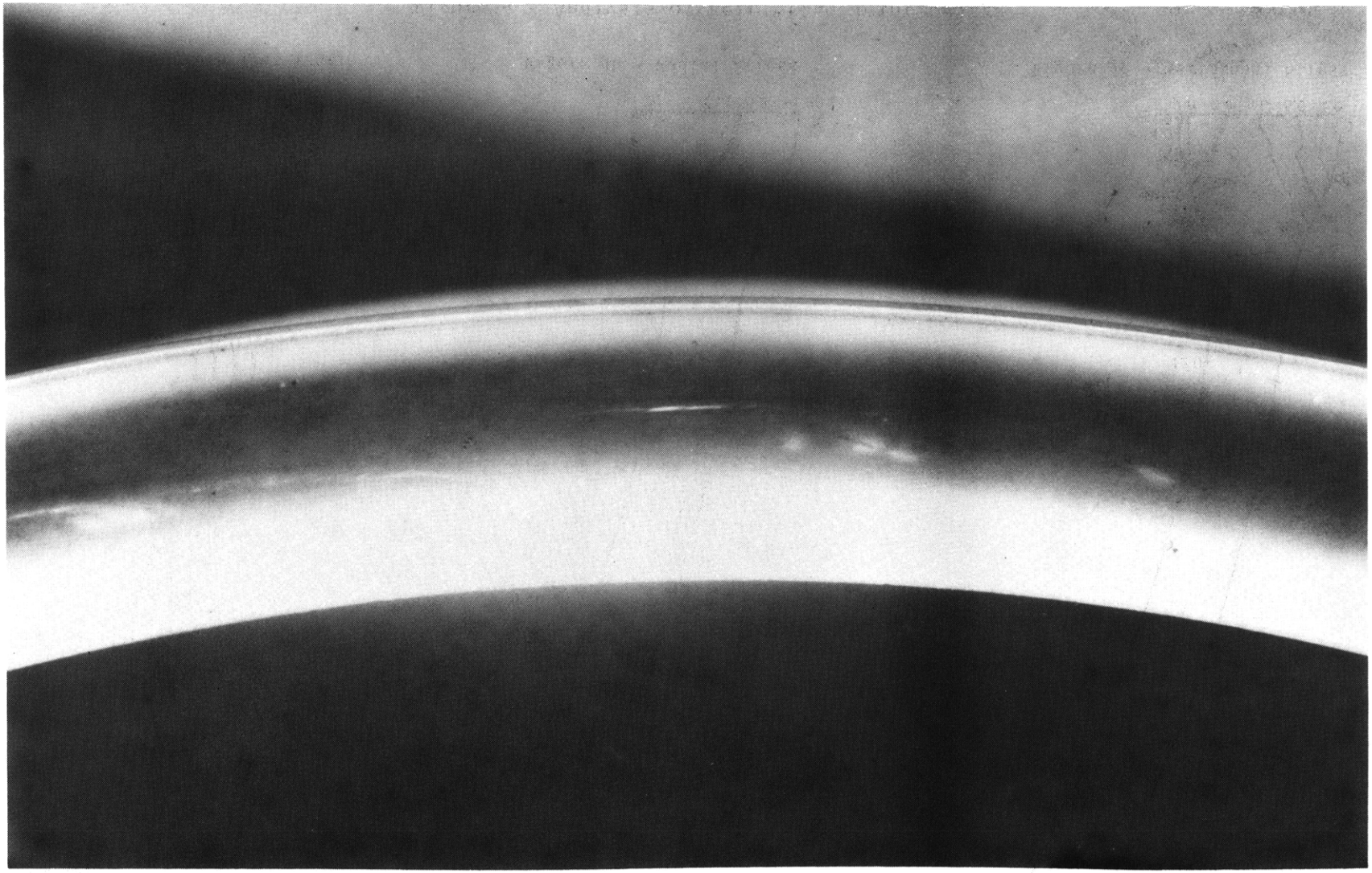

Figure 5 - Surface Compressed Hemisphere with Reinforced Joint after 10 Cycles to 10,000 psi

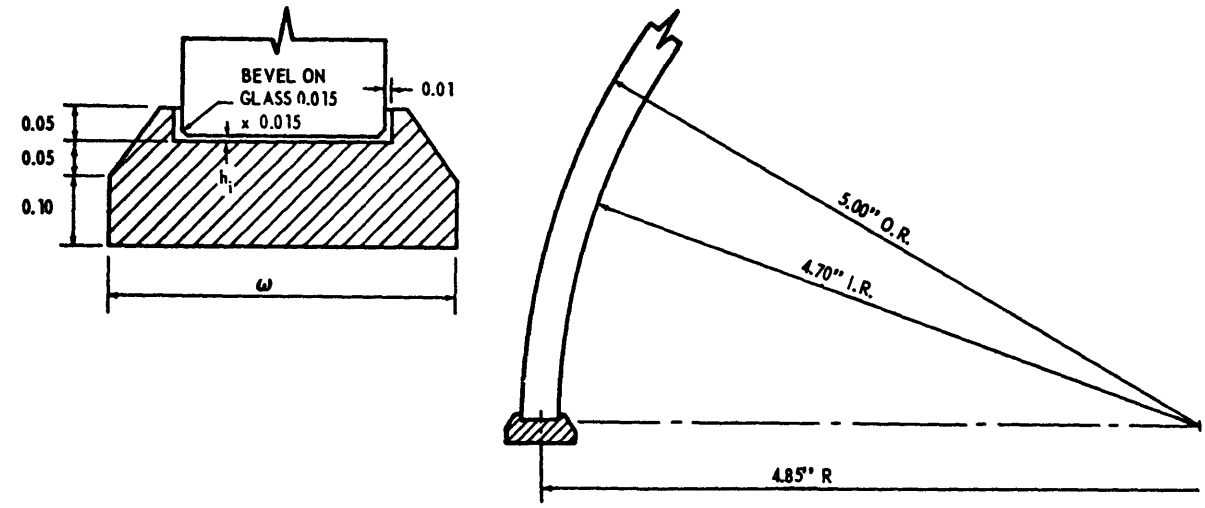

Figure 6a - Flat Juncture (G1)

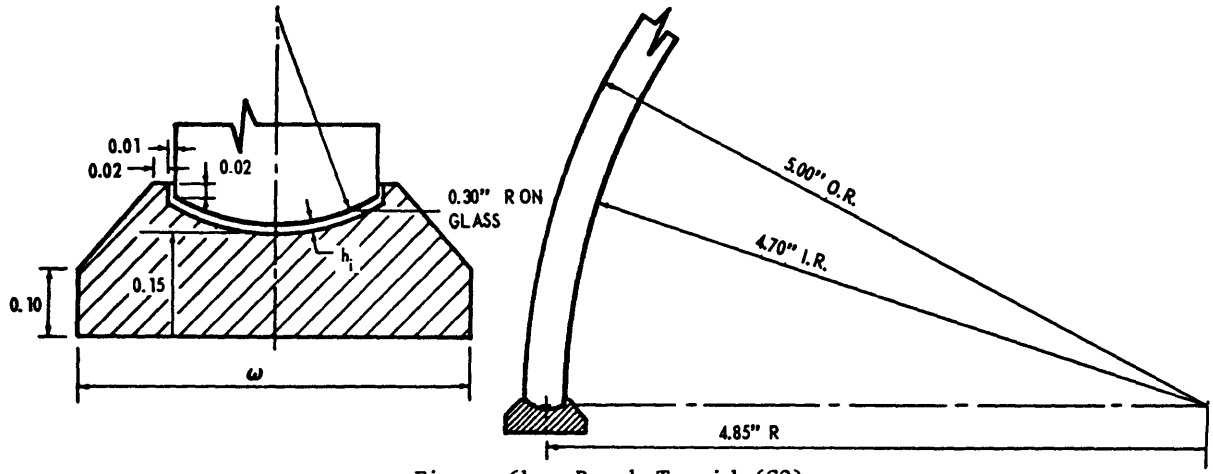

Figure 6b - R = h Toroid (G2)

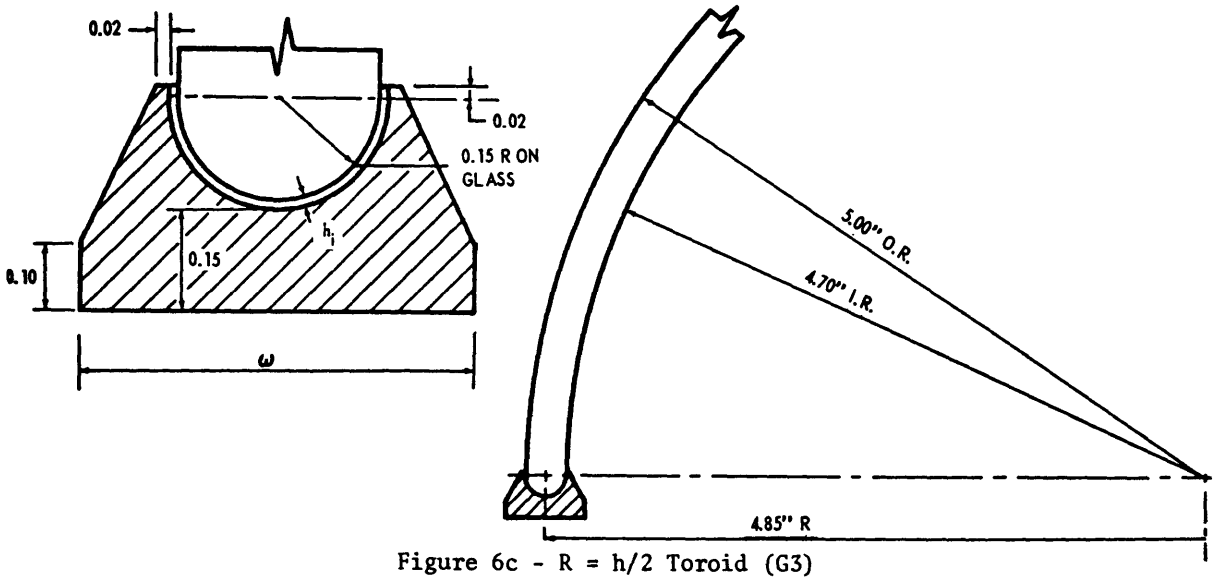

Figure 6c - R = h/2 Toroid (G3)

Figure 6 - Joint Geometries for Parametric Study

Figure 7 - Stress Contours

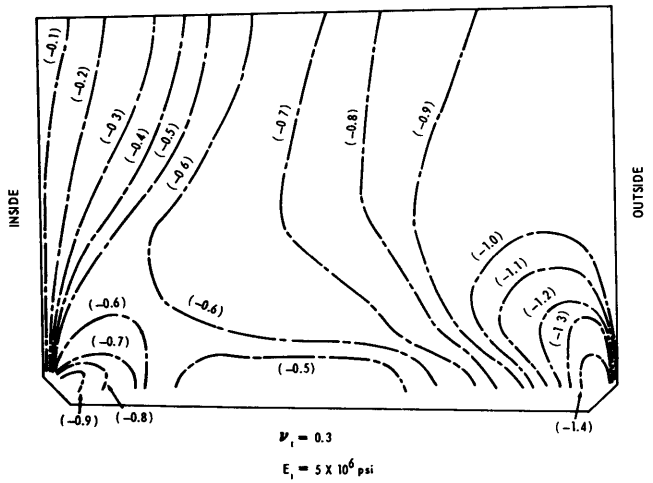

Model G11

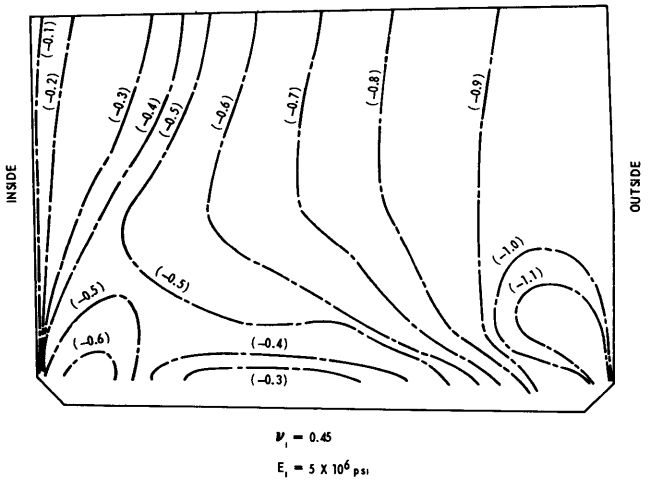

Model G12

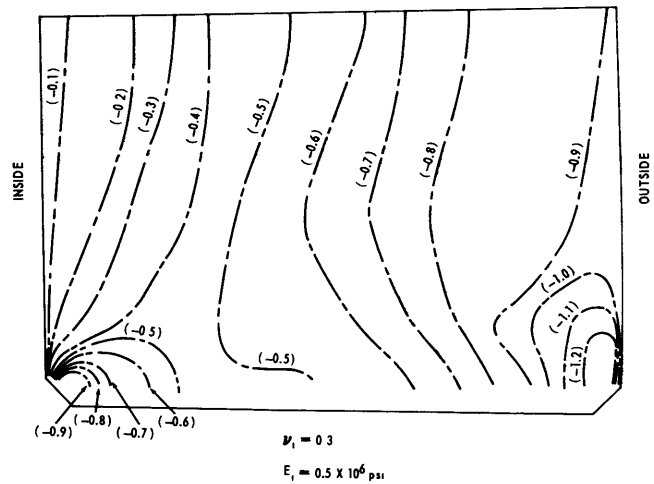

Model G13

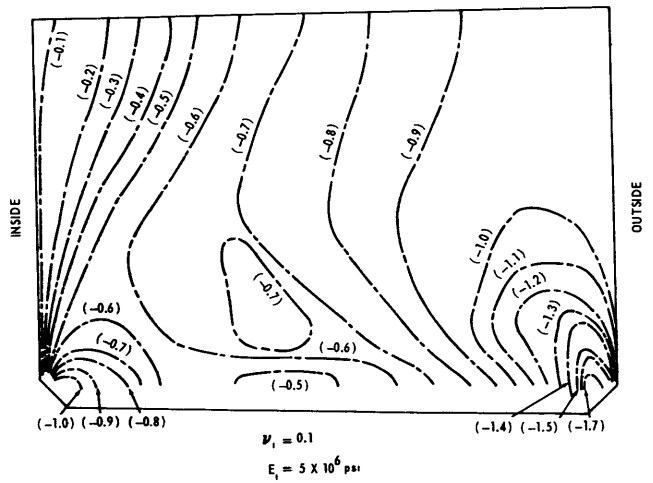

Model G14

Figure 7 (continued)

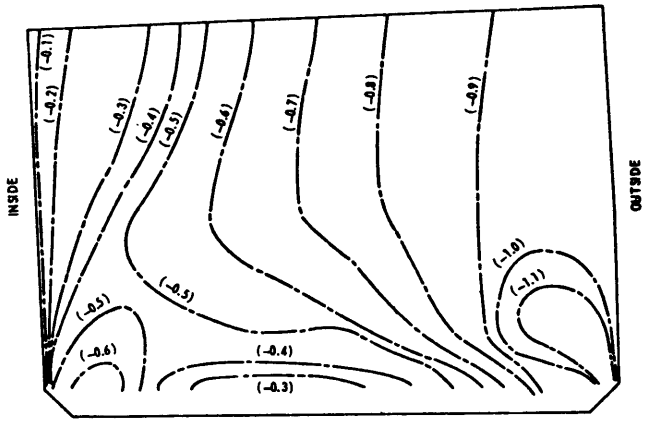

Model G15

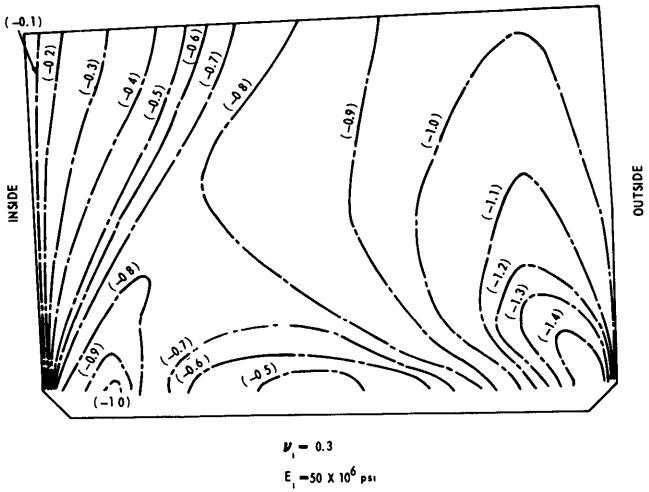

Model G16

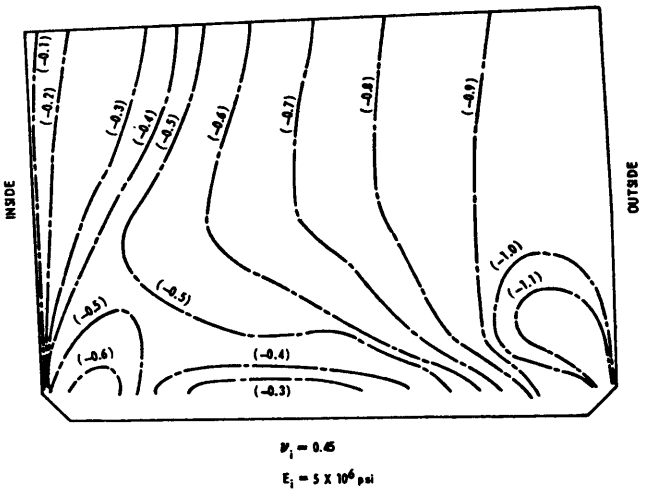

Model G17

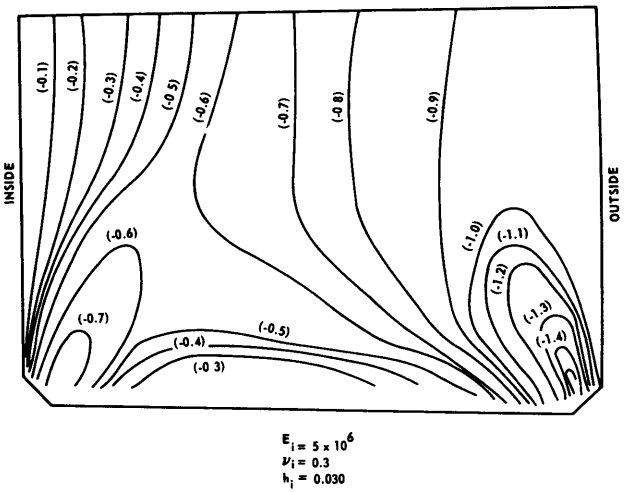

Model G18

Figure 7 (continued)

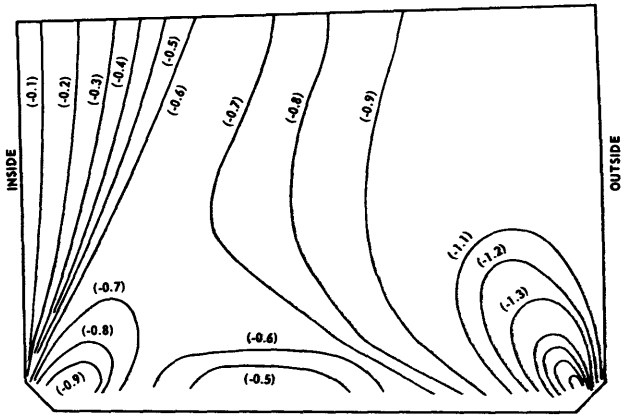

Model G18a

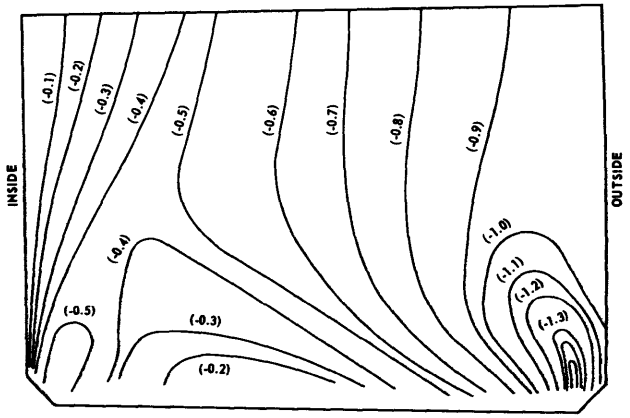

Model G19

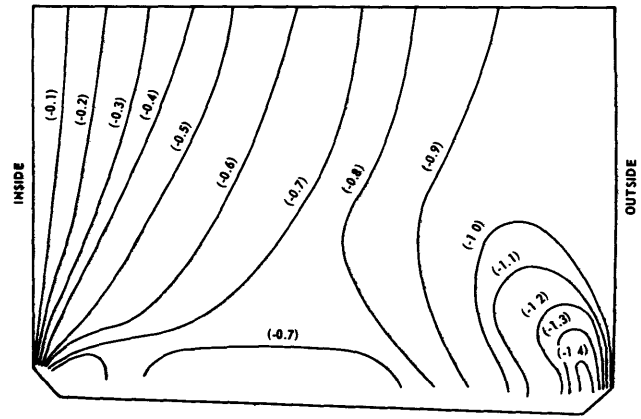

Model 19a

Figure 7 (continued)

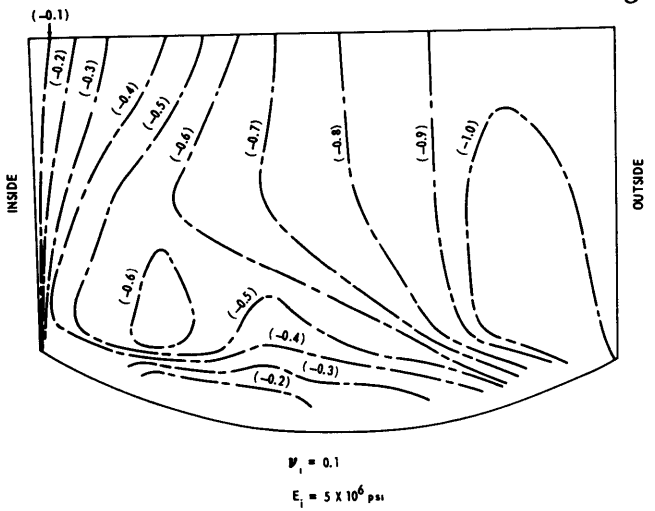

Model G21

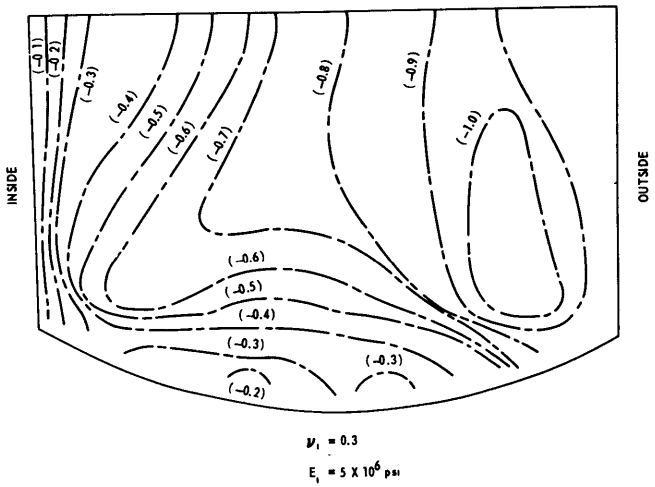

Model G22

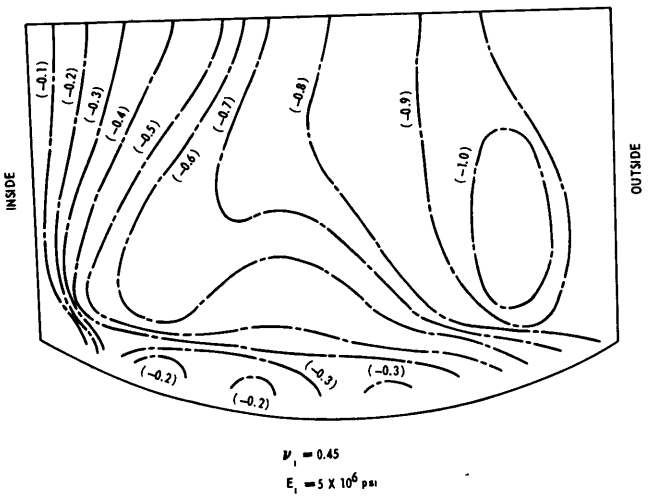

Model G23

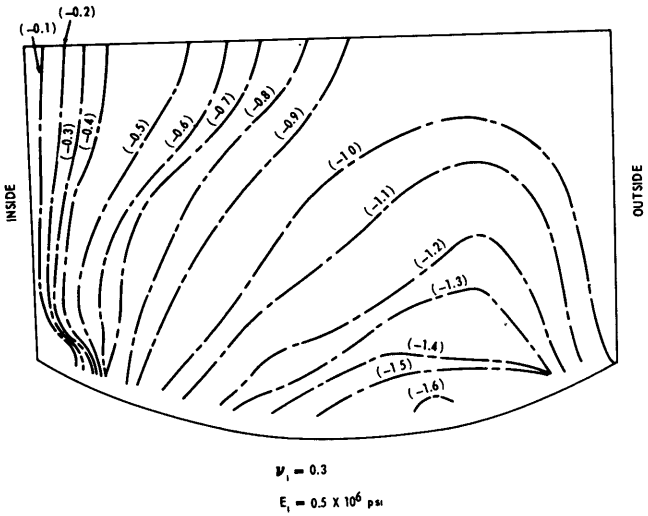

Model G24

Figure 7 (continued)

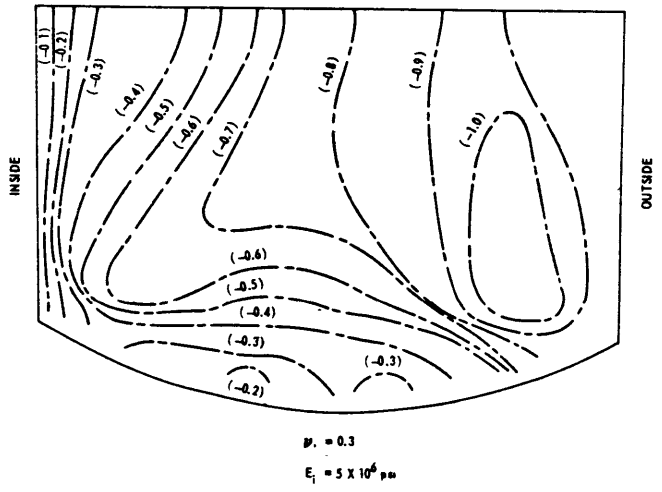

Model G25

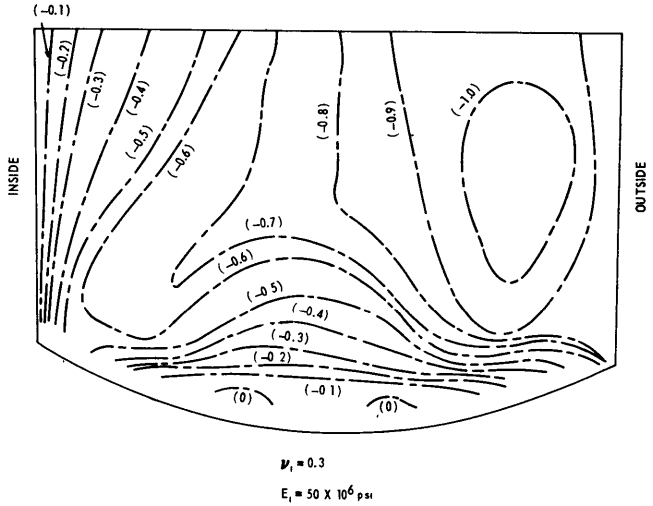

Model G26

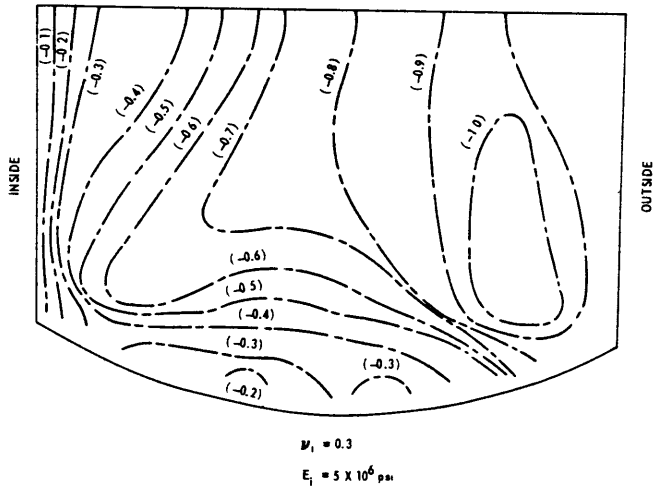

Model G27

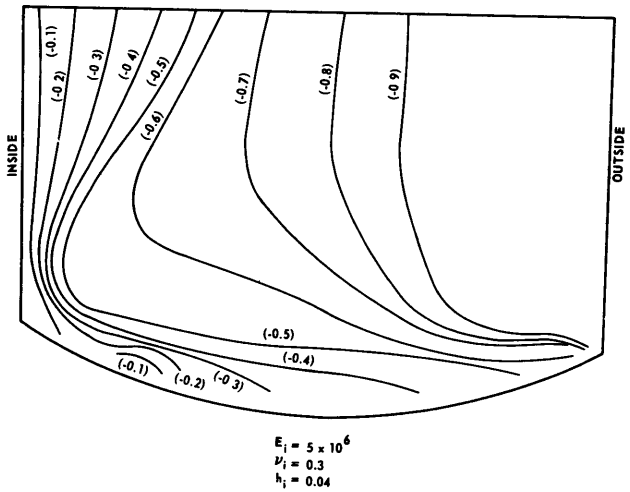

Model G28

Figure 7 (continued)

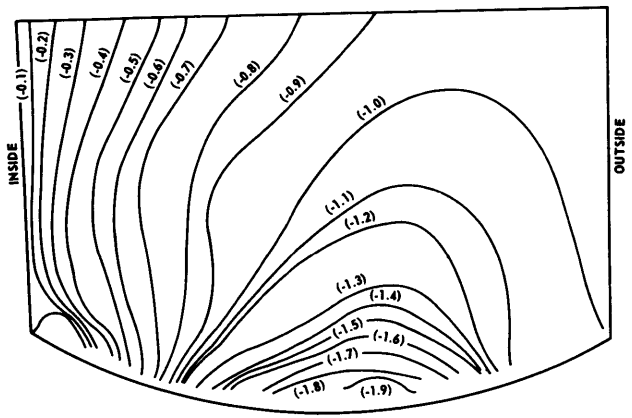

Model G28a

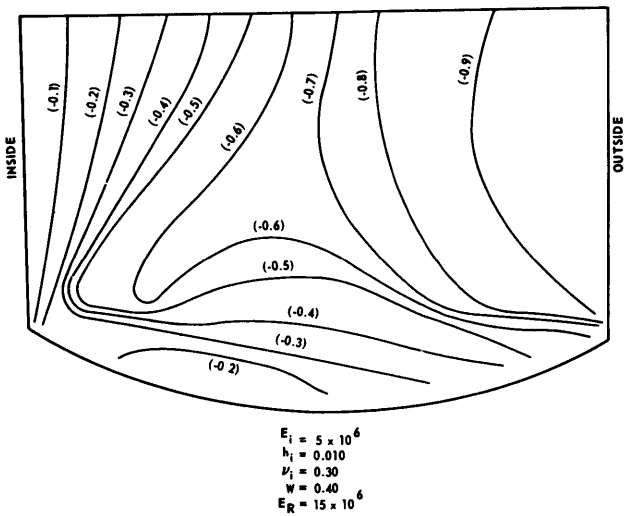

Model G29

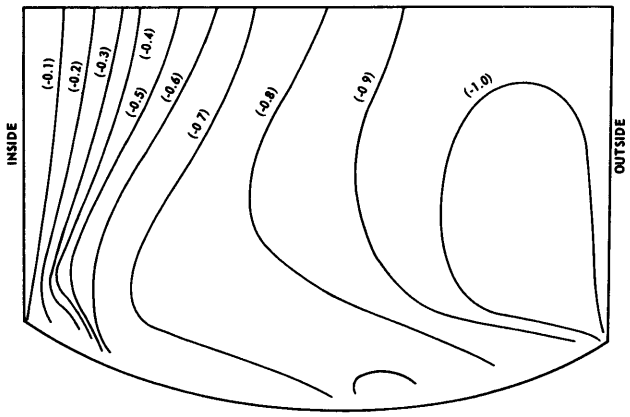

Model G29a

Figure 7 (continued)

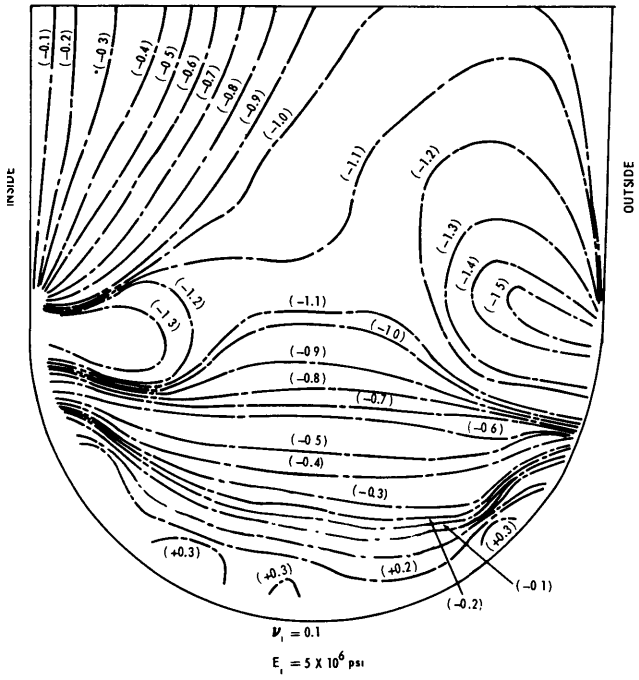

Model G31

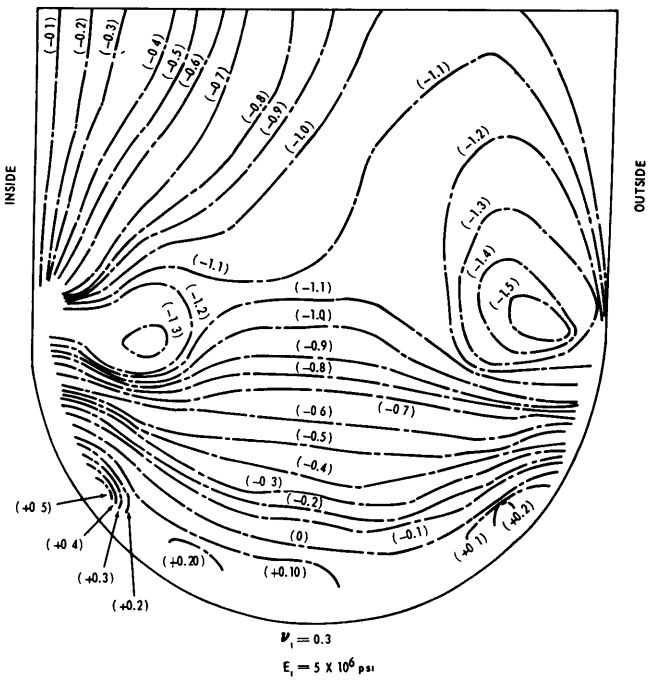

Model G32

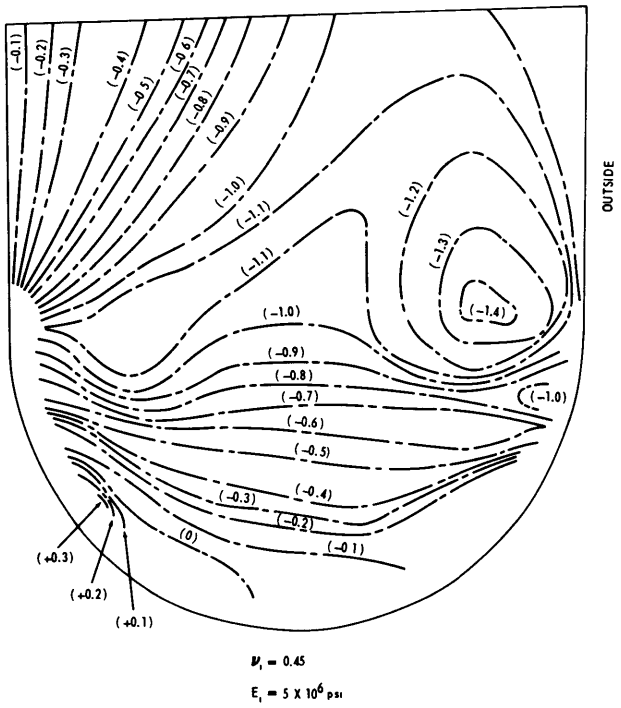

Model G33

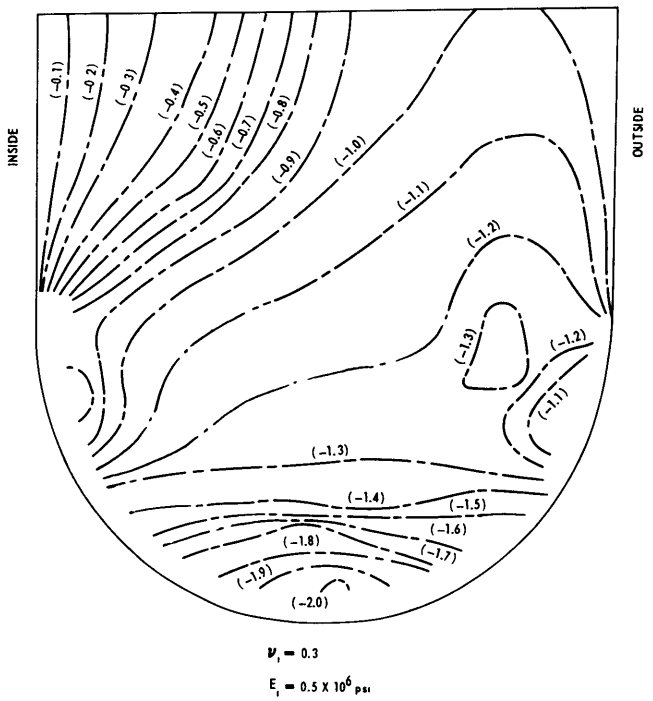

Model G34

Figure 7 (continued)

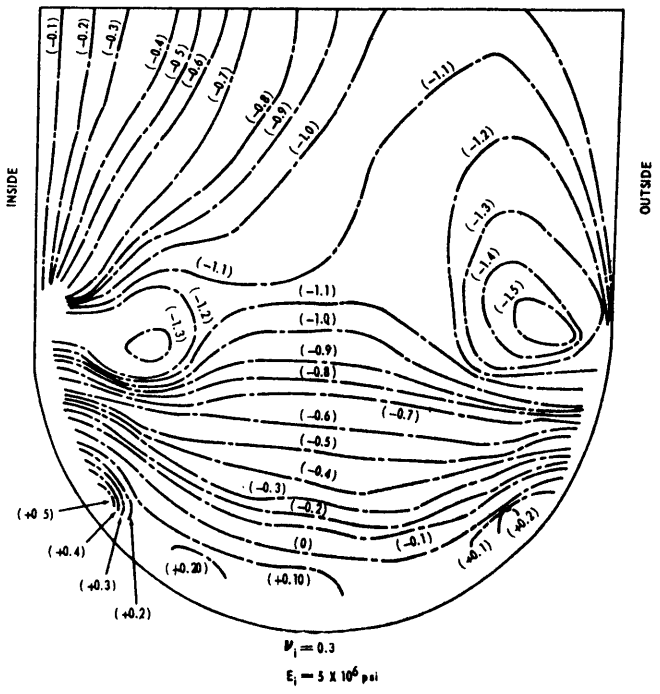

Model G35

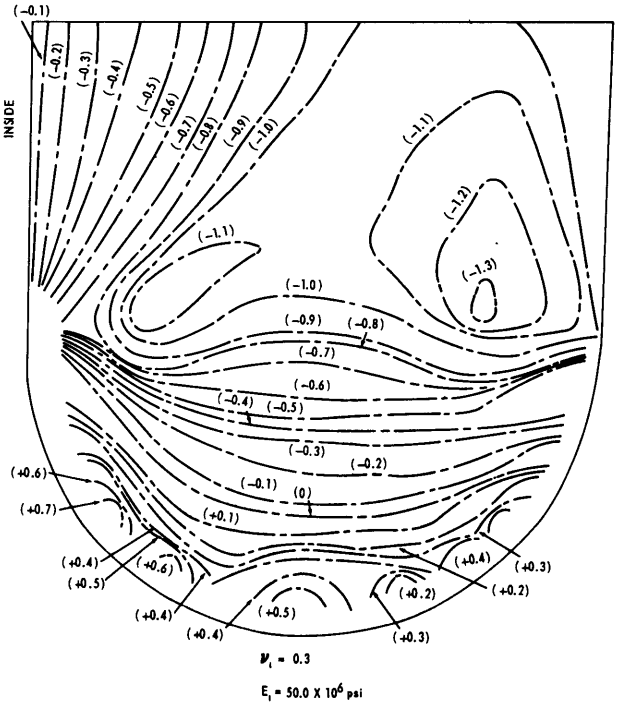

Model G36

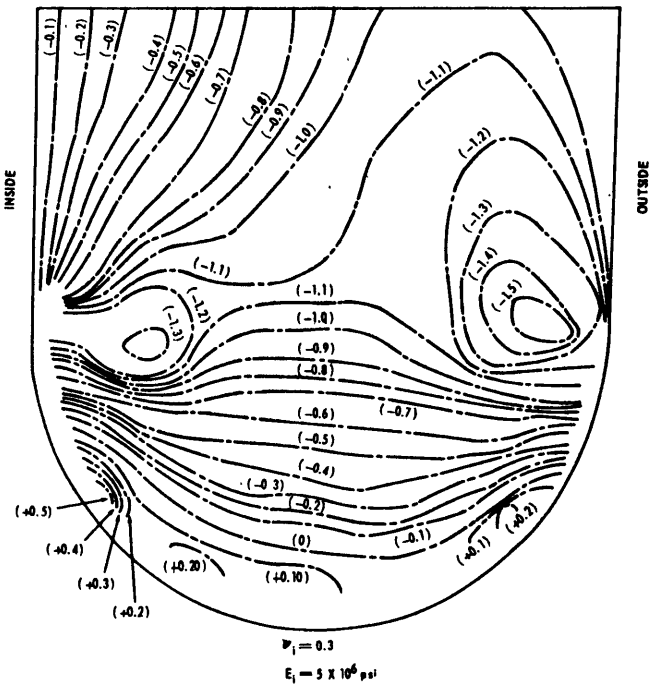

Model G37

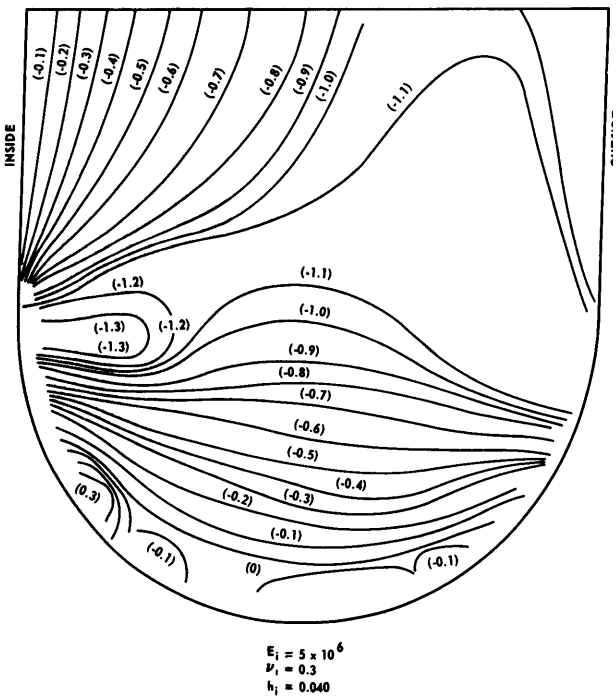

Model G38

Figure 7 (continued)

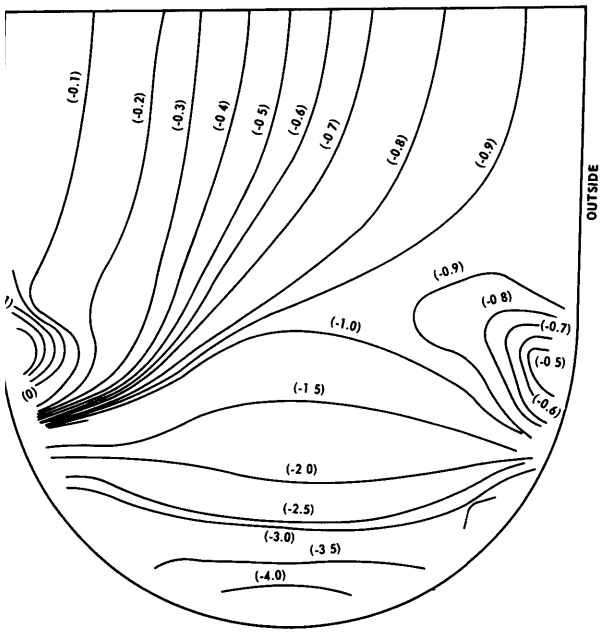

$E_i = 0.5 \times 10^6$
$\nu_i = 0.45$
$h_i = 0.040$

Model G38a

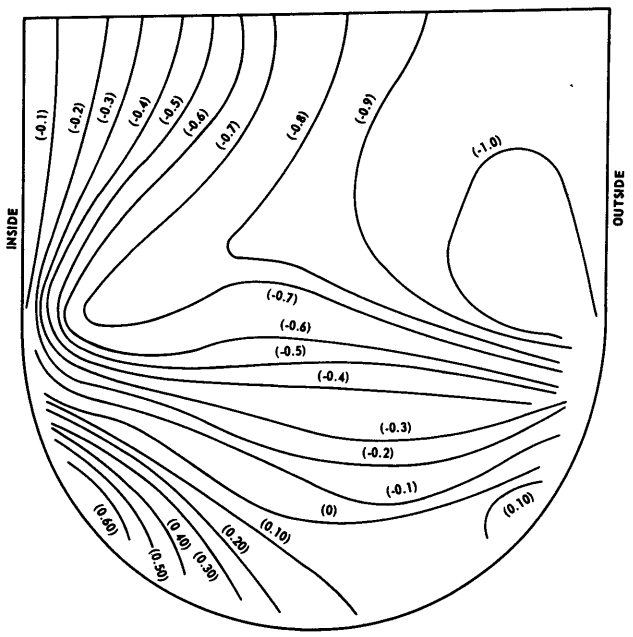

$E_i = 5 \times 10^6$
$h_i = 0.010$
$\nu_i = 0.30$
$W = 0.40$
$E_R = 15 \times 10^6$

Model G39

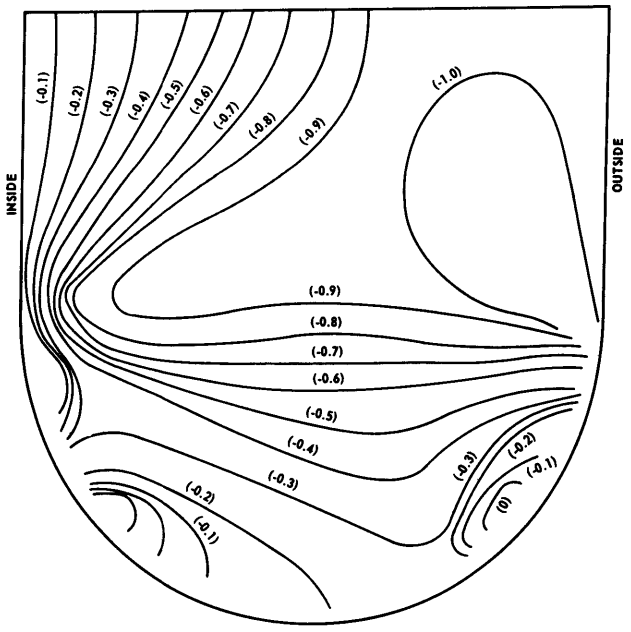

$E_i = 5 \times 10^6$
$h_i = 0.010$
$\nu_i = 0.30$
$W = 0.40$
$E_R = 30 \times 10^6$

Model G39a

0.28 WALL MODELS

0.36 WALL MODELS

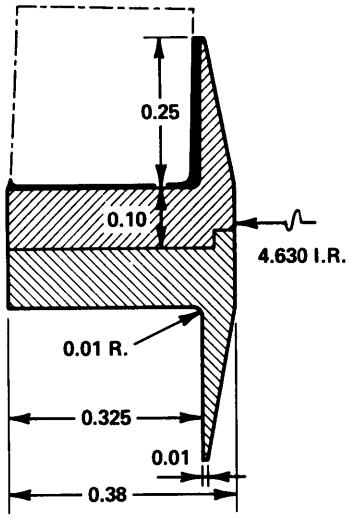

MOD 1

Figure 8a

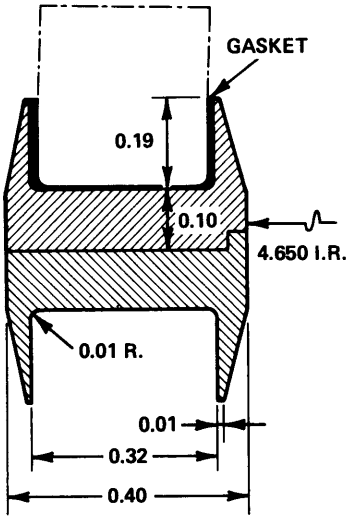

MOD 2

Figure 8b

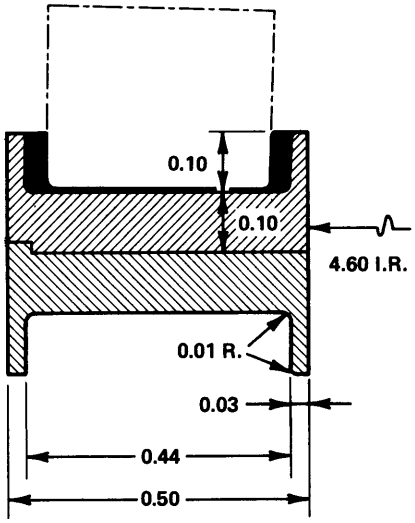

Figure 8c

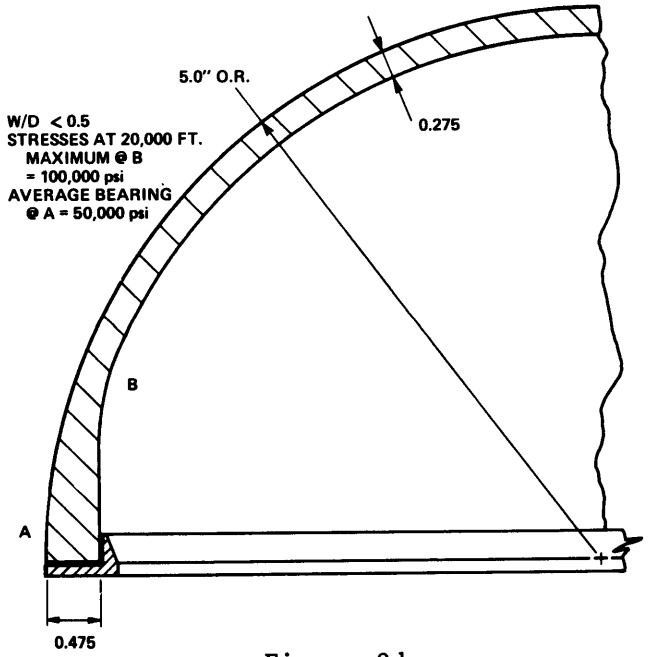

Figure 8d

Figure 8 - Final Joint Designs

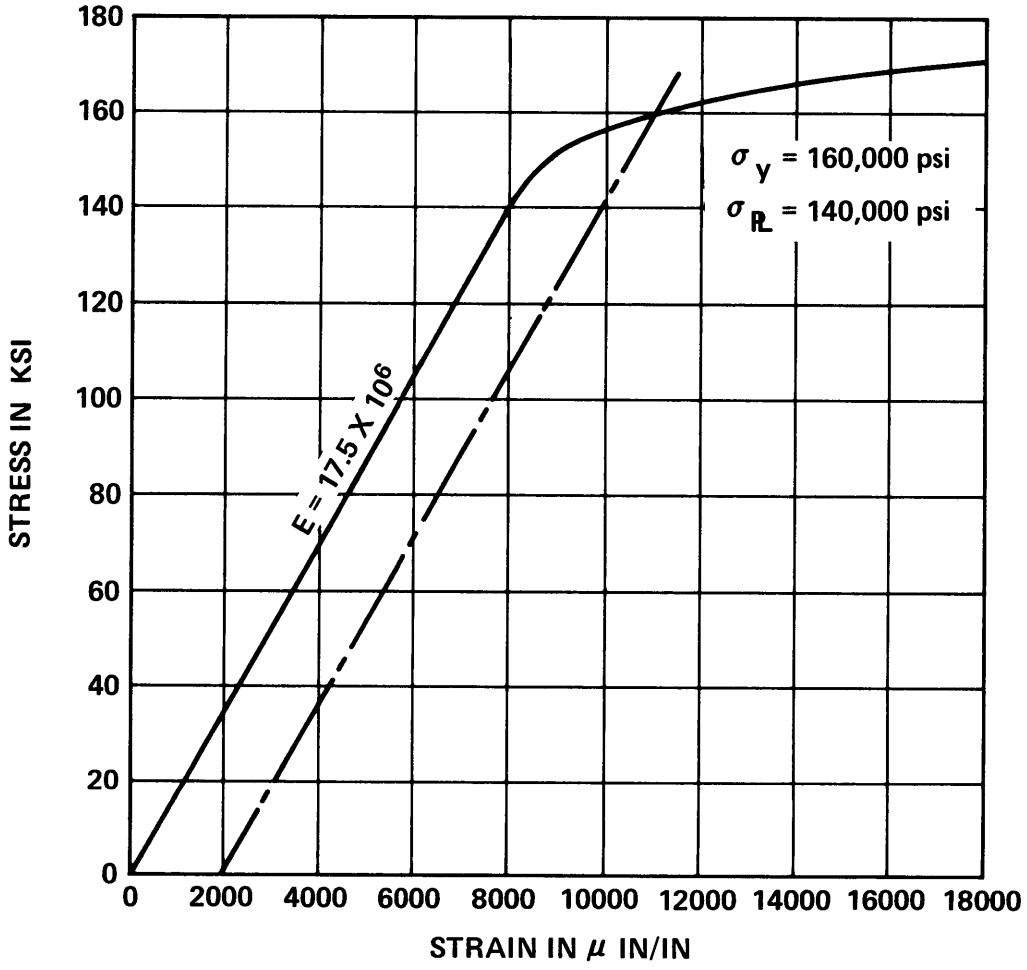

Figure 9 - Compressive Stress-Strain Curve for 662 Titanium

Figure 10 - Analysis of Final Joint Designs

MOD 1 MEMBRANE FOR 0.28 WALL GLASS HEMISPHERE

MATERIAL PROPERTIES:

TITANIUM	E = 17.5 X 10^6 psi
	y = 0.3
	σ_{RL} = 140,000 psi
GLASS	E = 10.5 X 10^6 psi
	y = 0.225
INTERFACE	E = 0.4 X 10^6 psi
	y = 0.4

LOADS:

INCREMENT 1	– 1 psi
FIRST YIELDING IN TITANIUM	– 9540 psi

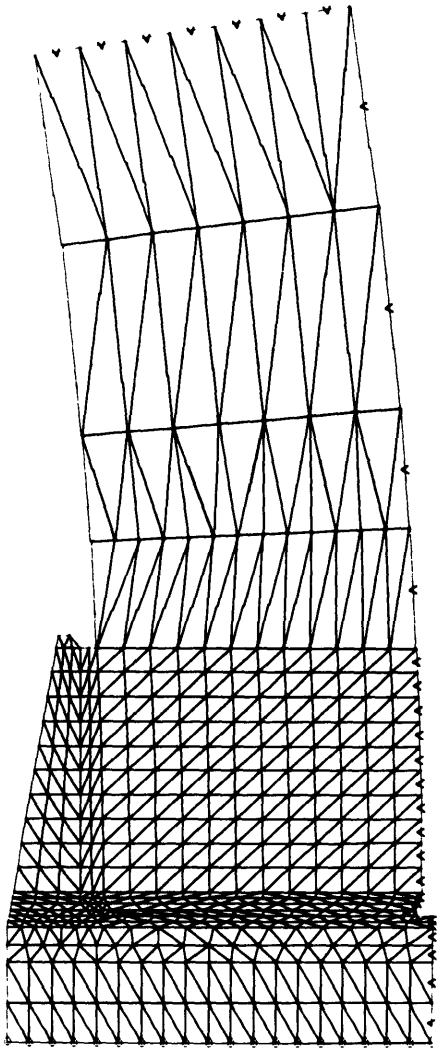

ZP26

STRUCTURAL IDEALIZATION

Figure 10a - Mod 1 Structural Idealization

MOD 1 MEMBRANE RING FOR 0.28 WALL GLASS HEMISPHERE

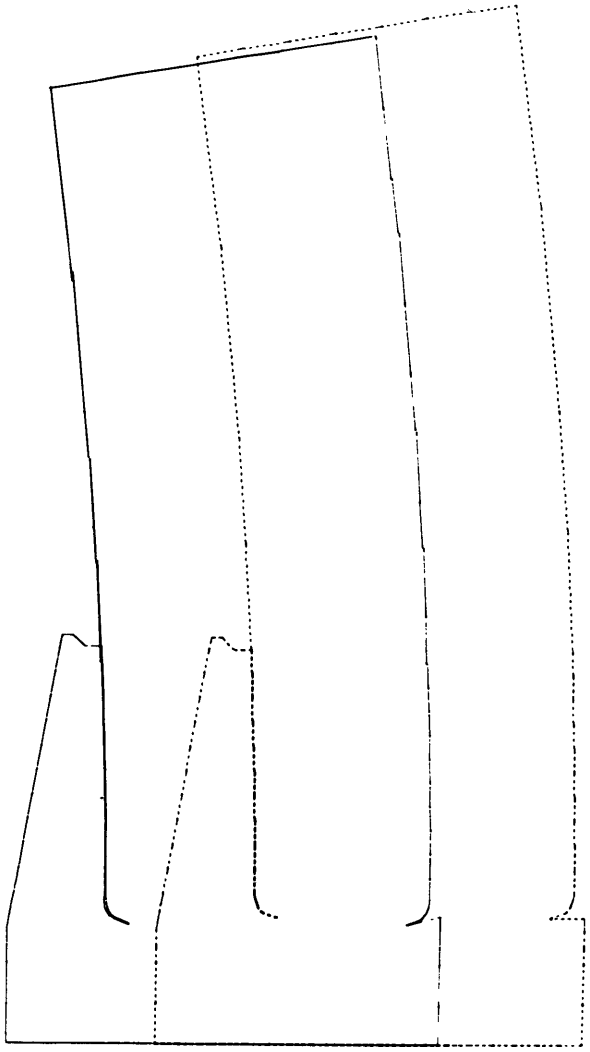

ZP26 DISPLACED STRUCTURE INCREMENT NUMBER 1

Figure 10b - Mod 1 Displaced Structure

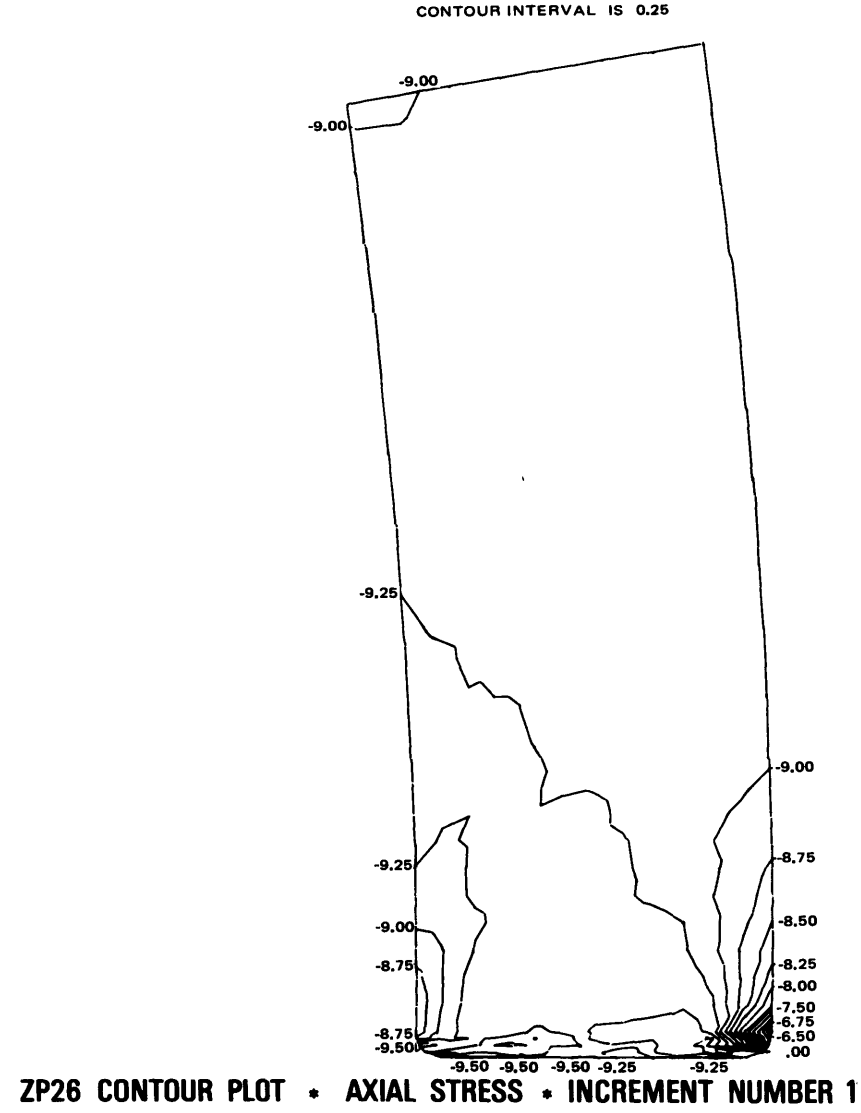

Figure 10c - Mod 1 Axial Stress

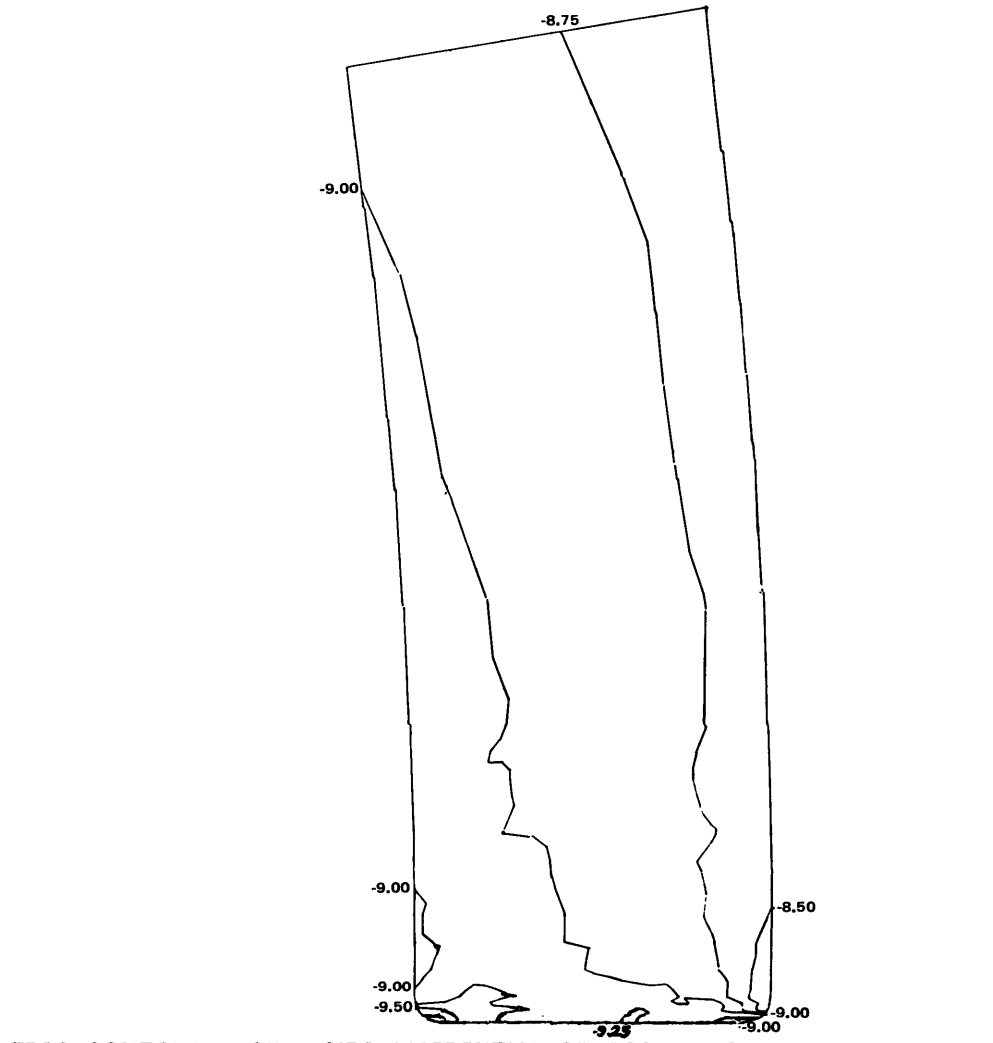

Figure 10d - Mod 1 Circumferential Stress

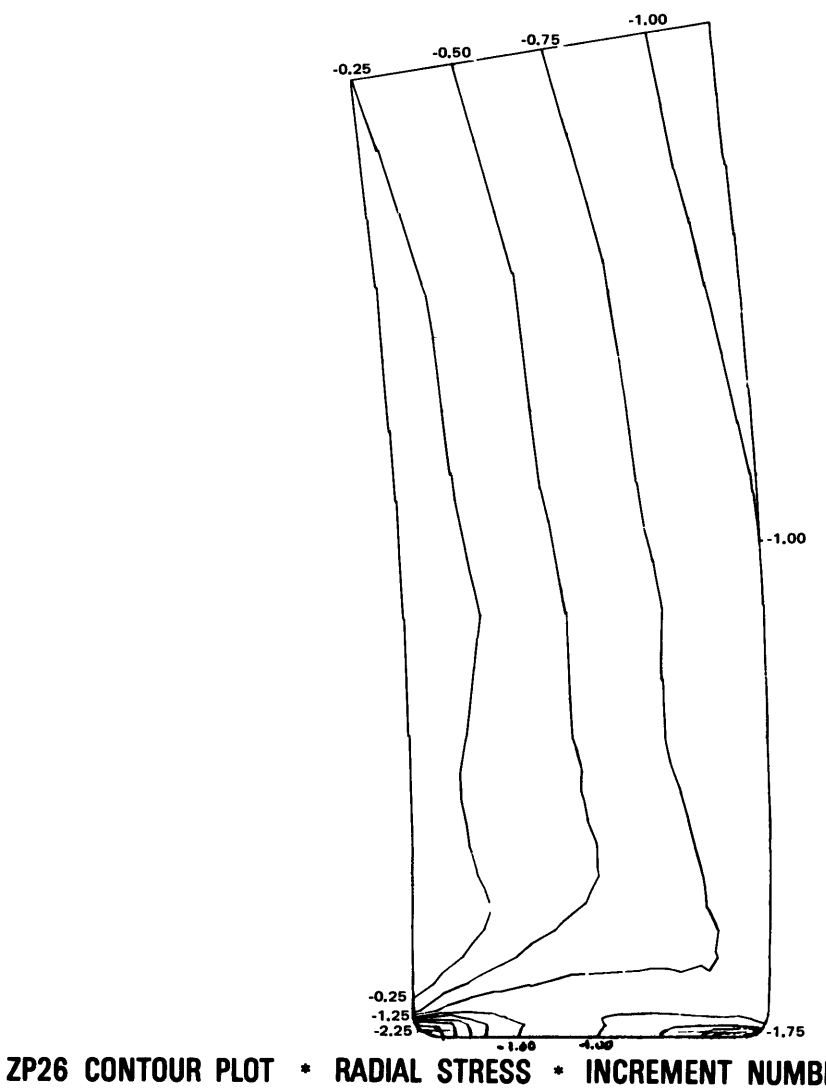

Figure 10e - Mod 1 Radial Stress

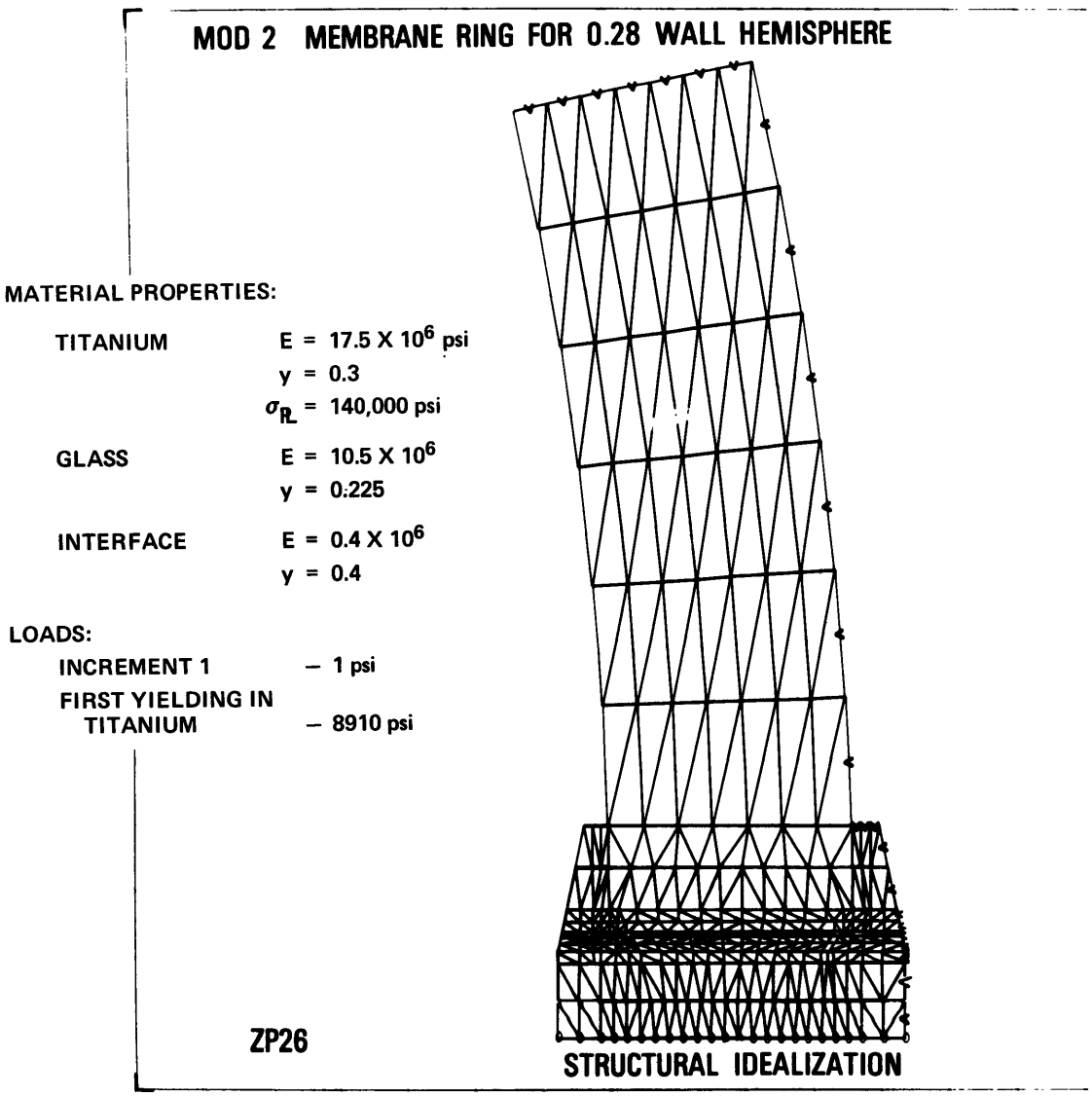

Figure 10f - Mod 2 Structural Idealization

MOD 2 MEMBRANE RING FOR 0.28 WALL HEMISPHERE

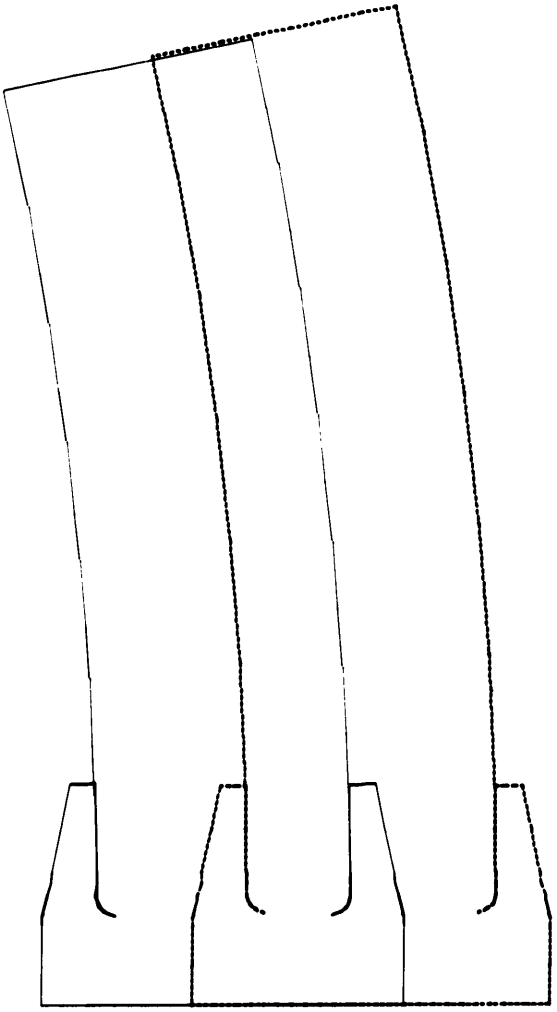

ZP26 DISPLACED STRUCTURE INCREMENT NUMBER 1

Figure 10g - Mod 2 Displaced Structure

MOD 2 MEMBRANE RING FOR 0.28 WALL HEMISPHERE

CONTOUR INTERVAL IS 0.50

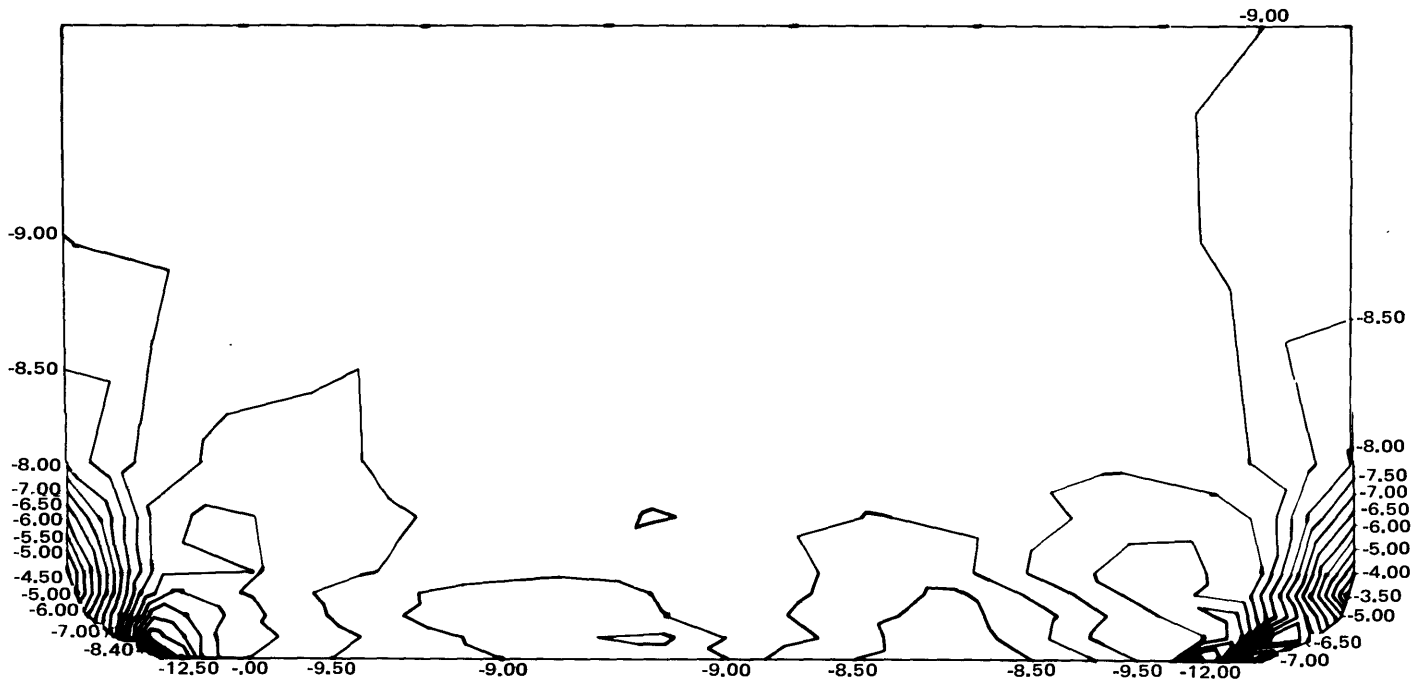

ZP26 CONTOUR PLOT * AXIAL STRESS * INCREMENT NUMBER 1

Figure 10h - Mod 2 Axial Stress

MOD 2 MEMBRANE RING FOR 0.28 WALL HEMISPHERE

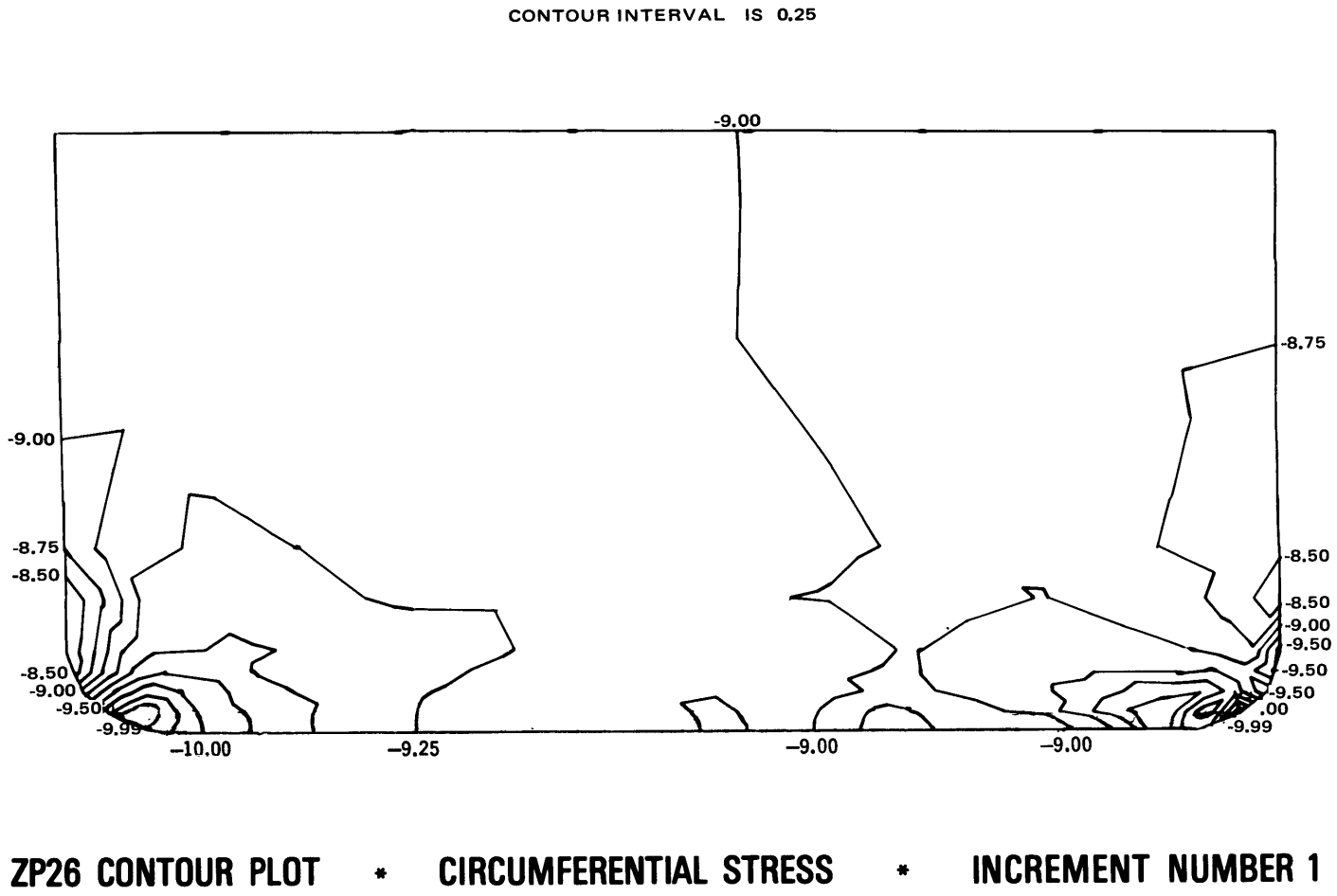

Figure 10j - Mode 2 Circumferential Stress

MOD 2 MEMBRANE RING FOR 0.28 WALL HEMISPHERE

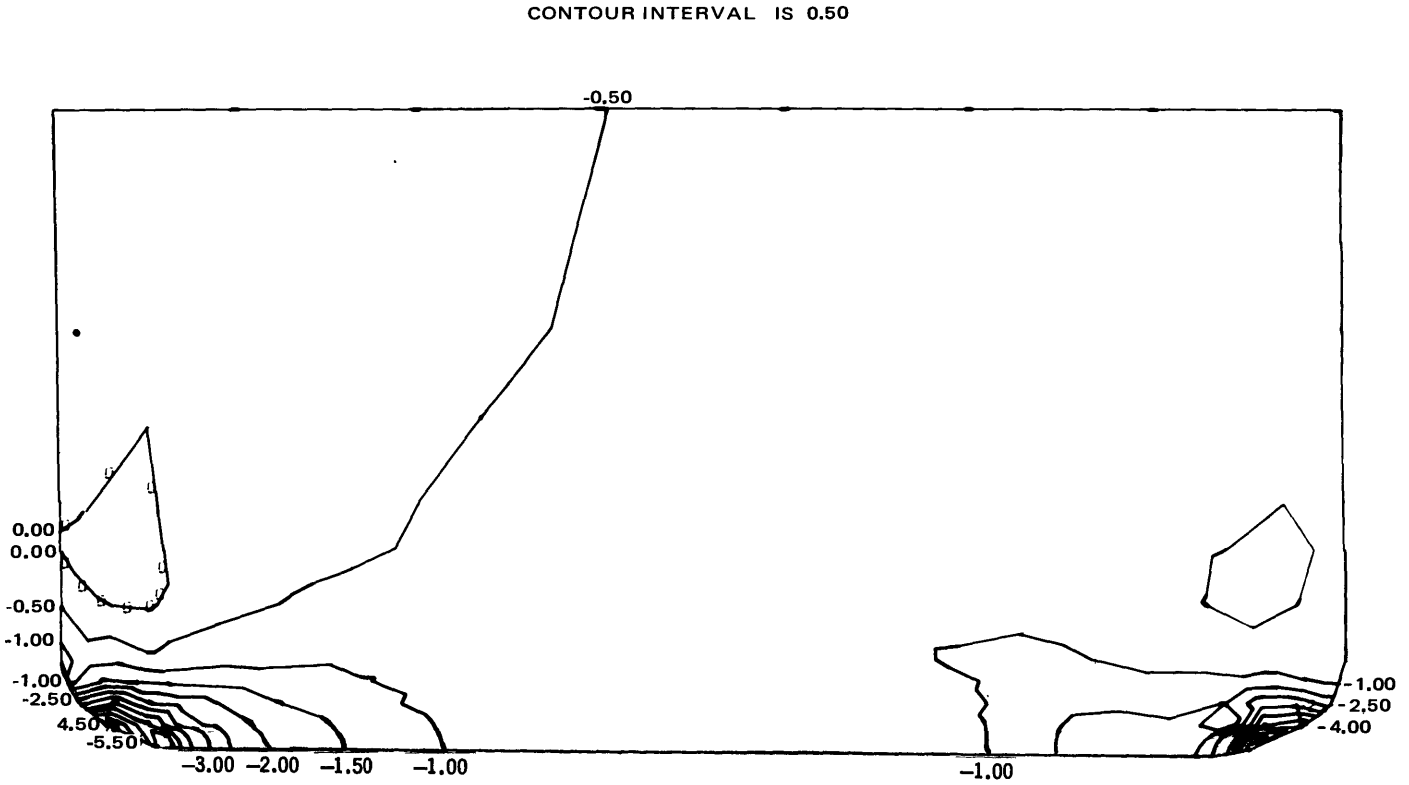

ZP26 CONTOUR PLOT * RADIAL STRESS * INCREMENT NUMBER 1

Figure 10k - Mod 2 Radial Stress

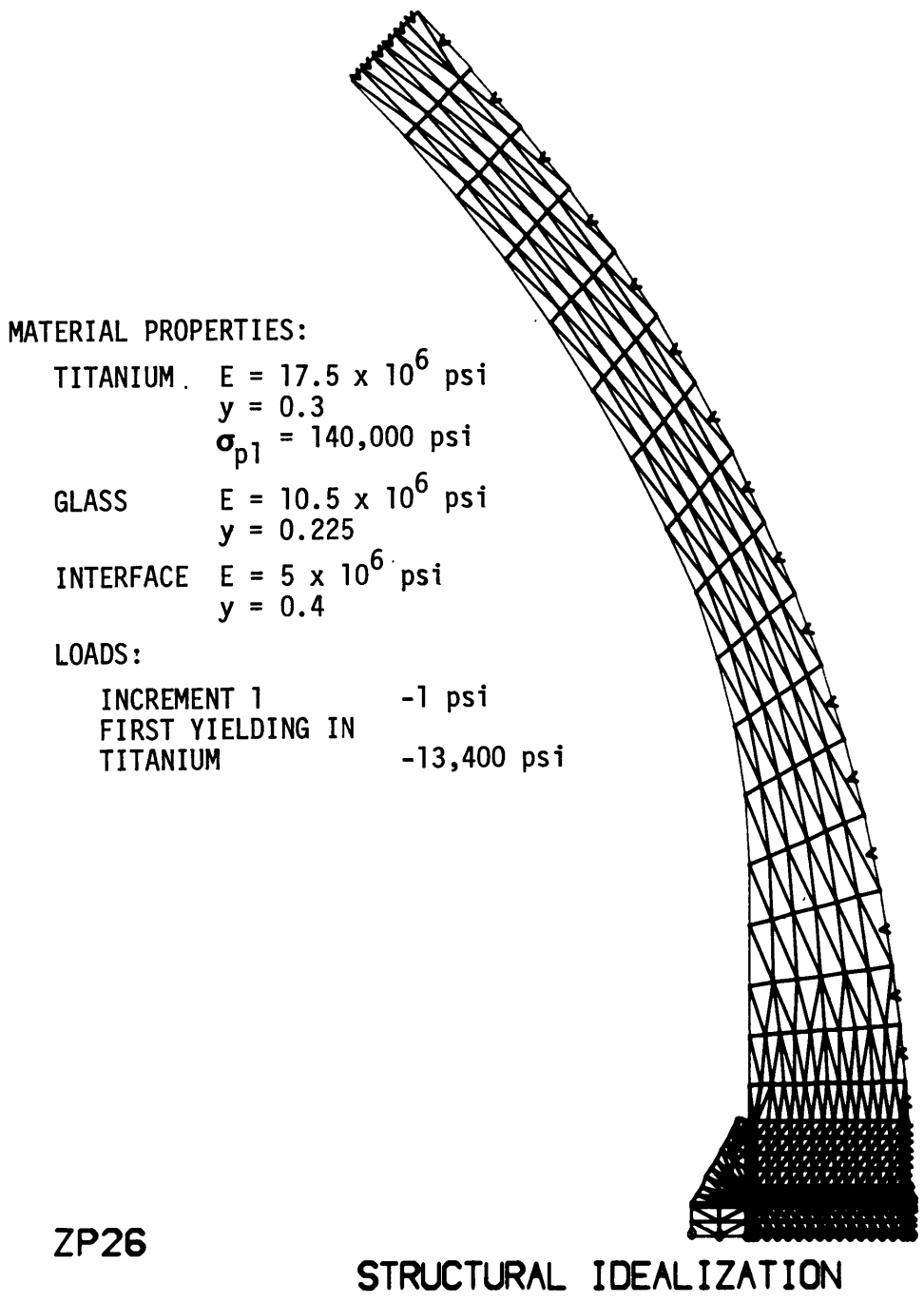

Figure 101 - Internally Reinforced Joint Structural Idealization

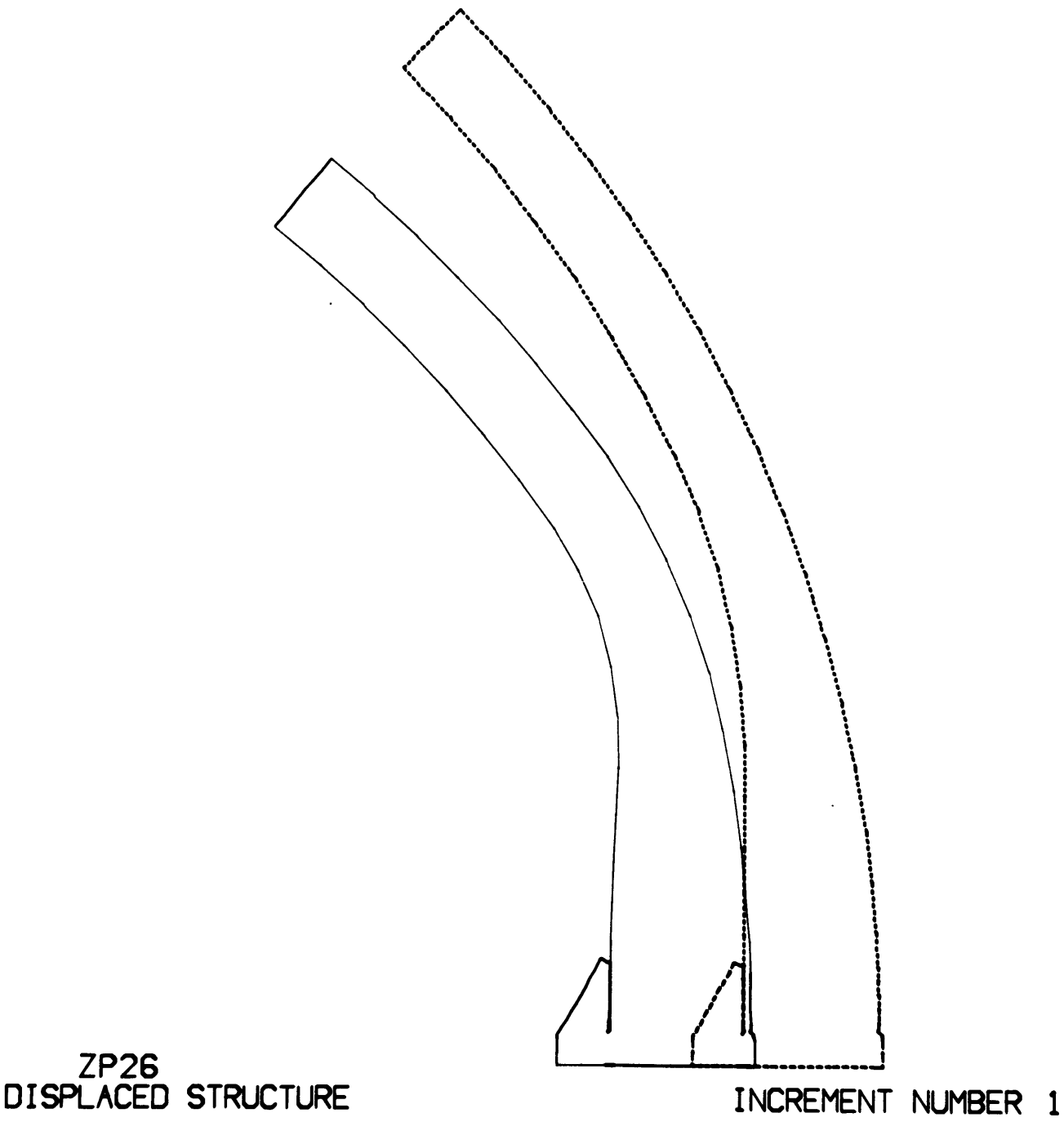

Figure 10m - Internally Reinforced Joint Displaced Structure

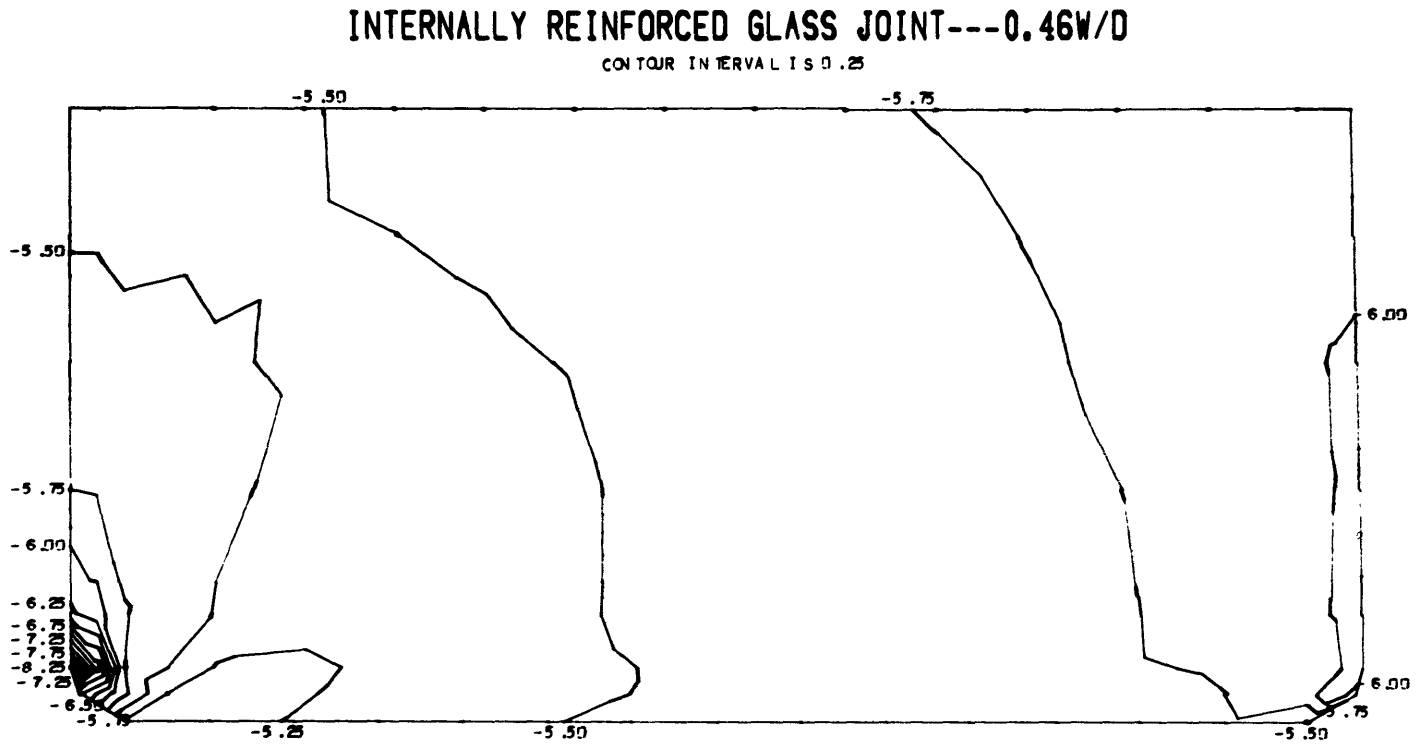

ZP26
CONTOUR PLOT * AXIAL STRESS * INCREMENT NUMBER 1

Figure 10n - Internally Reinforced Joint Axial Stress

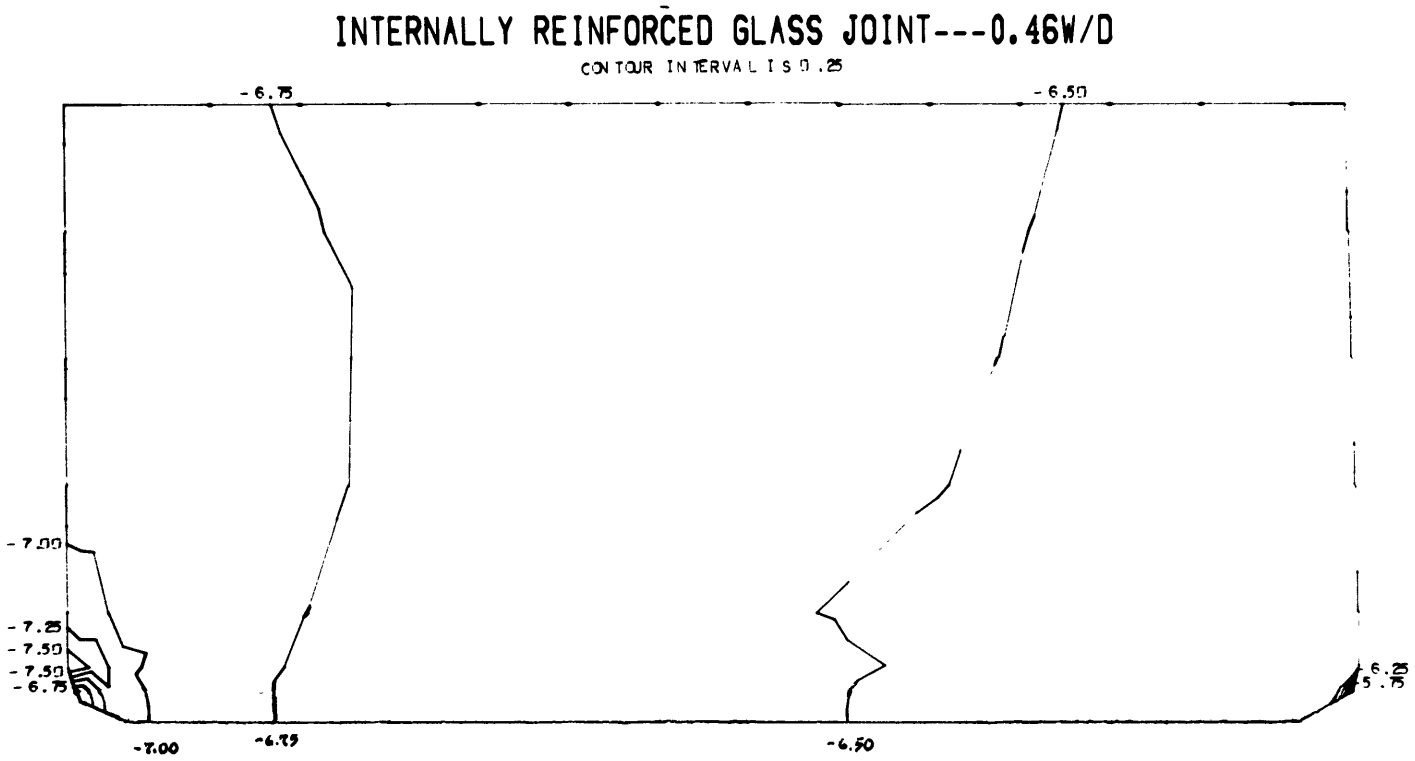

ZP26
CONTOUR PLOT * CIRCUMFERENTIAL STRESS * INCREMENT NUMBER 1

Figure 10p - Internally Reinforced Joint Circumferential Stress

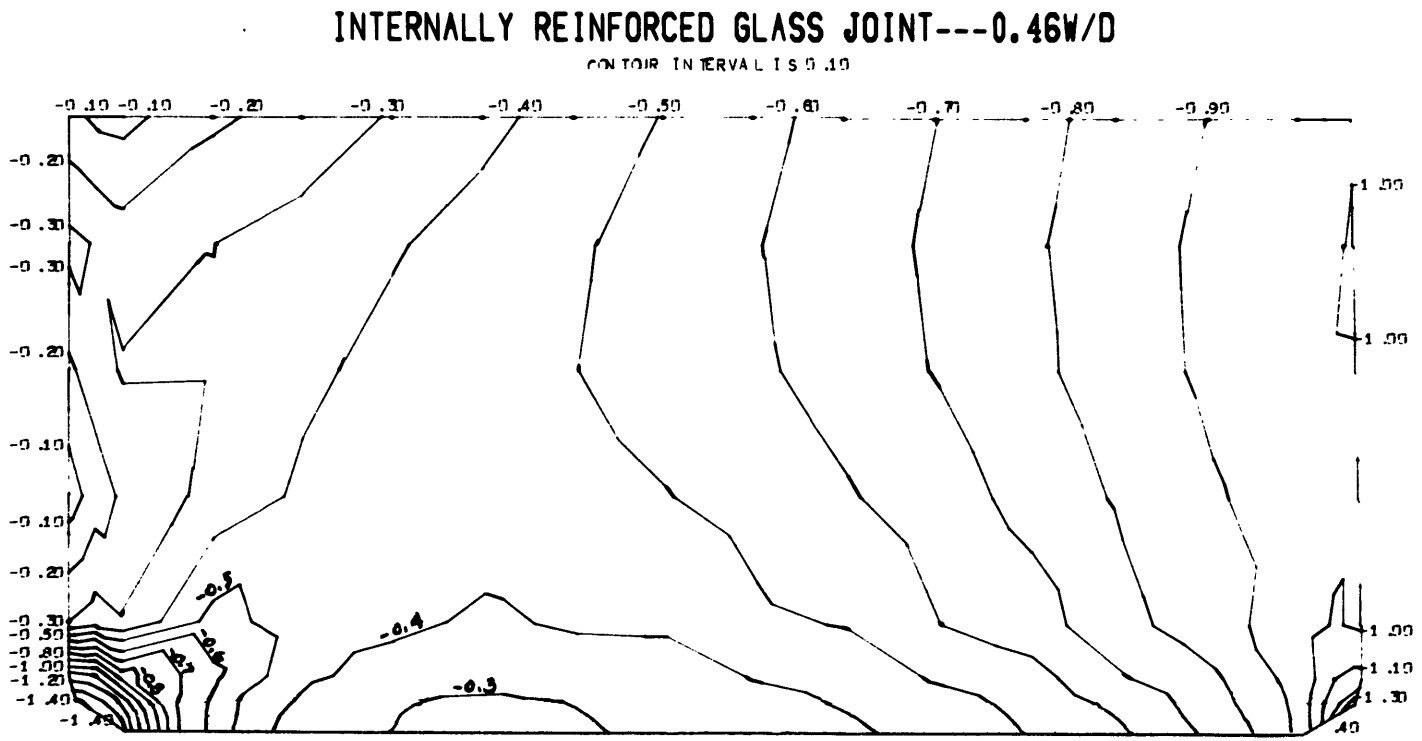

Figure 10q - Internally Reinforced Joint Radial Stress

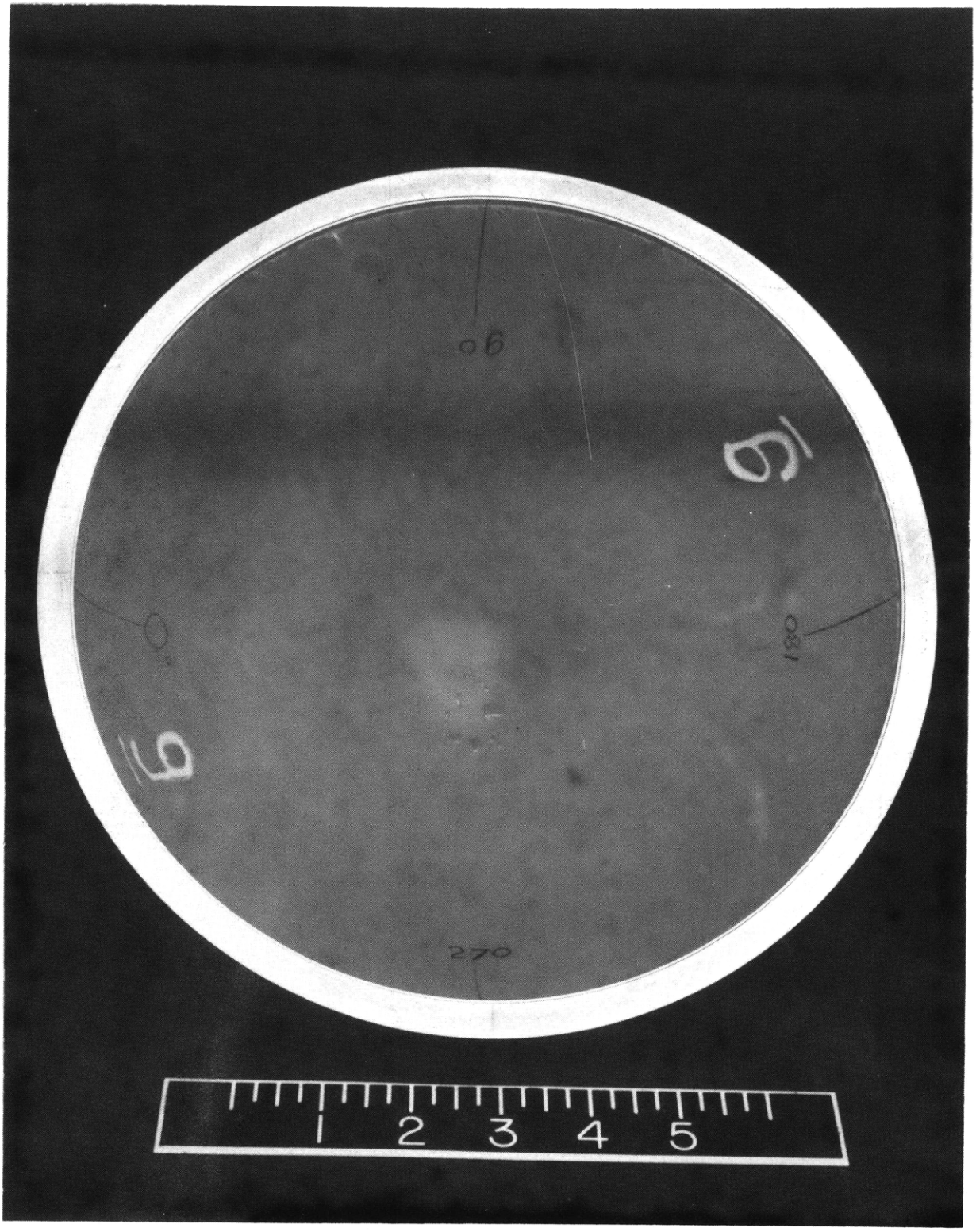

Figure 11 - Glass Hemispherical Shell

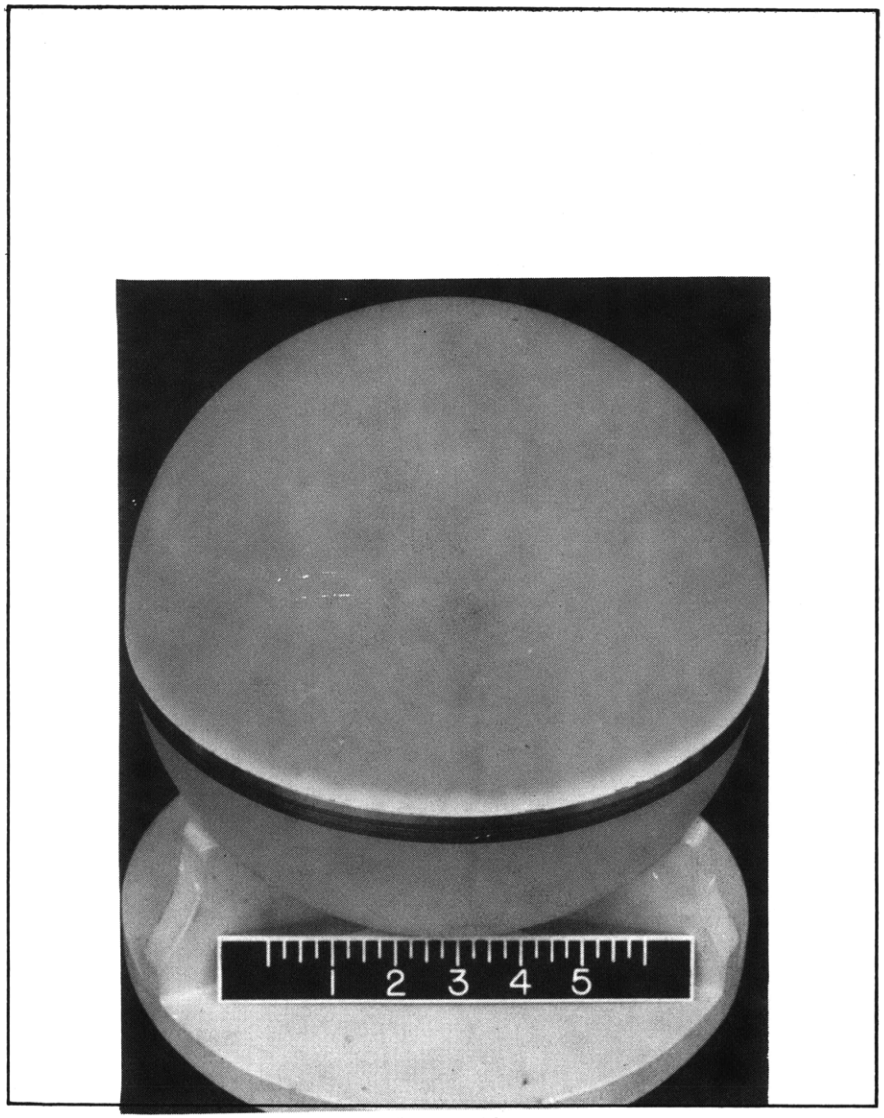

PPG 1578

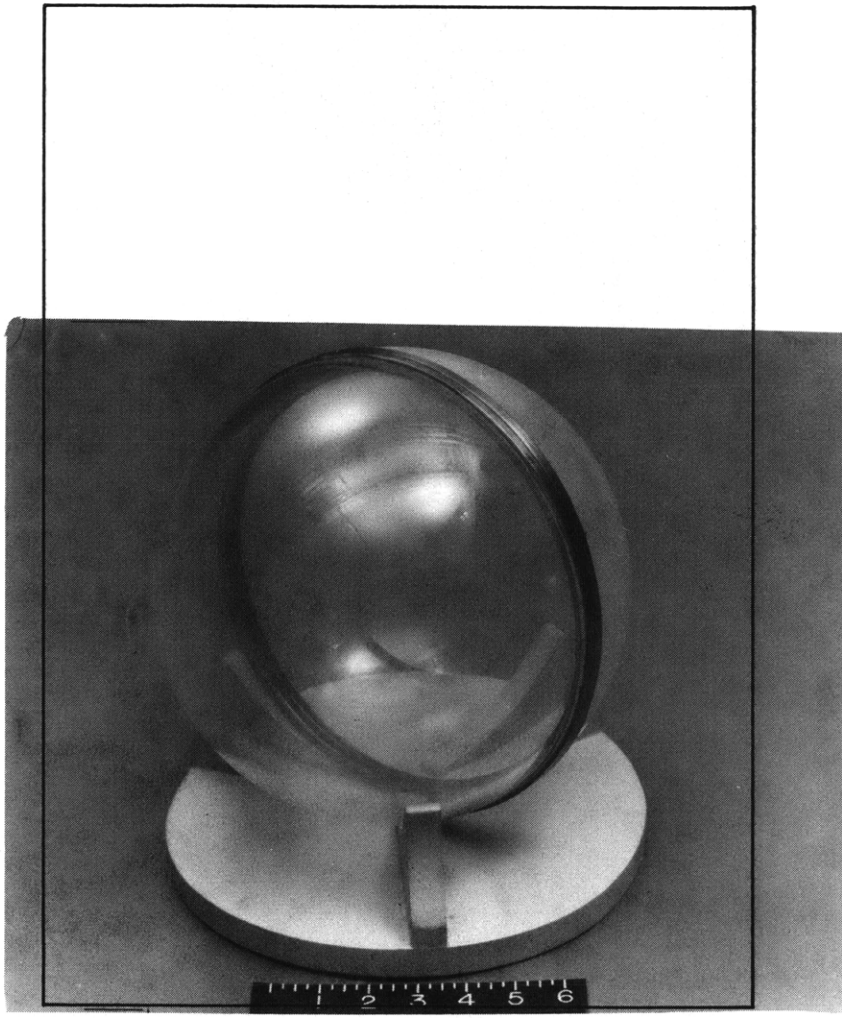

PPG 1080

Figure 12 - Assembled Spheres

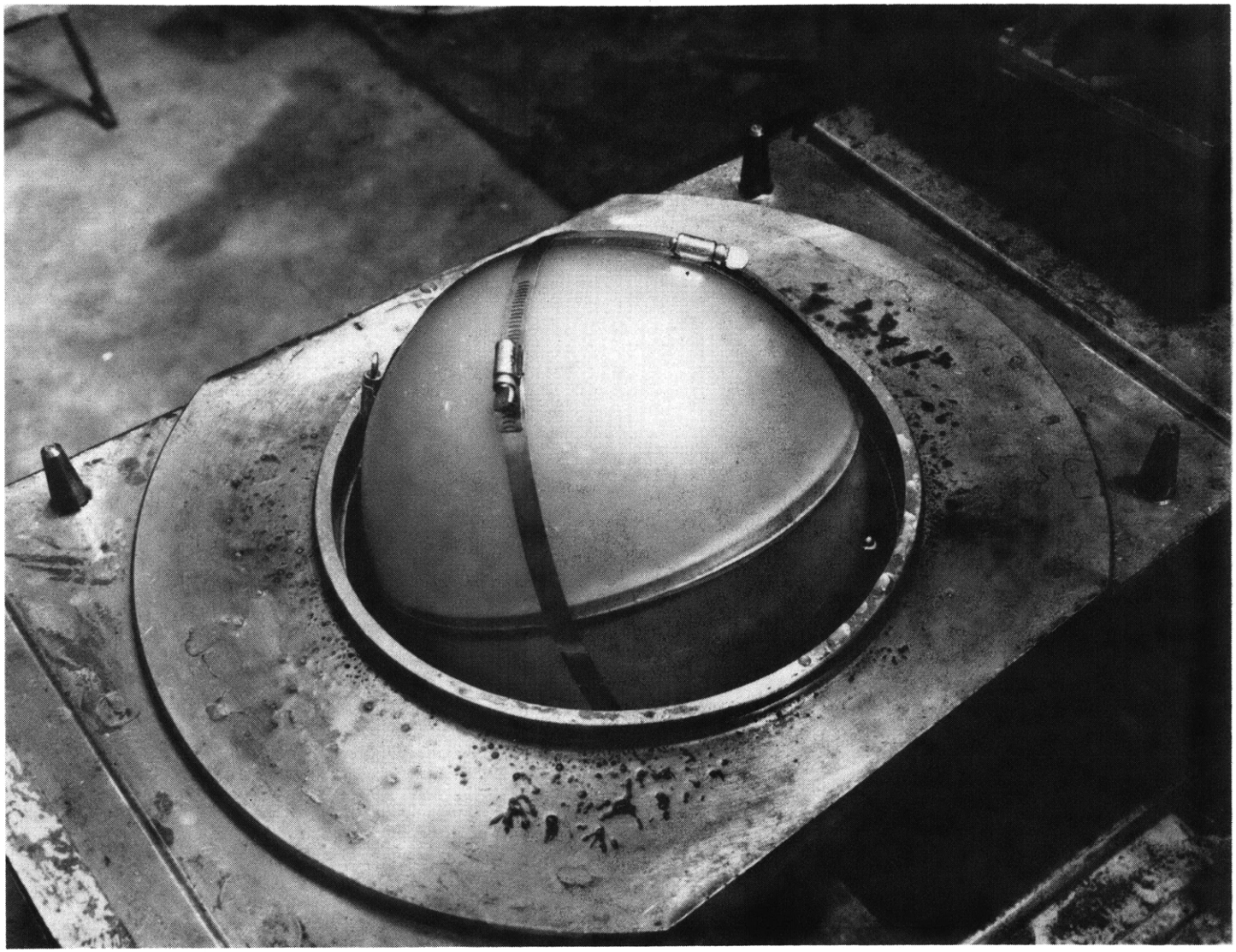

Figure 13 - Model in Test Facility

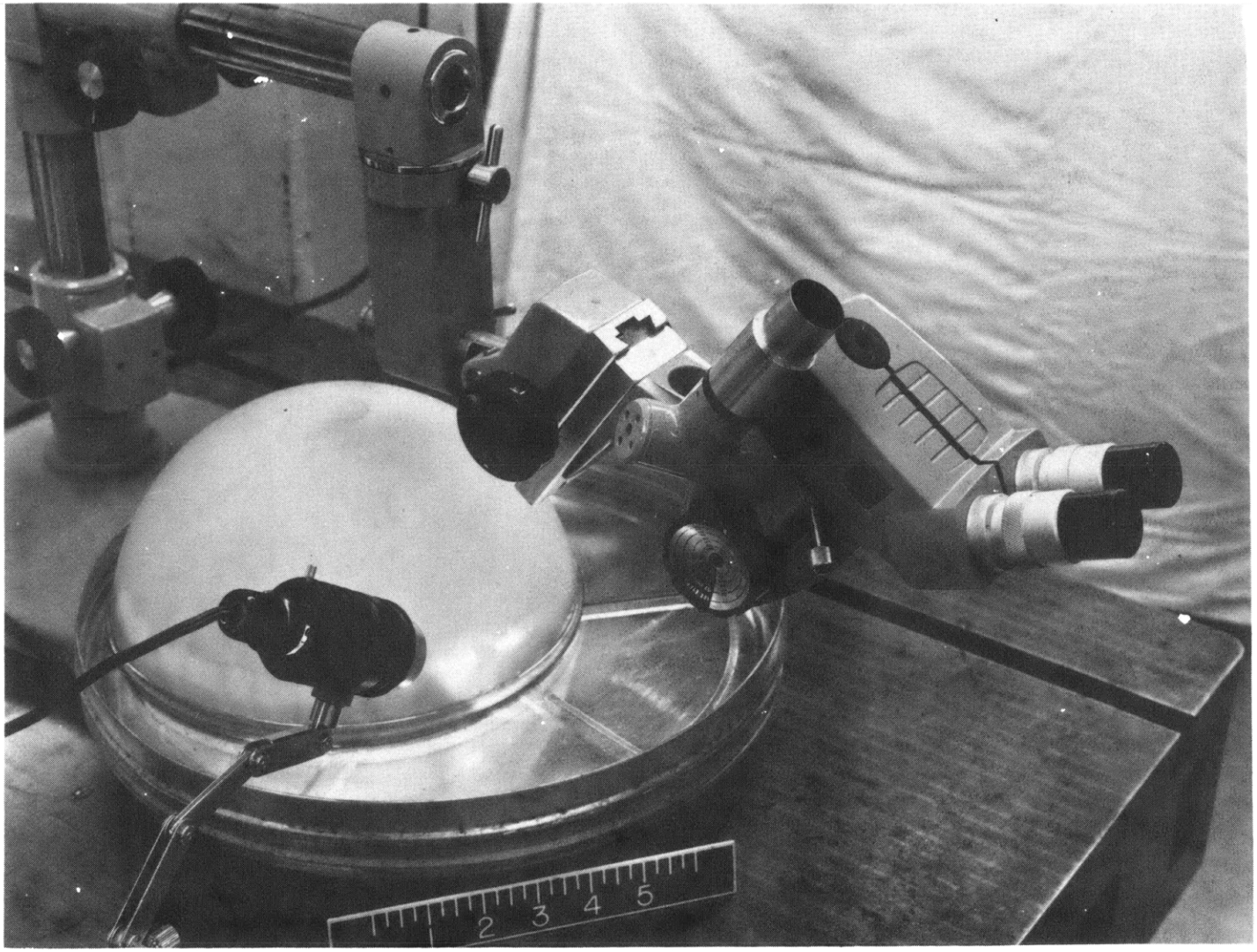

Figure 14 - Inspection Set Up

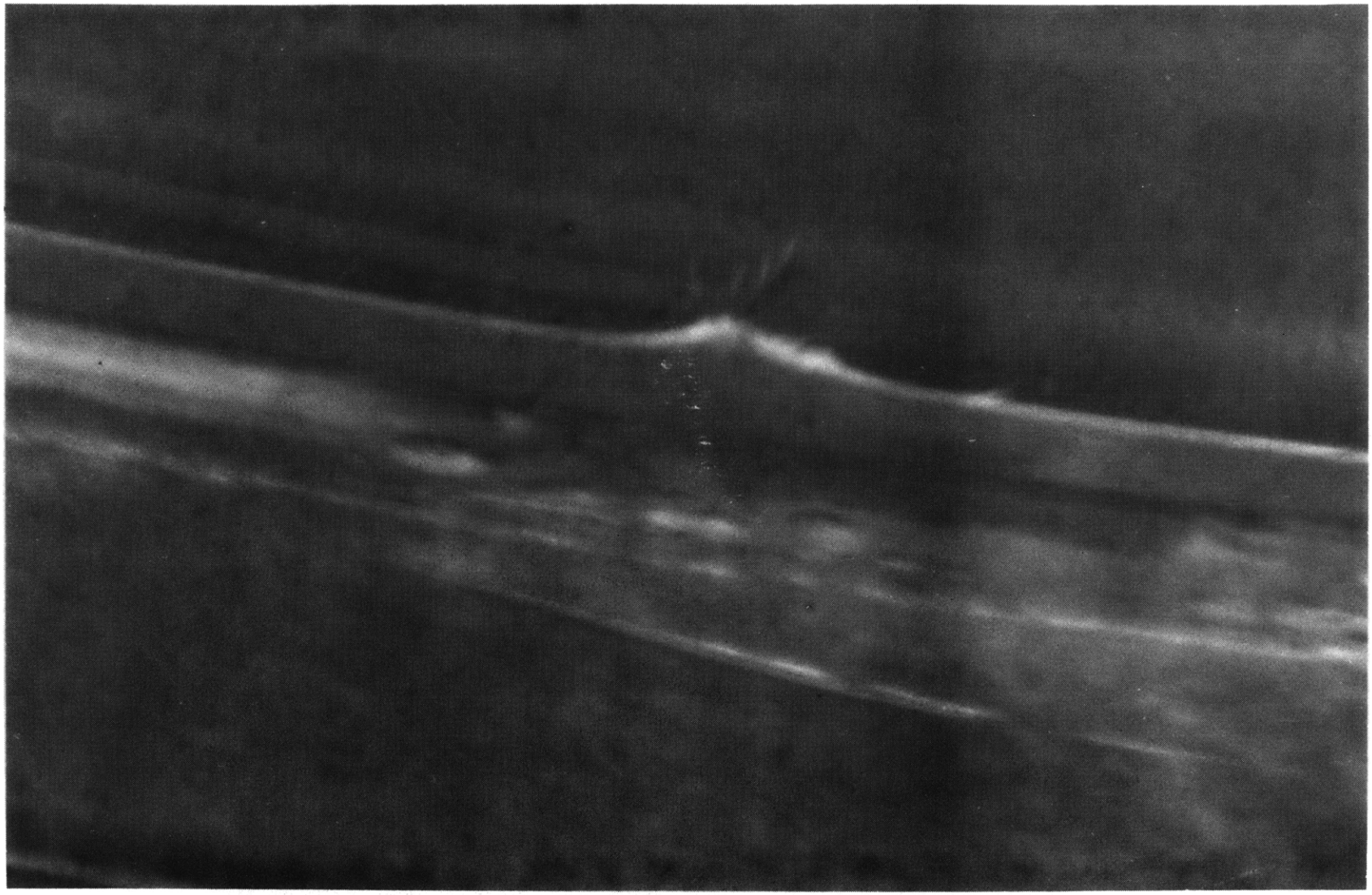

Figure 15 - Fracture on Hemisphere 15 after 100 Cycles to 6500 psi

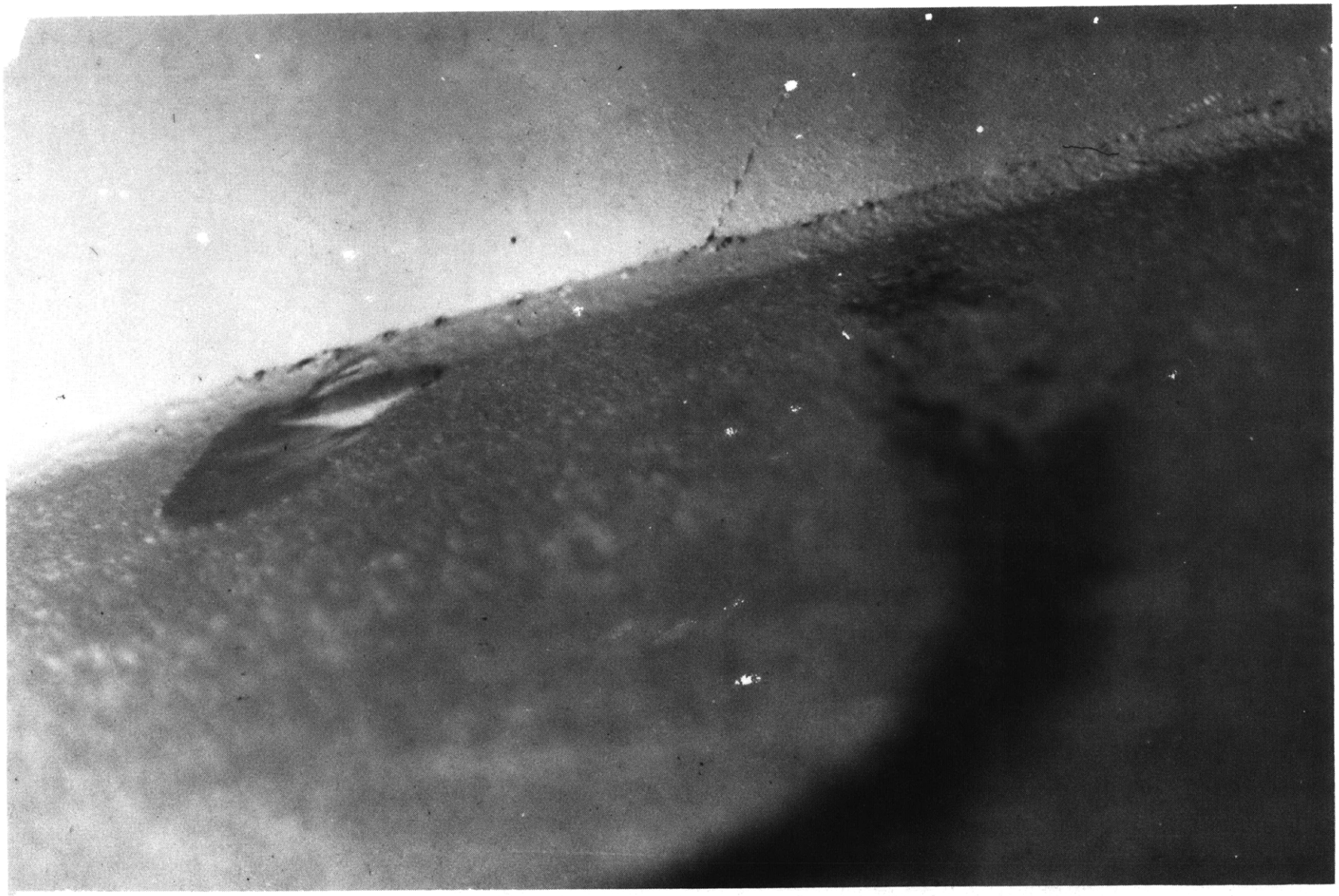

Figure 16 - Inside Edge Chip on Hemisphere 13 after 898 Cycles to 5000 psi

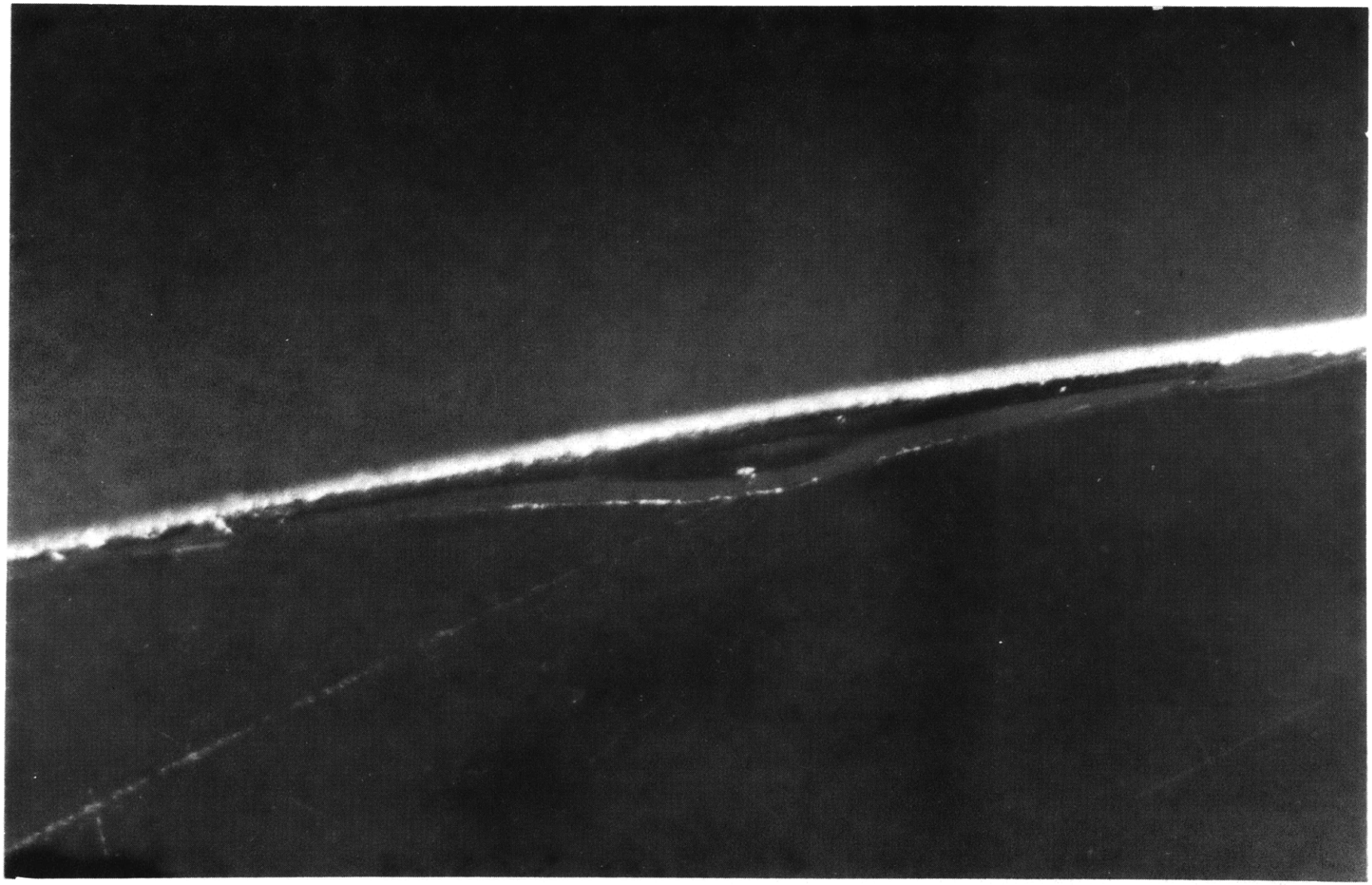

Figure 17 - Outside Edge Spall on Hemisphere 13 after 1048 Cycles to 5000 psi

Figure 18 - Flaw in Hemisphere 3

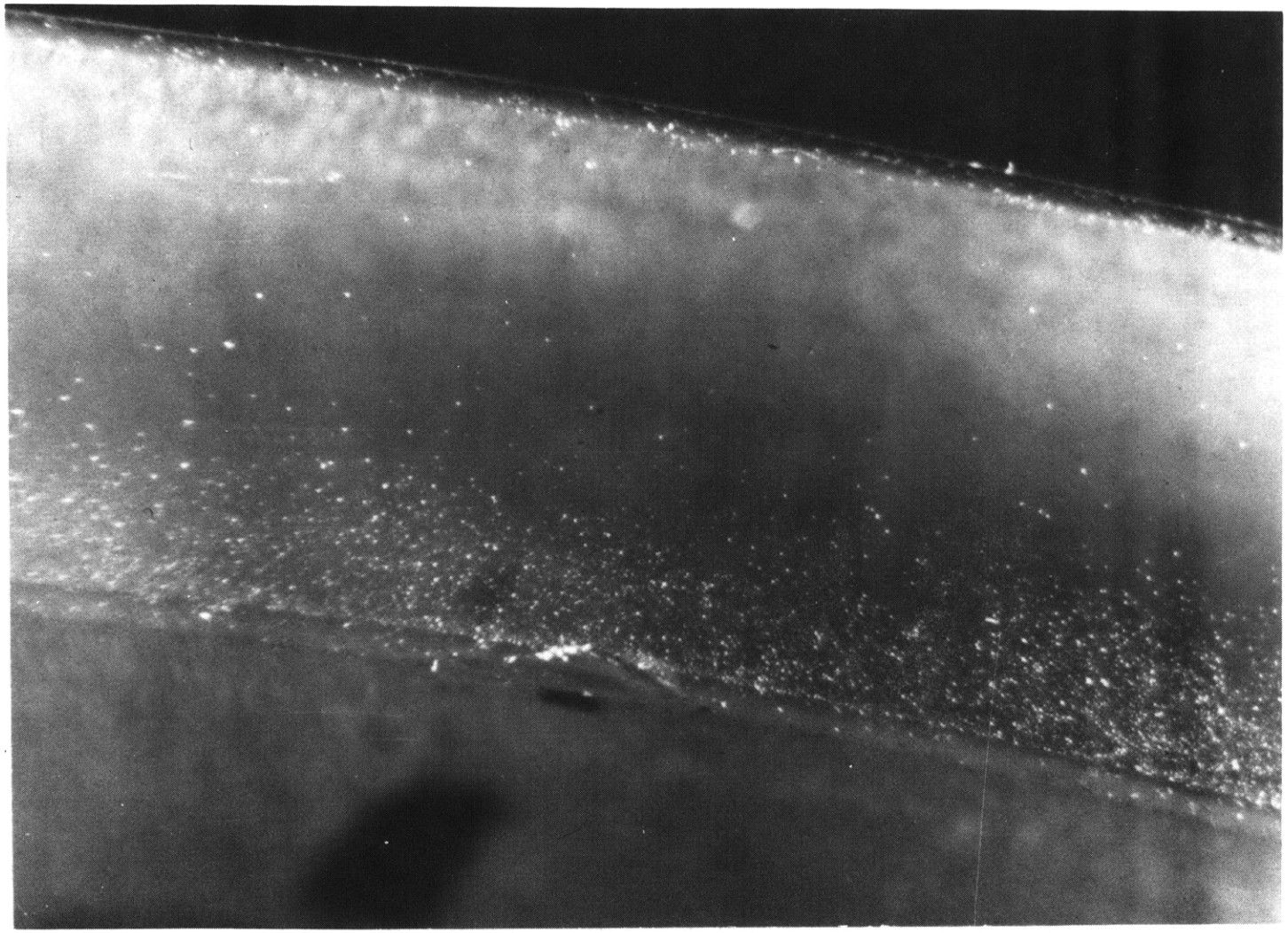

Figure 18a - Check at Inner Edge of Model Before Making Replica

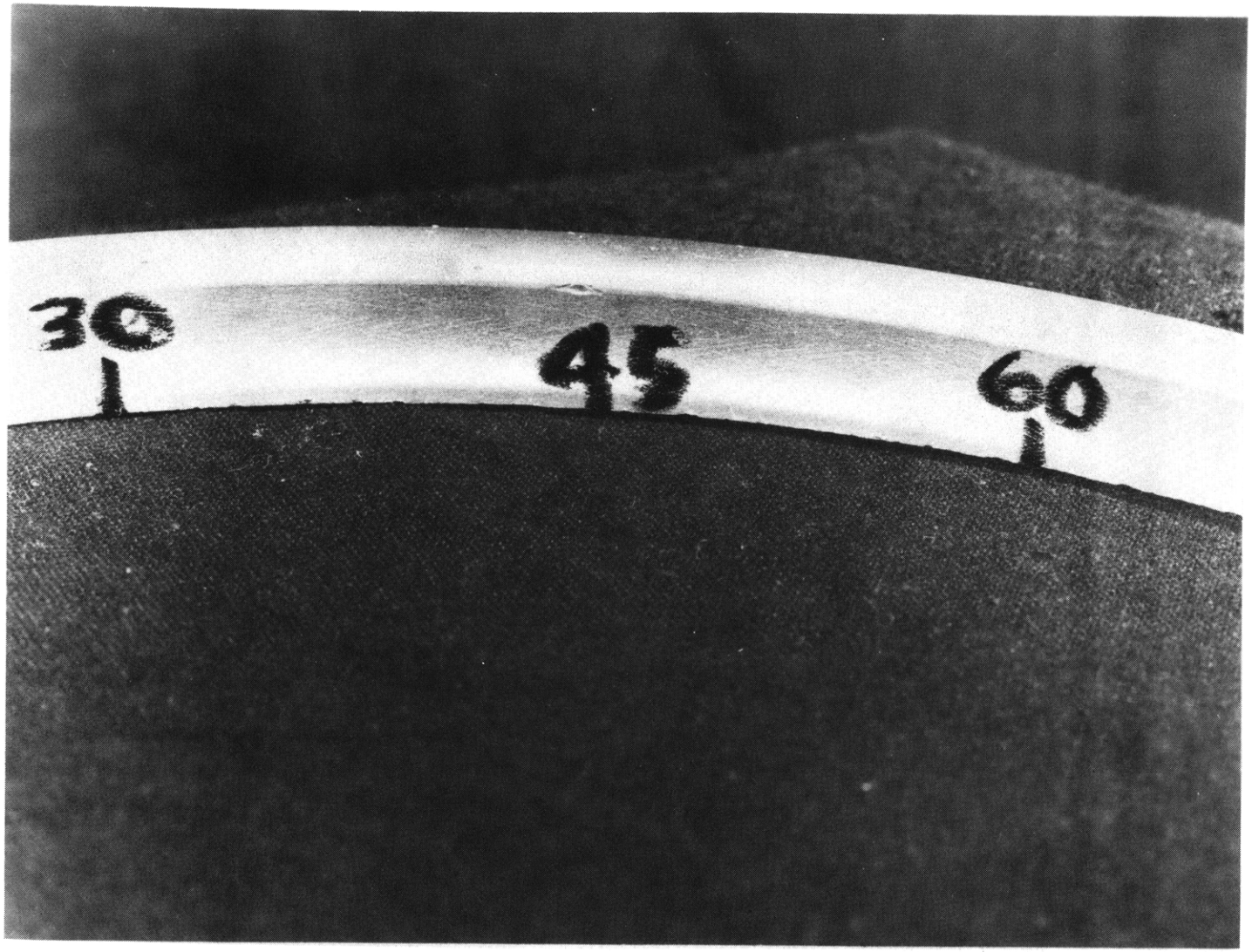

Figure 18b - Inner Edge Spall on Replica

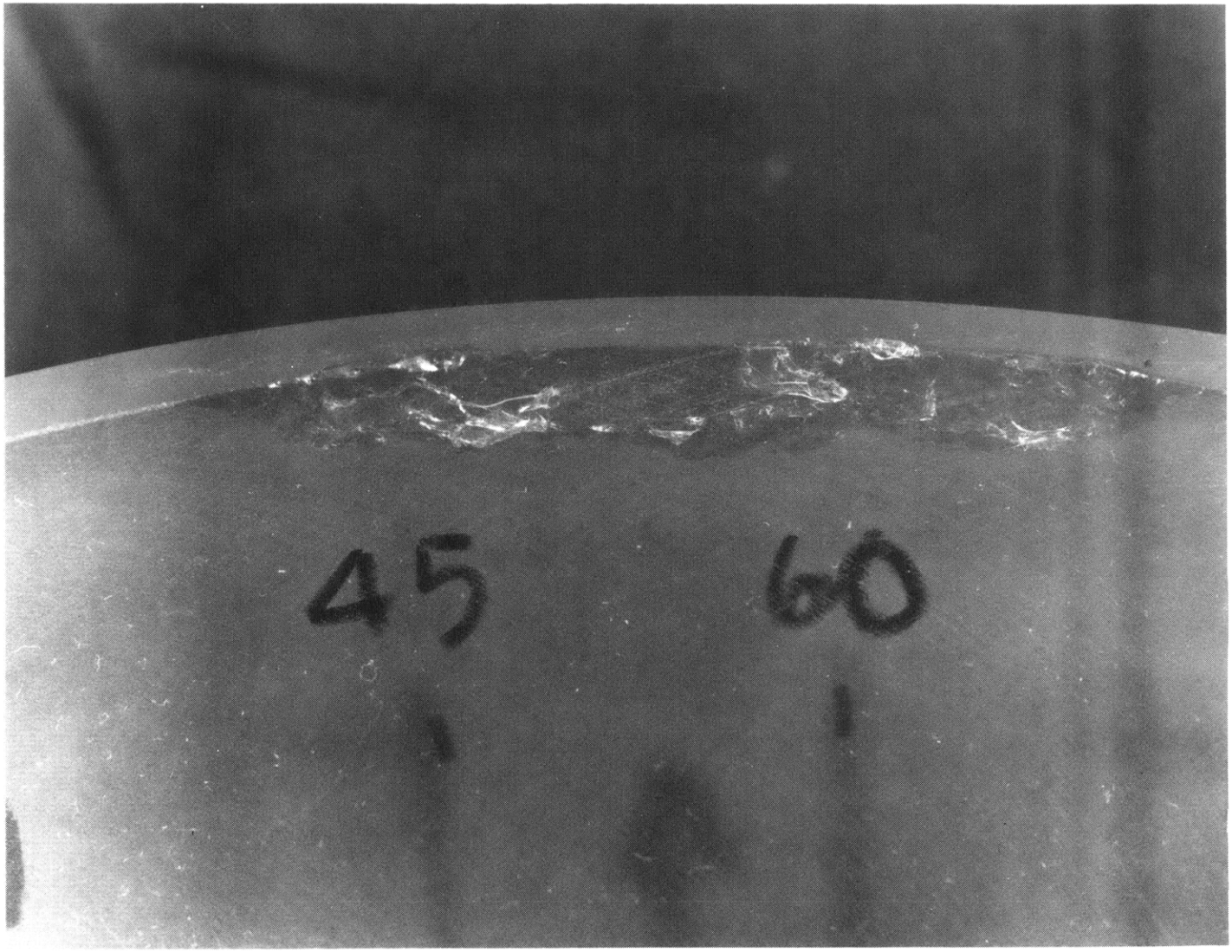

Figure 18c - Model After 3,000 Cycles to 5,000 psi

Figure 19 - Models after Test

Model 19a - HGS-14

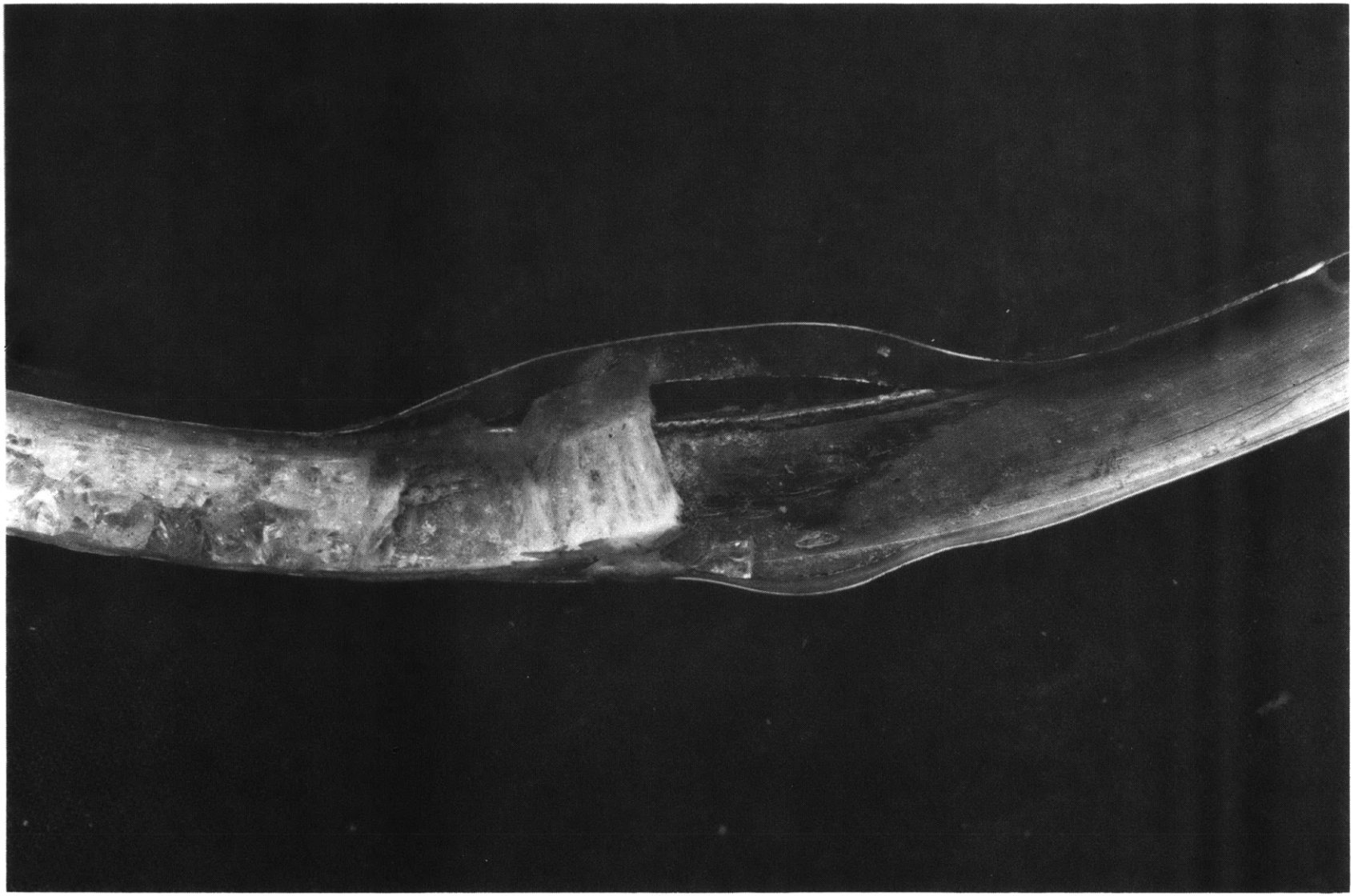

Figure 19b - HGS-17

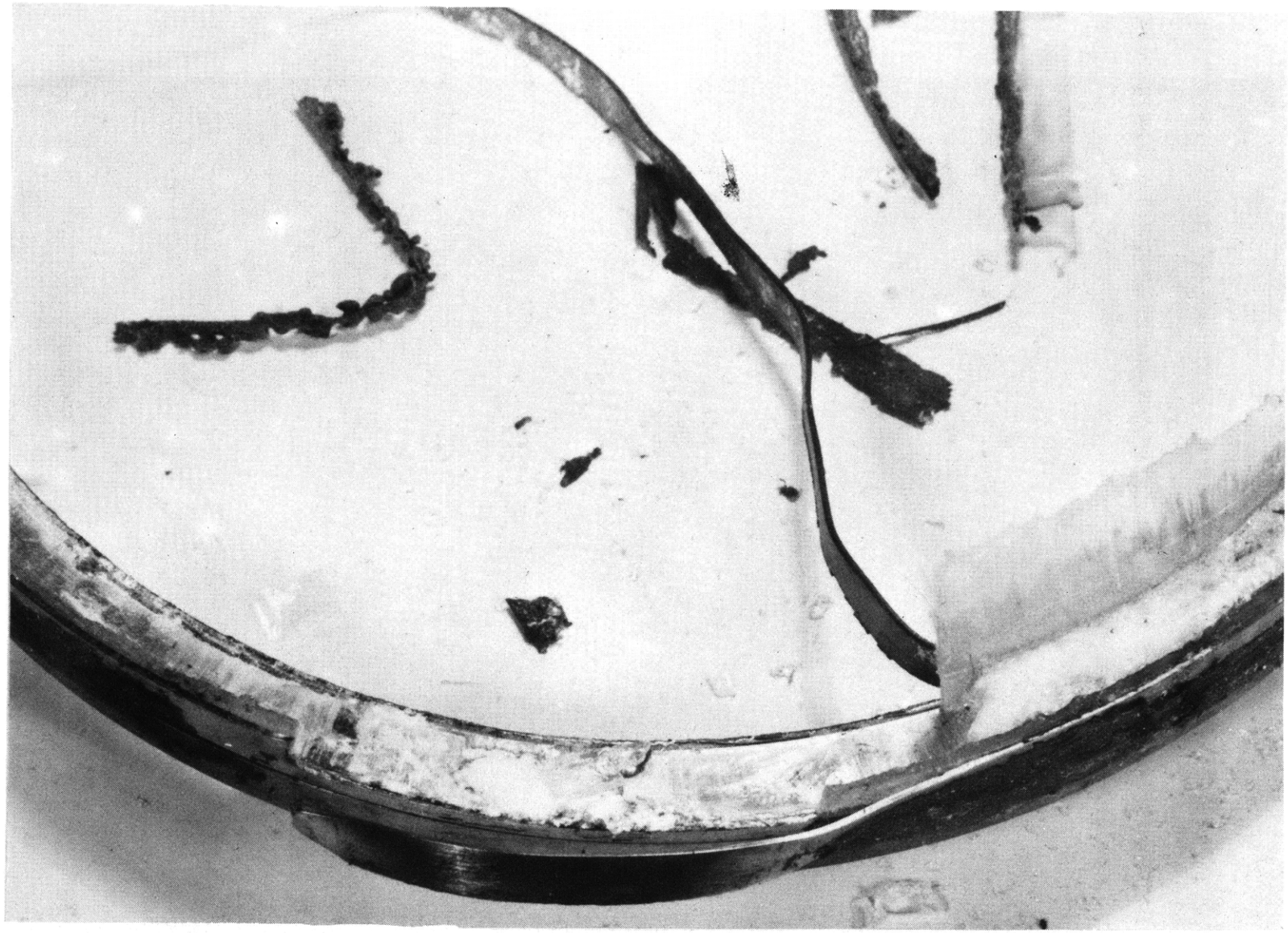

Figure 19c - HGS-3

TABLE 1 - SUMMARY OF GEOMETRIC AND MATERIAL PROPERTIES

TEST CASE NUMBER	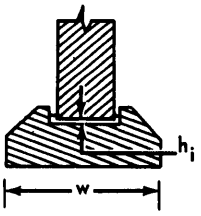 G1	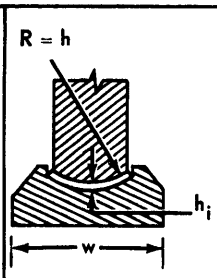 G2	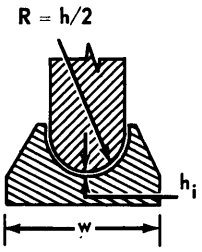 G3	CONSTANTS*
1	$\nu_i = 0.1$	$\nu_i = 0.1$	$\nu_i = 0.1$	$E_i = 5 \times 10^6$ $h_i = 0.010$ $w = 0.58$
2	$\nu_i = 0.3$	$\nu_i = 0.3$	$\nu_i = 0.3$	
3	$\nu_i = 0.45$	$\nu_i = 0.45$	$\nu_i = 0.45$	
4	$E_i = 0.5 \times 10^6$	$E_i = 0.5 \times 10^6$	$E_i = 0.5 \times 10^6$	$\nu_i = 0.30$ $h_i = 0.010$ $w = 0.58$
5	$E_i = 5.0 \times 10^6$	$E_i = 5.0 \times 10^6$	$E_i = 5.0 \times 10^6$	
6	$E_i = 50.0 \times 10^6$	$E_i = 50.0 \times 10^6$	$E_i = 50.0 \times 10^6$	
7	$h_i = 0.010$	$h_i = 0.010$	$h_i = 0.010$	$E_i = 5 \times 10^6$ $\nu_i = 0.30$ $w = 0.58$
8	$h_i = 0.030$	$h_i = 0.040$	$h_i = 0.040$	
8a	$h_i = 0.030$	$h_i = 0.040$	$h_i = 0.040$	$E_i = 0.5 \times 10^6$ $\nu_i = 0.45$ $w = 0.58$
9	$w = 0.40$	$w = 0.40$	$w = 0.40$	$E_i = 5 \times 10^6$ $h_i = 0.010$ $\nu_i = 0.30$
9a	$w = 0.40$	$w = 0.40$	$w = 0.40$	STEEL RING $E_R = 30 \times 10^6$

*UNLESS OTHERWISE INDICATED RING IS OF TITANIUM WITH $E_R = 15 \times 10^6$ AND $\nu_R = 0.3$

TABLE 2 - TEST RESULTS OF 0.28 IN. WALL--10-INCH-DIAMETER SURFACE COMPRESSED GLASS HEMISPHERES

PPG CODE 1578 GLASS[1]						
HEMI NO	ASSEMBLY NUMBER AND JOINT TYPE[3]	NUMBER OF CYCLES[2] SURVIVED AT				
		2500 psi σ_{AVG} = 23,000	3750 psi σ_{AVG} = 34,500	5000 psi σ_{AVG} = 45,900	6500 psi σ_{AVG} = 59,600	7700 psi σ_{AVG} = 70,600
4	HGS-10				3100	380 Collapsed
7	MOD-2				3100	380 Collapsed
9	HGS-11				100 No Damage	
15	MOD-2				100 Crack	
9	HGS-11a			3000	1494 Collapsed	
2	MOD-2			3000	1494 Collapsed	
13	HGS-12			898 Inside Edge Chip		
14	MOD-1			898 No Damage		
11	HGS-12a			3000	1342 Collapsed	
14	MOD-1			3000	1342 Collapsed	
18	HGS-13			3000	692 Crack	
19	MOD-1			3000	692 Crack	
1	HGS-14	3000	3000	3100	2000	30 Collapsed
12	MOD-2	3000	3000	3100	2000	30 Collapsed
16	HGS-15	3000	3000	3000	1500	
17	MOD-2	3000	3000	3000	1500	
3	HGS-16	3000	3000	3000 Crack		
5	MOD-1	3000	3000	3000 No Damage		
6	HGS-17	3000	3100	3000	2000	30 Collapsed
8	MOD-2	3000	3100	3000	2000	30 Collapsed
CORNING CHEMCOR 0313 GLASS						
6	CH-1			218 No Damage		
24	MOD-1			218 Collapsed		

1. Chemically strengthened in sodium salt bath. Surfaces of glass have residual compression stress of approximately 60,000 psi for 1578 models and 35,000 psi for 0313 models.
2. All tests were conducted in fresh water at a rate of approximately 1 cycle per minute.
3. See Figure 4 for joint geometry.

TABLE 3 - TEST RESULTS OF 10-INCH-DIAMETER 0.36 WALL PPG 1080 K+ SURFACE COMPRESSED GLASS HEMISPHERES

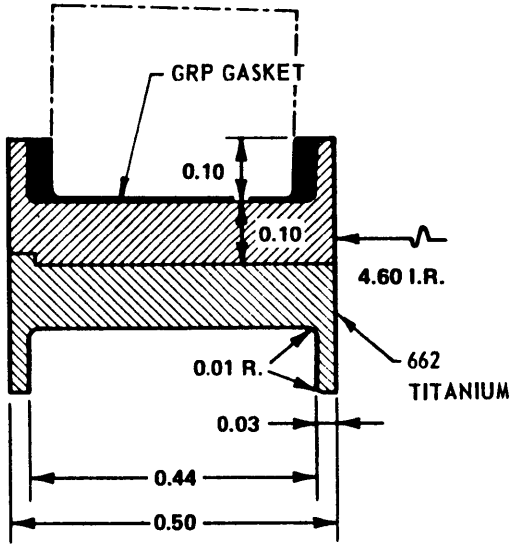

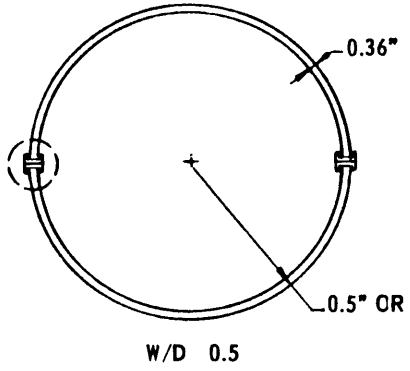

Model No.	Hemi No.	Number of Cycles Survived at 14,600 Ft σ_{Avg} = 46,900 psi	17,500 Ft σ_{Avg} = 55,400 psi	20,000 Ft σ_{Avg} = 64,200 psi	22,500 Ft σ_{Avg} = 72,100 psi	25,000 Ft σ_{Avg} = 74,900 psi	27,500 Ft σ_{Avg} = 87,700 psi	30,000 Ft σ_{Avg} = 96,500 psi
HGS 4	52*	2000	3000	3000	3000	1000	500	1
	99	2000	3000	3000	3000	1000	500	1
HGS 5	28	2000	3000	3000	3000	3000	2000	4
	33	2000	3000	3000	3000	3000	2000	Collapsed 4
HGS 6	64	2000	3000	3000	3000	1000	500	1
	104	2000	3000	3000	3000	1000	500	1
HGS 7	52*	2000	3000	3000	3700	1000	500	1
	55	2000	3000	3000	3700	1000	500	1
HGS 8**	1	2000	3000	3000				1
	3	2000	3000	3000				1

*Used twice.

**Hemispheres were ground and polished over entire surface. Thickness was about 0.02 in. less than unpolished models.

TABLE 4 - TEST RESULTS OF 10-INCH-DIAMETER VARIABLE WALL PPG 1578
SURFACE COMPRESSED GLASS HEMISPHERES

Assembly	Hemi No.	Number of Cycles Survived at						
		6500 psi σ_{Avg} = 38,000	7700 psi σ_{Avg} = 43,000	8900 psi σ_{Avg} = 50,000	10,000 psi σ_{Avg} = 56,000	11,100 psi σ_{Avg} = 62,000	12,200 psi σ_{Avg} = 68,000	13,400 psi σ_{Avg} = 75,000
HGS-20	7	2000	3000	3000	3000	2000	1000	1000
	9	2000	3000	3000	3000	2000	1000	1000
HGS-21	1	2000		300 Collapsed				
	3	3000		300 Collapsed				
HGS-22	2	1532 Collapsed						
	4	1532 Collapsed						

APPENDIX

BACKGROUND ON GLASS AND CERAMIC SPHERICAL SHELLS

Numerous tests had been conducted prior to initiation of the DOT massive glass effort. A number of these studies will be discussed with emphasis on those conducted at the Center.

SPHERICAL SHELLS FOR BUOYANCY SPHERES

Although the pressure hull of a deep submergence vehicle may be positively buoyant, the complete vehicle is usually not because of instruments, machinery and outer structure weight. The approach taken to provide positive buoyancy is to surround the structure with syntactic foam, a composite of glass microballoons in a plastic matrix. Until recently the best foam available for 20,000 feet had a density on the order of 42 pounds per cubic feet. As a possible alternative, glass and alumina spherical shells were investigated at the Center in the Search Vehicle program of DSSP. At the time these studies were to be undertaken two of the more promising production techniques for buoyancy spheres were Corning Glass Work's fusion sealing of annealed Pyrex glass hemispheres and Coors Procelain Company's casting method for monolithic alumina spheres.

The glass spherical shells investigated were 10 inch diameter by 0.28 wall Corning Code 7740 annealed Pyrex glass. This glass has a Young's modulus of approximately 9.1×10^6 psi, Poisson's ratio of 0.2, and a density of 139 $lb/ft.^3$ The W/D ratio of the glass spheres were 0.36. The spheres are formed by butting together two hemispherical shells, heating the area of the glass joint, and passing an electric arc across the butt joint to make a fusion weld. Through the period between 1964 and 1968, nearly 100 model tests were conducted to observe static and cyclic performance of fusion welded spheres. Kiernan[1] conducted collapse tests of 18 models. The results are shown in Figure 20. Subsequently tests[15] were

---

[15]Nishida, K., "Static and Cyclic Fatigue Tests of Fusion Sealed Pyrex Glass Spheres," David Taylor Model Basin Report 2246 (Sep 1966).

conducted to study effects of loading rate, pressure medium, and sealing technique on short term static strength. These results are shown in Tables 5 and 6 and also in Figure 20. In addition to static tests, 10 models were tested under cyclic conditions. The results are shown in Table 7. The interesting points of the data are:

1. There was no apparent effect of loading rate on collapse strength when tests were conducted in simulated sea water at three rates of compressive stress. Nine spheres were each tested at rates of 140,000, 3500, and 200 psi/min. The average collapse strengths were 31,700, 31,600, and 32,500 feet.

2. No appreciable difference in collapse strength was obtained when simulated sea water and oil were used as pressure medium. The average collapse strength for 9 models in sea water was 31,600 feet and for 9 models in oil was 34,000 feet.

3. The static strength of fusion sealed annealed glass spheres is dependent on sealing technique. Three sets of glass spheres gave average collapse depths of 32,000 feet, 38,000 feet, and 47,000 feet. The early models tested were characterized by large internal beads at the fusion sealed seam. This was subsequently improved with some modification in the manufacturing procedure. Figure 21 shows the difference in the weld seams before and after the change.

4. The 10 spheres tested cyclically survived 5000 cycles 22,500 feet. One sphere may have suffered fatigue damage after 3000 cycles at the fusion welded seam. Each sphere had been proof tested to 30,000 feet prior to cycling. Five spheres including the damaged one were collapsed after cycling. In each case the collapse pressure was considerably higher than the initial proof pressure.

In addition to the data of 0.28 wall models, 6 collapse tests were conducted on 10-in.-diameter 0.36 wall fusion sealed spheres. The results are summarized in Table 8. The empirical elastic buckling pressure for this geometry is about 40,000 psi. The 6 models failed at pressures significantly below this and thus, it is concluded that all failed by stress induced conditions. All of these models were sealed with the early technique. No data was generated with the modified sealing process.

Two 44 inch diameter fusion sealed annealed Pyrex glass spheres were tested[16] as a part of the evaluation of fusion sealed seams. These two tests were preceded by a series of static tests on 10 inch diameter versions. Nominal model dimensions for the 10 and 44 inch models are shown in Figure 22. A summary of the results of the five 10 inch models is shown in Table 9. Note that the experimental collapse pressures were within 10 percent of the calculated values based on near perfect geometry. The excellent results obtained in these tests are attributed to the quality of the fusion sealed seam. The thinner shell wall (0.23 against 0.28 for unpenetrated uniform wall models) and the fact that air pressure was applied inside the model through the penetration made it possible to obtain a better fusion sealed seam. Physically this resulted in a zone much more uniform than those observed for the 0.28 wall spheres.

The fusion sealed seams of the 10 inch models were not representative of the 44 inch models. The two 44 inch models had sharp notches at the inner surface of the fusion sealed seam. In the case of Model 44-1 this caused a reduction in wall thickness of nearly 50 percent at the base of the notch.

The two 44 in. glass spheres were hydrostatically tested in the Center's 4 ft 15,000 psi high pressure test facility. A photograph of a model being lowered in the test facility is shown in Figure 23. The tests were conducted in fresh water. In the case of Model 44-1 a hydrostatic pressure of 3500 psi was applied at which point sharp cracking sounds were audible from distances fairly remote to the test facility. The strain gages in the area of the fusion sealed seam also indicated a sharp change in strain. Typical examples of this behavior are shown in Figure 24. The test was terminated at this point and pressure was slowly reduced. Inspection of the model after test revealed heavy spalling in the inner and outer surfaces of the fusion sealed seam. Typical photographs of the damaged areas are shown in Figure 25. Strain sensitivities, defined as the slopes of the pressure strain diagram are shown in Figure 26. The maximum stress calculated from strain gage data was 70,000 psi.

---

[16]Nishida, K., "Structural Studies of Massive Glass: Sep 1968-May 1969," NSRDC Report 3180 (Aug 1969).

Model 44-2 exhibited similar behavior. However, sharp cracking sounds were not audible in this case. The test was terminated when a sharp change in strain was detected at a pressure of 4500 psi. The spalling on 44-2 was mainly on the inner surface.

The results obtained on the two 44 inch models are similar to that obtained by the Woods Hole Oceanographic Institute in a test of a 44 inch model for Bell Telephone Laboratories. These tests suggest that a considerable effort is required before large fusion sealed glass spherical shells can be considered practical for deep submergence buoyancy spheres.

Alumina spherical shells were also tested extensively for possible application as buoyancy spheres. Most of the tested were 10 inch diameter 0.18 in. wall of AD 99C and fabricated by Coors Porcelain Company. AD 99C has a Young's modulus of 52 x $.0^6$ psi, a Poisson's ratio of 0.22, and a density of 238 $lb/ft.^3$ The spheres tested had a W/D ratio of 40 percent. The spherical shells are formed while in the "green" state by a casting technique. The shells are then fired for curing. The tests carried out on alumina spheres were similar to those conducted on Pyrex glass. The results are discussed in detail in Reference 17, and are also tabulated in Table 10. The interesting points of the tests were.

1. The static strength of alumina spherical shells was quite encouraging. Stress levels in excess of 500,000 psi were achieved in many of the tests.

2. Loading rate does not appear to have a very significant effect on compressive strength based on tests conducted at rates between 350 and 400,000 psi/min. The average compressive stress of the 8 models tested at 350 psi/min was 460,000 psi, 3 models at 9000 psi/min was 510,000 psi, and 8 models at 400,000 psi/min was 500,000 psi.

3. Two 40 percent W/D alumina spheres survived proof tests of 30,000 ft and 5000 cycles of pressure to 22,500 feet. The two models were then collapsed at depths equal to about 60,500 feet. Thus, it appears that cycling did not affect the collapse strength of the models.

---

[17]Reardon, E.F., " Exploratory Tests of Aluminum Spheres Under External Pressure," NSRDC Report 3013 (Apr 1969).

Attempts to manufacture larger alumina spheres by the casting method was not very successful as the shell had a tendency to sag of its own weight while the material was in the "green" state. This created undesirable flatspots at the apex. A fusing technique to form larger spheres was also attempted. However, poor tests were obtained on 10 inch models of this type primarily because of a notch effect at the inner surface of the joint. This defect was very similar to those observed on the 44 inch diameter fusion sealed Pyrex glass spheres. Electron beam and laser welding were also explored on 3 inch diameter by 0.1 wall hemispheres.[18] This work indicated additional effort was required to eliminate thermal stress cracking and incomplete penetration welds. The data indicate that further development is required before large alumina spheres can be considered practical for deep submergence buoyancy spheres.

MECHANICAL COMPRESSION JOINTS

A pressure vessel designed to house instruments or man will require at least one mechanical joint. This problem has been under study for a number of years and has proven to be one of the more difficult ones encountered. Very exploratory work conducted by Krenzke and Charles[19] on the static strength of 2 inch diameter annealed Pyrex glass hemispheres were quite encouraging. The collapse strength of the hemispheres could be predicted by elastic theory up to stresses as high as 300,000 psi. Kiernan[1] subsequently conducted experiments on larger 18 inch diameter hemispheres of annealed and surface strengthened glass and alumina. Various types of gaskets were also explored. A summary of the interesting points are:

1. Generally, chemically strengthened glass (Herculite II) performed better than thermally tempered and annealed glasses as expected.
2. In the limited number of tests conducted, gasket material with various combinations of teflon, lead, alumina and titanium foil gave no better results than glass-to-glass tests.

---

[18] Benecke, M.W., "Electron Beam and Laser Welding of Aluminum Oxide Hemispheres," Prepared by Boeing Company for U.S. Navy under Contract N00600-69-C-0370 (May 1967).

[19] Krenzke, M.A. and R.M. Charles, "The Elastic Buckling Strength of Spherical Glass Shells," David Taylor Model Basin Report 1759 (Sep 1963).

3. Of the nearly 50 collapse tests conducted, less than 10 percent could be associated with elastic shell buckling. All other failures were attributed to stress conditions at the joint.
4. Collapse tests of 8 alumina spherical shells with W/D ratios of about 25 percent indicated that the joint problem in alumina ceramic may not be as severe as in glass. Four of the spheres were cast monolithically and four were formed by butting together a pair of hemispheres. No reduction in strength could be attributed to the presence of the joint.

Additional static and cyclic tests of Herculite II glass hemispherical shells not reported in Reference 20 have been conducted. The results are shown in Table 11. Five collapse tests of models butted together glass-to-glass were performed. The bearing stresses at collapse ranged from 127,000 to 219,000 psi. Fatigue tests were attempted on models also assembled glass-to-glass. None of the 3 models cycled survived more than 30 cycles of pressure which ranged from 10,000 to 13,333 psi. Similar results have been reported by Perry of NOL for this glass.

In view of the scatter of the data and the limited number of tests conducted under identical conditions an extensive effort to study the joint problem under more rigidly controlled conditions was attempted. All of the hemispherical shells tested were 10 inch diameter 0.28 inch wall of annealed Pyrex glass. Two sets of tests were conducted. One to observe the effects of surface flatness and the other the effect of "soft" gasket materials. The results of these tests are summarized in Tables 12 and 13. It is interesting to note the following trends indicated by the tests.

1. As might be expected, surface flatness appears to have an effect on collapse strength. The average collapse strength of 16 spherical assemblies formed by butting together two hemispherical shells which were finished at the bearing edge with 1200 mesh diamond dust abrasive was nearly 30 percent higher than the average collapse strength of 17 spherical assemblies

---

[20]National Materials Advisory Board, "Massive Glass as a Naval Structural Material," NMAB-262, April 1970.

whose hemispheres were finished at the bearing edge with 150 grit diamond embedded carbon wheel. Interestingly, the lowest collapse strength of the finely finished models (11,125 psi) was higher than the highest collapse strength of the roughly finished models (10,650 psi).

2. The data indicates that "soft" gasket materials can have a beneficial effect on short term static collapse strength. However, in a number of individual cases of gasket tests the models did no better than glass-to-glass tests. The average of 6 models with gaskets of glass fiber cloth impregnated with epoxy were 20 percent higher than glass-to-glass models of the same surface finish. The average collapse strength of 6 models with glass fiber cloth impregnated with synthetic sulfide rubber was nearly 50 percent better than glass-to-glass models of the same surface finish.

The better performance of gasketed models is attributed to the more even distribution of stress it creates. The compliant gasket material has a tendency to reduce the significance of contact stresses which are most likely the cause of premature failures in glass-to-glass models. None of the glass-to-glass models failed at a pressure that could be associated with the elastic buckling strength, which for this geometry is approximately 20,000 psi. In a number of cases of models with gaskets, the short term collapse strength could be associated with elastic buckling. It is also of interest to note that the collapse pressures of 3 models with glass reinforced rubber were actually not catastrophic. These tests were terminated when a slight drop in the pressure gage was noted. Inspection of these models indicated that the edges of the bearing surface had spalled off on both the inner and outer wall. Figure 3 is a photograph of a model terminated at a pressure of 17,000 psi.

Fatigue tests have been conducted on annealed Pyrex glass hemispherical shells utilizing glass reinforced plastic gaskets. Although the static tests suggested that rubber was probably the better matrix material for short term static strength, inspection of these gaskets after a single application of pressure indicated that extrusion and deterioration were serious problems. Thus, two types of epoxy were used for the matrix:

(1) Hysol, a quick setting epoxy, and (2) high strength resin EPON 828. The cyclic tests of glass reinforced plastic (Hysol) have been disappointing. None of the three spherical assemblies survived more than 6 cycles of pressure to maximum depth of 22,500 ft.

The results of models with glass reinforced plastic (EPON 828) also were disappointing. The test results are summarized in Table 14. The five models designated C1 through C5 were cycled to depths of 11,250, 13,500, 18,000, and 22,500, respectively. A proof test of 30,000 feet was applied to Model 65 only. Inspection of Models C1 through C4 after 50 cycles of pressure indicated slight spalling at the inner edge of the bearing surface. Glass chips about 1/4 by 1/32 in. were observed. When Model C3 (15,750 ft cyclic depth) was reinserted in the test facility, it failed after a total of 197 cycles. Model C4 (18,000 ft cyclic depth) failed after a total of 150 cycles and C5 after 706 cycles. Models C1 and C2 survived 1000 cycles and were reinspected; further cyclic damage was observed in both cases. Model C1 exhibited spalling on the inner surface of the bearing edge. The spalled area was approximately 1 1/2 by 3/8 in. Model C2 spalled at the outer surface at the bearing edge. A photograph of this damage is shown in Figure 27. The models were reinserted in the tank for further cycling. Model C2 failed after a total of 2015 cycles. Model C1 survived 3000 cycles although further cyclic damage was quite obvious. Relatively large spalled areas were observed on the inner surface as well as the outer surface at the joint. A photograph of the damage after 3000 cycles is shown in Figure 27. No further testing was attempted on the model.

In addition to tests of annealed Pyrex glass, compression studies were conducted on PPG Industries' 1080 glass. The models are 10 in. diameter by 0.36 in. All models were tested in the annealed condition. Most had bearing surfaces prepared with No. 120 grit wheel. These models were tested in simulated sea water at various loading rates and held at constant pressure in some cases. A summary of the test results is presented in Table 15. All models, except two hemispheres tested on hardened steel surface, were formed by butting two hemispheres together glass-to-glass. It can be observed that the range of stresses obtained on these tests were 99,000 to 158,000 psi, excluding tests of glass hemispheres on

hardened steel. It is interesting to note that the two lowest test results were those conducted with steel as the bearing surface. It should be recognized that different loading rates, limited cycling, and sustained loading were involved for the glass-to-glass tests. This should be considered when comparing individual tests within the group. For example, it can be observed that most of the lower stresses at collapse were obtained on models that were cycled and held at pressure for a period of time. This is to be expected.

One static test of a 5 inch diameter by 0.11 inch wall glass ceramic hemispherical shell was conducted at the Center. The material was Corning's Pyroceram 9606 which has a Young's modulus of 17.3×10^6 psi, Poisson's ratio of 0.245, and a density of 163 $lb/ft.^3$ The weight-to-displacement ratio for the hemisphere was 32 percent. A sketch of the model is shown in Figure 28. The hemisphere was tested by placing it on a hardened steel block in the NSRDC 30,000 psi 12 in. spherical pressure chamber. Simulated sea water was used as the pressure medium and an external pressure loading rate of 400 psi/min was used. The model was pressurized to the rated operating capacity of the chamber, 30,000 psi, at which point the loading was terminated. Upon releasing pressure, the model failed catastrophically at a pressure of 15,000 psi. At the maximum static pressure of 30,000 psi the membrane stress in the shell was 352,000 psi. The calculated elastic buckling strength of the hemisphere based on the empirical formula was 27,000 psi. Thus, the model exceeded the calculated empirical pressure by nearly 10 percent. The failure of the model upon releasing the pressure is probably associated with local yielding at the bearing surface of the hardened steel block. Permanent set takes place on the load application phase which inhibits the Pyroceram shell to relax to its original shape upon unloading.

Tests of glass ceramic structures have also been conducted by the Lockheed Missiles and Spacecraft Company (LSMC) and the General Electric Company (GE). The LSMC model was a bi-spherical structure with the juncture portion of titanium and the end closures of Pyroceram. The GE model was a geodesic structure with the lattice of titanium and the inserts of Pyroceram. A summary of the tests is presented in Reference 20.

A slightly different approach to solving the joint problem was investigated utilizing chemically strengthened Chemcor 0312 glass. The area of the bearing joint is reinforced so that the thickness at the bearing face is nearly twice the thickness of the uniform portion of the wall. The increased thickness at the bearing face reduces the bearing stresses and thus could reduce the contact problem. Several models have been statically tested to observe response. Two different loading rates were utilized to determine the effect of strength. These models were handlapped prior to testing. Measurements taken before and after lapping indicated that approximately 0.002 to 0.003 in. of the glass surface was removed as a result of lapping. In addition to static tests, a few cyclic tests have been conducted. All tests of chemically strengthened glass hemispheres have been conducted in simulated sea water.

The results of static tests of chemically strengthened glass hemispheres are presented in Table 16. The models were formed by butting two hemispheres together glass-to-glass. It is somewhat surprising to see that the average stress at collapse for the models tested at a slow loading rate (20 psi/min) was higher than the average for the fast rate tests (15,000 psi/min). Apparently an undesirable effect, possibly from friction, is created at the bearing surfaces of the model during a fast rate test.

The elastic buckling pressure for the uniform wall (0.23) portion of the shell is in the order of 14,000 psi. Although the collapse pressures could be associated with elastic buckling in some cases, the majority of models more likely failed by stress controlled conditions.

All static tests of Chemcor glass models were prior to tests conducted on annealed glass models with gaskets described previously. Since improvement in short term static strength was apparent in tests of annealed glasses, several cyclic tests of Chemcor 0312 glass hemispheres with reinforced bearing surfaces and glass reinforced plastic gaskets were conducted. A summary of these tests is included in Table 17. The results have been encouraging considering the rather severe conditions of the tests. A maximum cyclic pressure of 10,000 psi and a cyclic rate of approximately one cycle per minute were utilized in these tests. Thus, the loading rate was greater than that utilized for static tests of

glass-to-glass models tested at the fast loading rate. Five of the seven models cycled survived at least 3000 cycles to 10,000 psi. However, two failed after application of only 86 and 110 cycles. Based on present knowledge, it is concluded that some strength degradation resulted from the lapping. Although only 2-3 mils of glass was removed, the depth of surface compression for Chemcor 0312 glass is only about 5 mils. Thus, much of the residual surface compression was lost by the lapping operation and most likely influenced the test results. In view of this shortcoming in the specimen, the fact that 5 of 7 models survived 3000 cycles to 22,500 ft is quite encouraging.

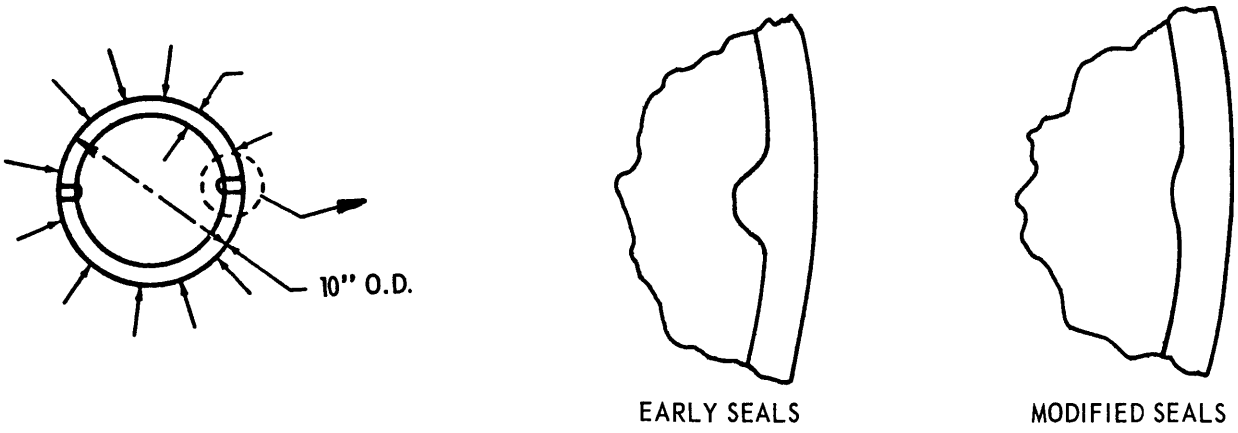

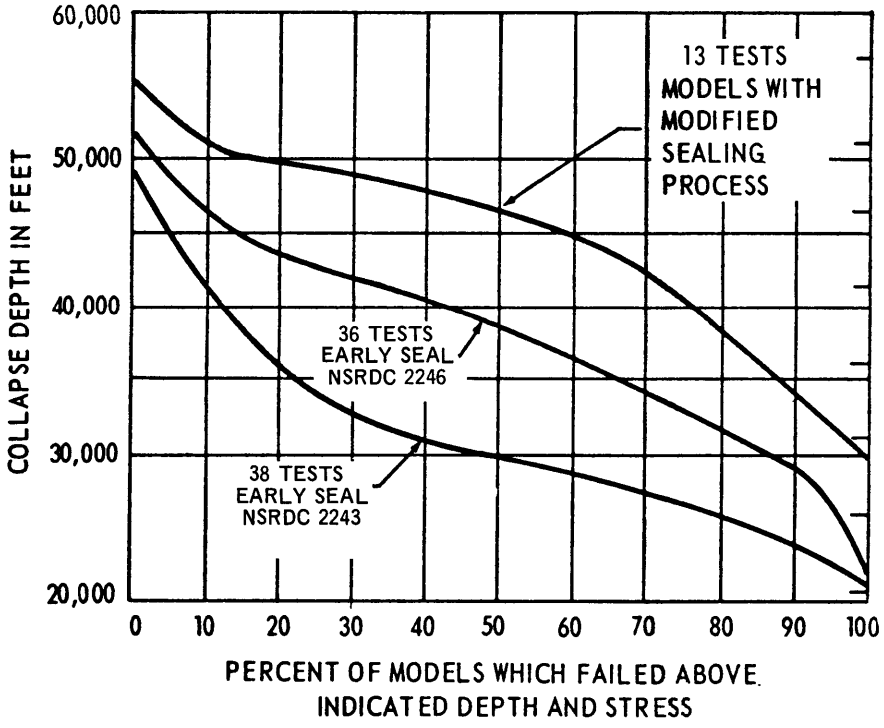

Figure 20 - Summary of Test Results of 10-Inch-Diameter 0.28 Wall Fusion Sealed Annealed Pyrex Glass Spheres

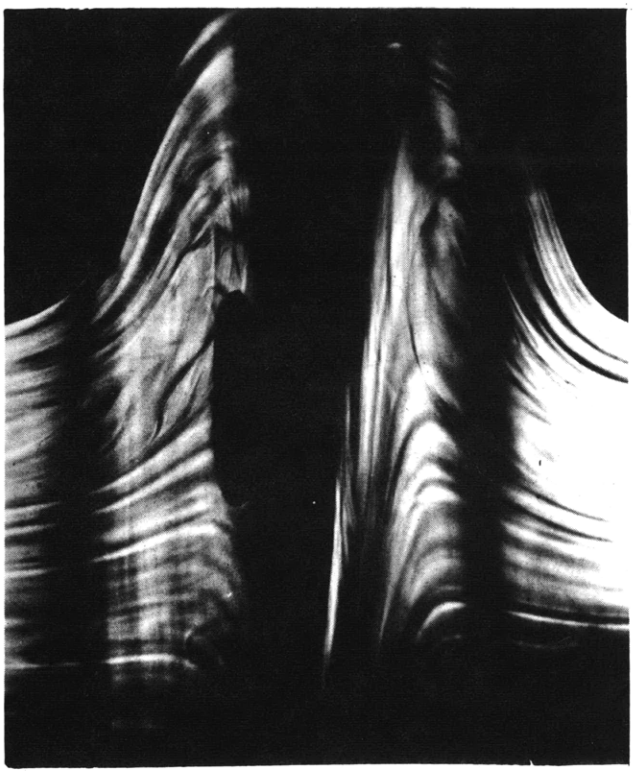

Figure 21a - Earlier Type Seam

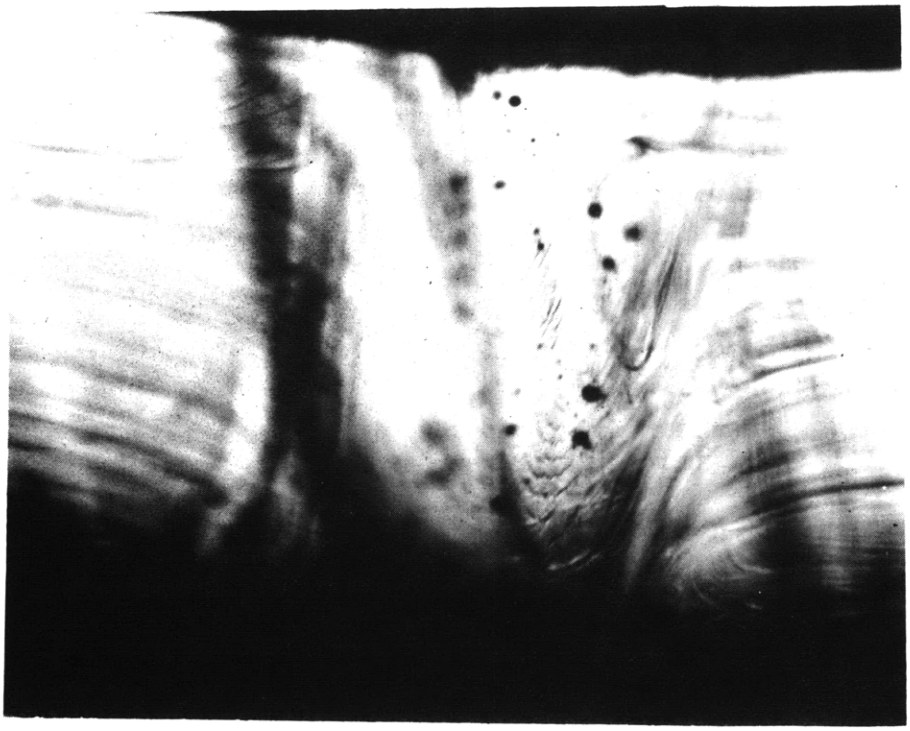

Figure 21b - Modified Type Seam

Figure 21 - Examples of Fusion Sealed Seams

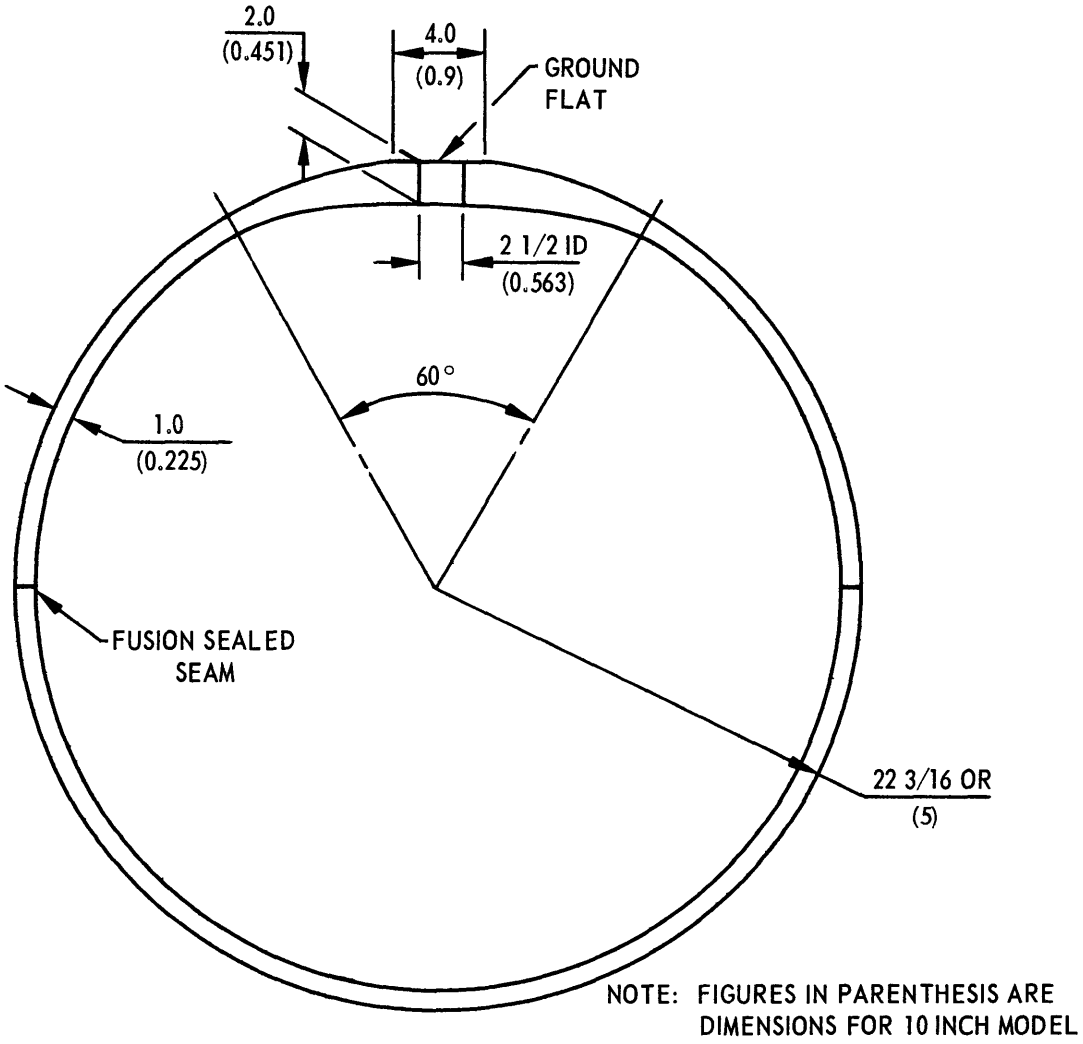

Figure 22 - Nominal Model Dimensions for Fusion Sealed Spheres with Penetration

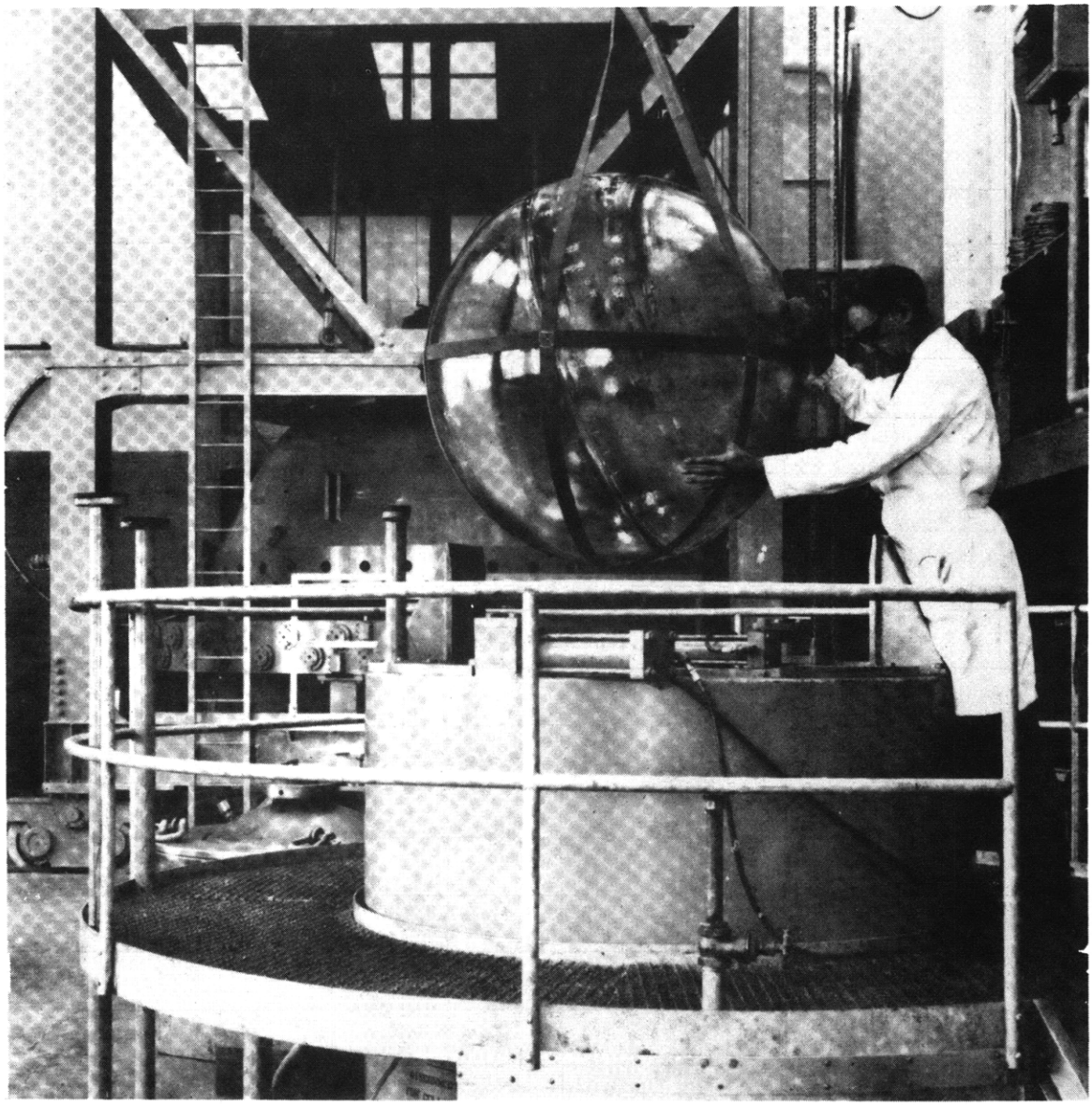

Figure 23 - 44 Inch Diameter Fusion Sealed Annealed
Glass Sphere

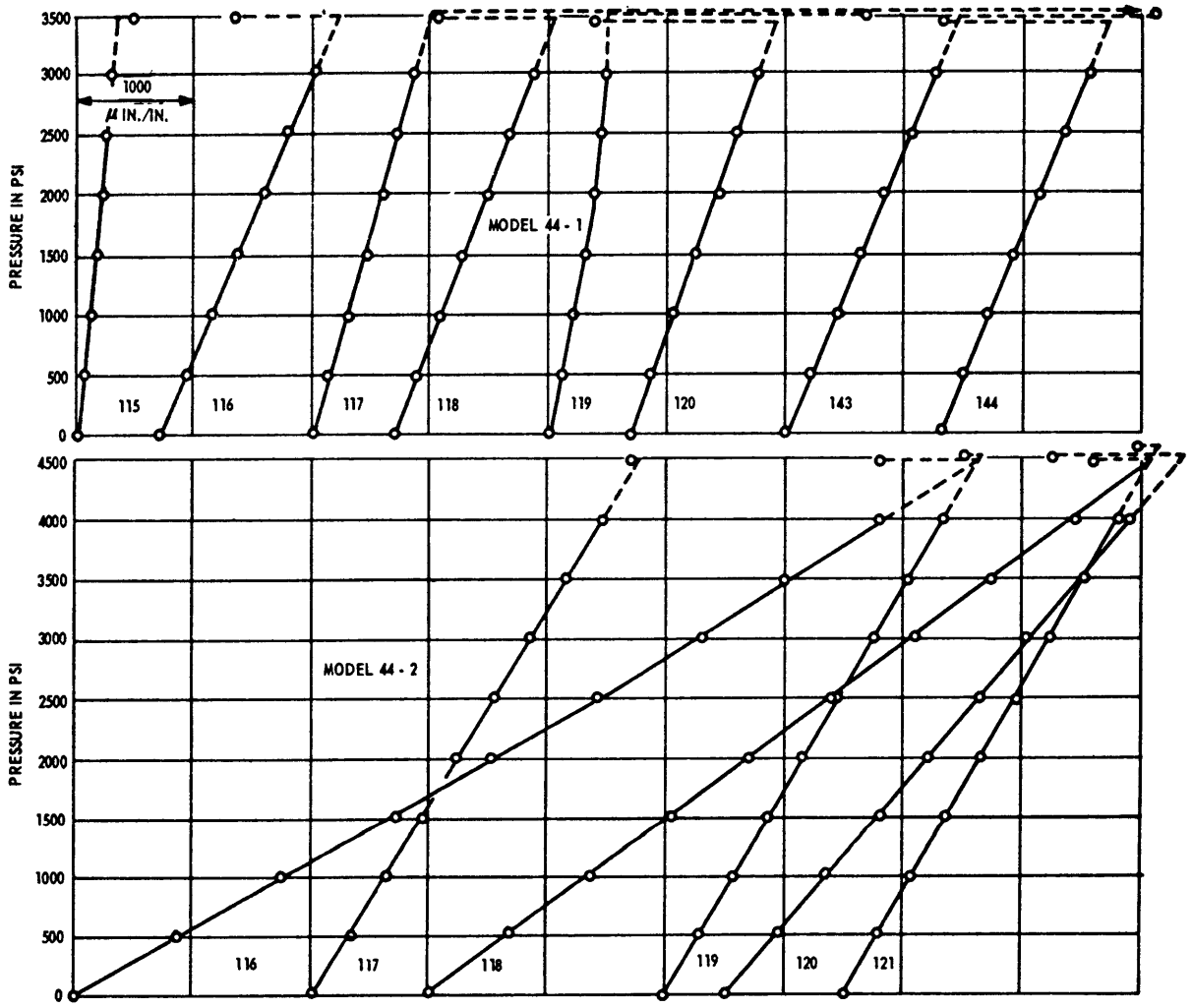

Figure 24 - Pressure Strain Plots for 44 Inch Glass Sphere

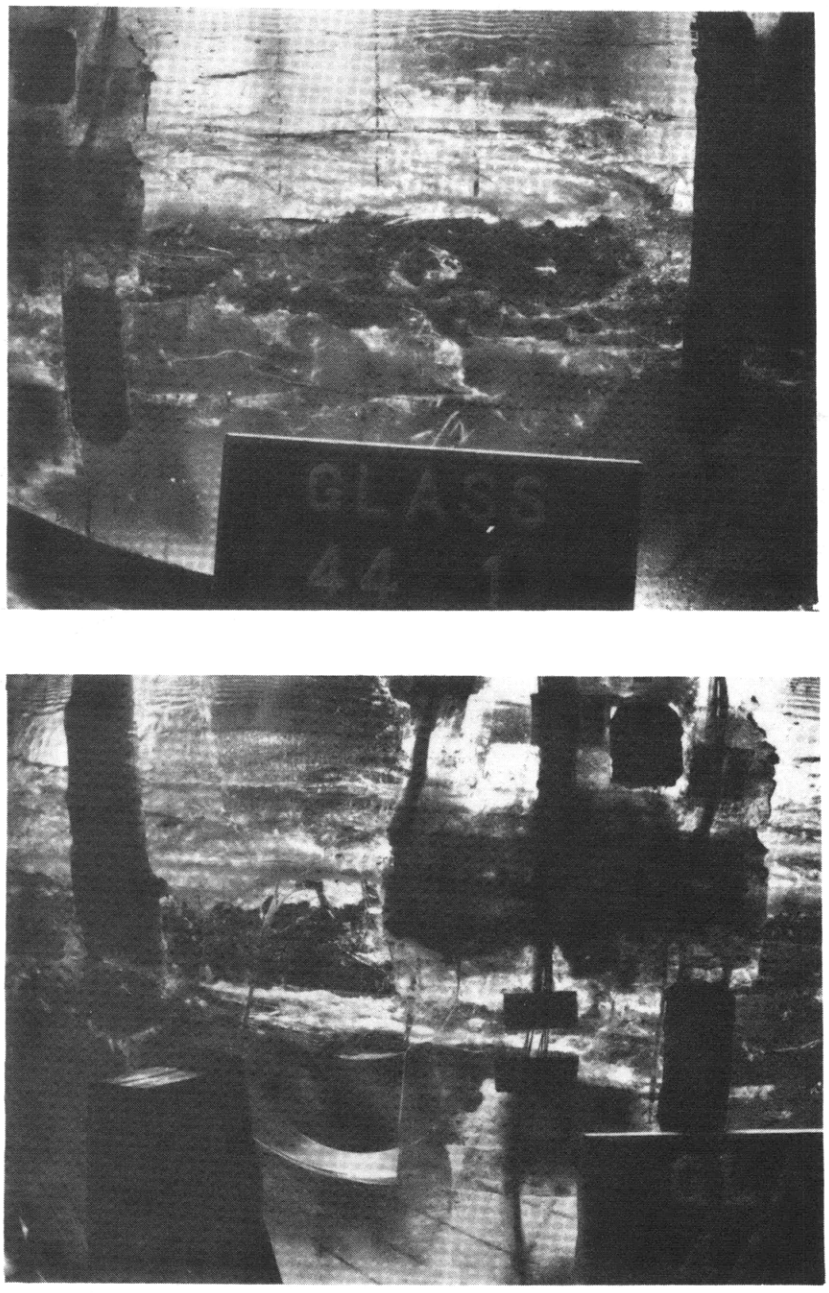

Figure 25 - Damage to Model 44-1 after 3500 psi

Figure 26 - Gage Locations and Strain Sensitivities for 44 Inch Sphere

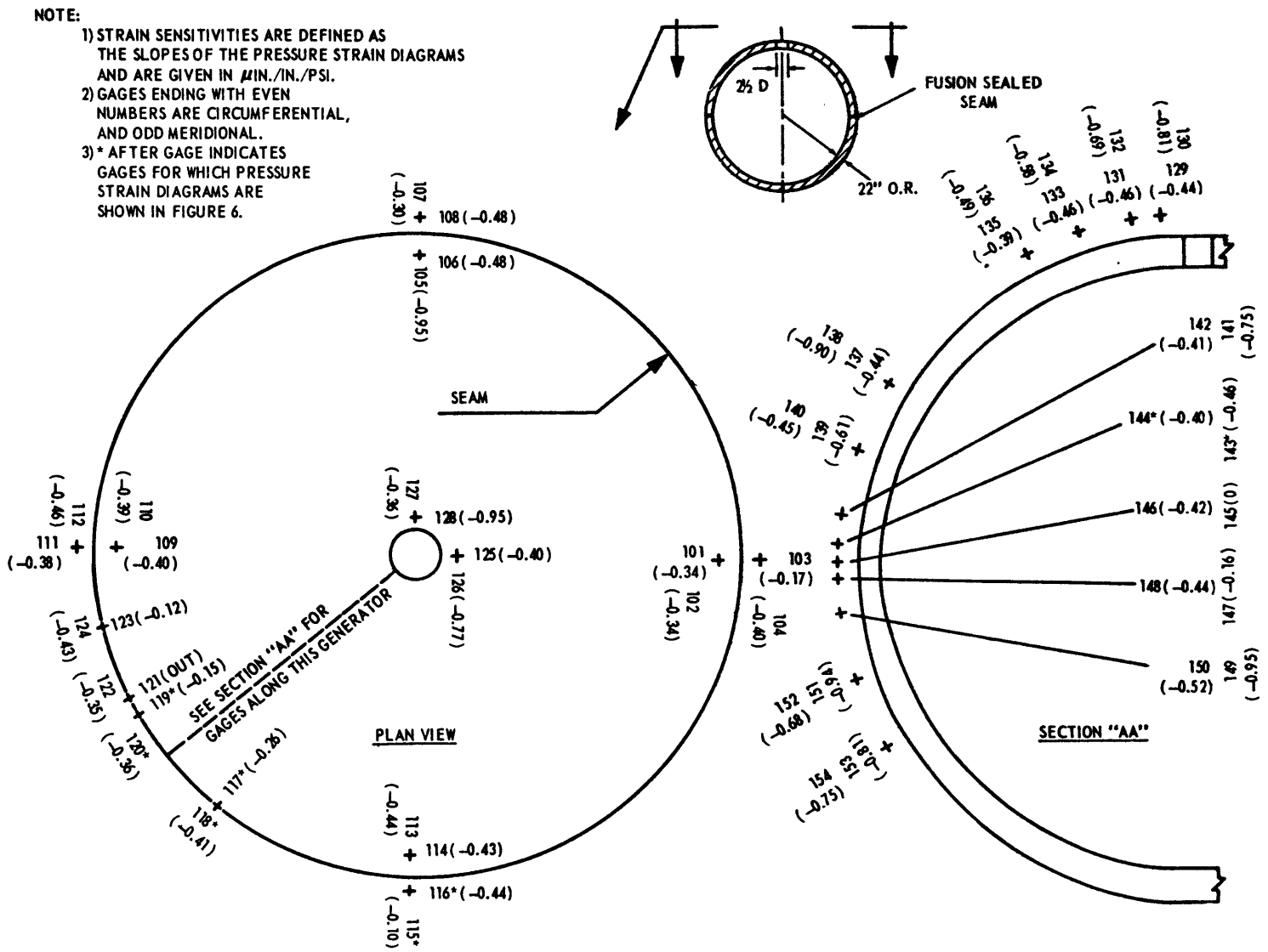

Figure 26a - Model 44-1

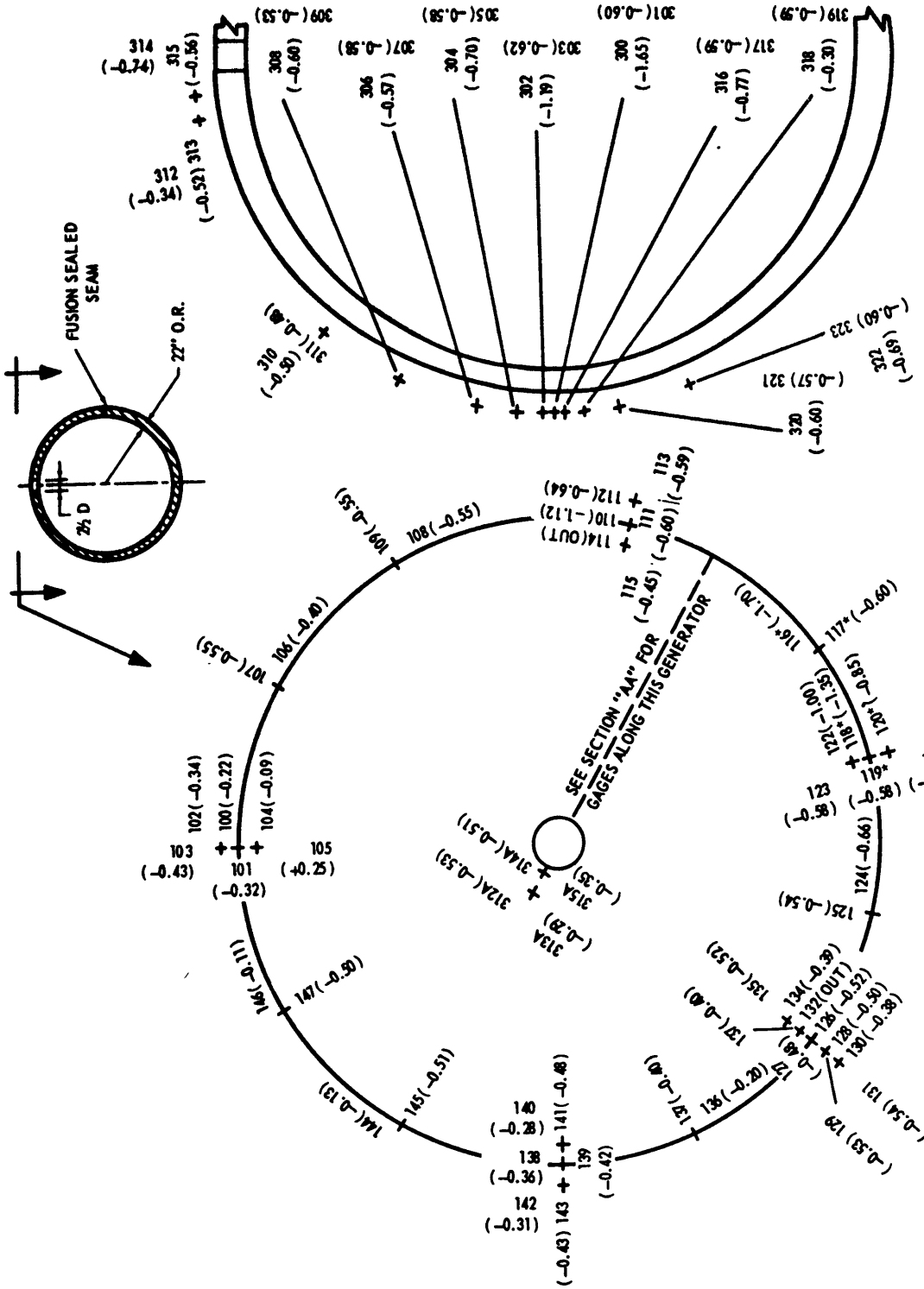

Figure 26b - Model 44-2

Figure 27a - After 1000 Cycles (3X)

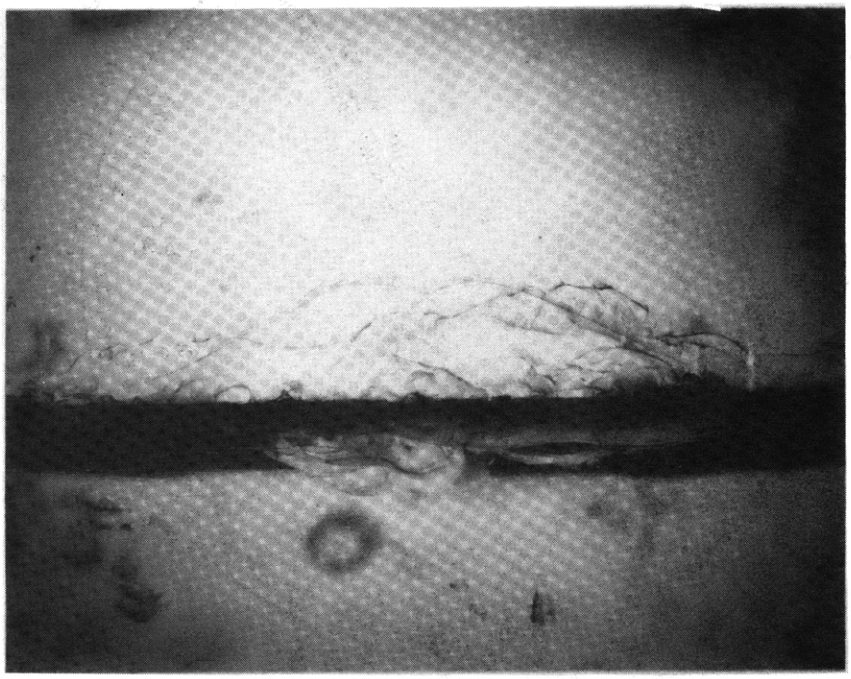

Figure 27b - After 3000 Cycles (3X)

Figure 27 - Damage to Model C-2 After Cycling to 5000 PSI

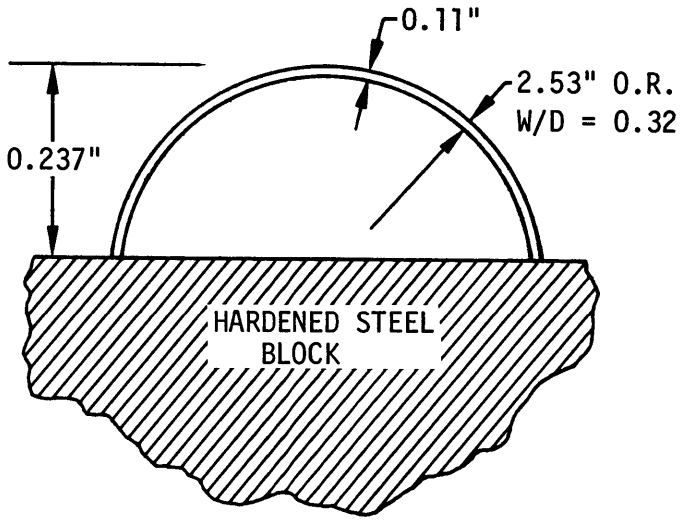

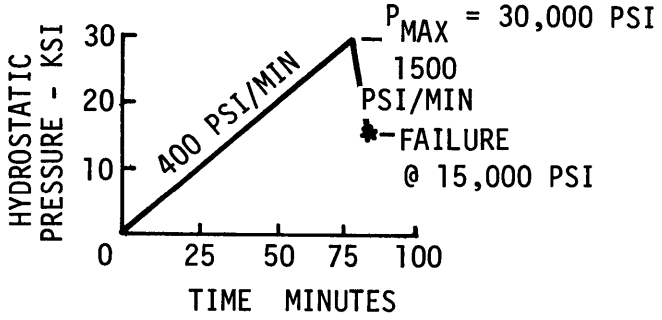

LOAD PROFILE

Material Properties:

$E = 17.3 \times 10^6$ psi

$\nu = 0.245$

$\gamma = 163$ #/ft^3

Loads:

Calculated Collapse Pressure - 27,000 psi

Experimental Pressure - 30,000 psi*

Membrane Stress - 352,000 psi

*Model did not fail at maximum applied load. Failure occurred during release of pressure. See Load Profile.

Figure 28 - Nominal Model Dimensions and Test Result of 5 Inch Diameter Pyroceram Hemisphere

TABLE 5 - EFFECT OF LOADING RATE AND PRESSURE MEDIUM ON COLLAPSE STRENGTH

Series	Model	Experimental Collapse		Average Stress in Shell at Collapse
		psi	ft	psi
I (Tests in sea water at compressive stress rate of 140,000 psi/min)	1	20,625	46,400	183,000**
	2	19,250	43,300	166,000**
	3	14,200	31,900	126,000
	4	14,100	31,700	119,000
	5	13,400	30,100	117,000
	6	12,750	28,700	112,000
	7	12,625	28,400	105,000
	8	10,550	23,700	89,000
	9	9,550	21,500	83,000
II (Tests in sea water at compressive stress rate of 3500 psi/min)	10	18,500	41,600	157,000
	11	17,700	40,000	155,000
	12	15,450	34,700	136,000
	13	14,300	32,200	125,000
	14	13,875	31,200	122,000
	15	13,200	29,700	115,000
	16	11,800	26,500	103,000
	17	11,000	24,700	97,000
	18	10,500	23,600	91,000
III (Tests in oil at compressive stress rate of 3500 psi/min)	19	22,600	50,800	199,000**
	20	17,125	38,600	149,000
	21	16,100	36,000	140,000
	22	15,650	35,200	138,000
	23	15,300	34,400	131,000
	24	14,300	32,200	123,000
	25	13,400	30,100	117,000
	26	12,550	28,300	111,000
	27	9,050	20,300	81,000
IV (Tests in sea water at compressive stress rate of 200 psi/min)	28*	22,010	49,500	191,000**
	29	16,550	37,300	142,000
	30	15,710	35,300	136,000
	31	14,030	31,500	122,000
	32	13,640	30,700	118,000
	33	13,390	30,100	115,000
	34	12,150	27,300	104,000
	35	11,950	26,900	103,000
	36	10,550	23,700	92,000

*Model was not collapsed.
**Stress levels which may be associated with elastic buckling failure.

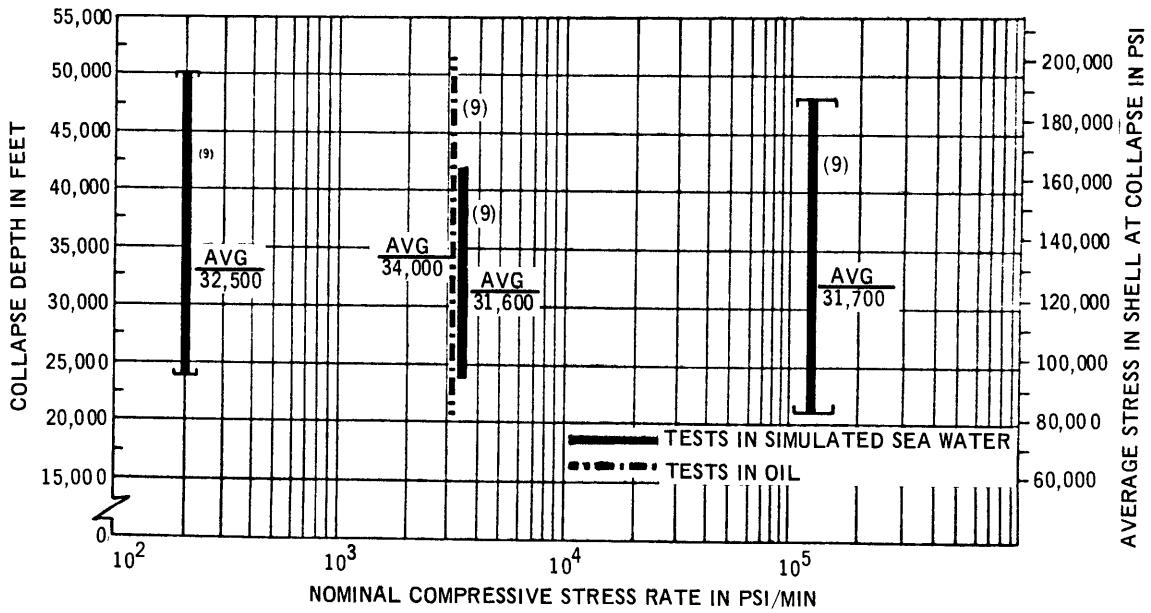

TABLE 6 - COLLAPSE STRENGTH OF 10-INCH-DIAMETER 0.28 WALL FUSION SEALED ANNEALED PYREX GLASS SPHERES WITH MODIFIED SEAMS

Model	Collapse Pressure		Stress*
	psi	ft	
IFS 7	13,600	30,600	119,000
IFS 13	14,450	32,500	126,000
IFS 5	15,200	34,200	134,000
IFS 4	18,100	40,700	160,000
IFS 9	19,900	44,800	174,000
IFS 14	20,500	46,000	181,000
IFS 12	20,625	46,300	179,000
IFS 1	21,050	47,400	188,000
IFS 8	21,425	48,300	187,000
IFS 6	26,625	48,600	190,000
IFS 11	22,375	50,400	197,000
IFS 3	23,150	52,100	201,000
IFS 10	25,050	56,400	222,000

*Based on average measured thickness.

TABLE 7 - CYCLIC TESTS OF 10-INCH-DIAMETER 0.28 WALL FUSION SEALED ANNEALED PYREX GLASS SPHERES

Model	Seal Type	Run No.	Test	Pressure	
				psi	ft
C-1	Early	1	Proof	13,333	30,000
		2	Cyclic 5000 cycles	10,000	22,5000
		3	Collapse	19,600	44,000
C-2	Early	1	Proof	13,333	30,000
		2	Cyclic 5000 cycles	10,000	22,500
		3	Collapse	21,090	47,600
C-3	Early	1	Proof	13,333	30,000
		2	Cyclic 5000 cycles	10,000	22,500
		3	Collapse	16,425	37,000
C-4	Early	1	Proof	13,333	30,000
		2	Cyclic 5000 cycles	10,000	22,500
		3	Collapse	16,025	36,100
28	Early	1	Proof	22,010	49,500
		2	Cyclic 5000 cycles	10,000	22,500
		3	Collapse	22,250	50,000
2A	Modified	1	Proof	13,333	30,000
		2	Cyclic 5000 cycles	10,000	22,500
6A	Modified	1	Proof	13,333	30,000
		2	Cyclic 5000 cycles	10,000	22,500
9A	Modified	1	Proof	13,333	30,000
		2	Cyclic 5000 cycles	10,000	22,500
10A	Modified	1	Proof	13,333	30,000
		2	Cyclic 5000 cycles	10,000	22,500
3A	Modified	1	Proof	13,333	30,000
		2	Cyclic 5000 cycles	10,000	22,500

TABLE 8 - COLLAPSE STRENGTH OF 10-INCH-DIAMETER 0.36 WALL FUSION SEALED ANNEALED PYREX GLASS

Model	Collapse Pressure		Stress*
	psi	ft	
319	19,000	43,700	136,000
313	21,925	49,400	155,000
314	22,200	50,000	155,000
316	22,090	49,600	158,000
320	23,000	51,700	163,000
317	23,200	52,200	164,000

*Based on average measured thickness.

TABLE 9 - SUMMARY OF STATIC TESTS OF 10-INCH-DIAMETER FUSION-SEALED ANNEALED PYREX GLASS SPHERES WITH PENETRATIONS

Model	Collapse Pressure		h_a[1] (in.)	Average Stress at Collapse (psi)	P_e[2] (psi)	P_{EXP}/P_e
	psi	ft				
GS-1	15,475	34,800	0.220	180,000	14,300	1.08
GS-2	15,550	35,000	0.232	172,000	15,900	0.98
GS-3	14,475	32,600	0.225	165,000	14,900	0.97
GS-4	15,150[3]	34,100	0.222	174,000	14,600	1.04
GS-5	13,333	30,000	0.223	152,000	14,700	0.91

1 – Minimum measured thickness.

2 – P_e calculated from equation $P_e = 0.83\ E\left(\frac{h_a 1}{R_o}\right)^2$ where $R_o = 5$ in.

3 – Test conducted in two runs.

TABLE 10 - STATE CYCLIC TESTS OF 10-INCH-DIAMETER 0.18 WALL MONOLITHIC ALUMINA SPHERES

STATIC TESTS

Model No.	P_3'	Experimental Pressures		Calculated Failure Stress	
	psi	psi	ft	Average ksi	Local ksi
AL- 92	30,080	25,400	57,200	429	484
AL- 95	30,080	27,825	62,600	468	534
AL- 98	27,200	28,475	64,000	497	572
AL- 99	28,510	20,400	46,000	373	402
AL-105	28,070	27,125	61,100	412	542
AL-106	23,860	26,875	60,500	500	574
AL-108	30,080	25,500	57,375	442	490
AL-109	36,030	22,450	50,500	370	410
AL- 94	36,500	26,875	60,500	410	468
AL-104	25,600	26,850*	60,400	395	560
AL-107	33,200	26,875*	60,500	395	495
AL- 91	28,740	20,100	45,300	350	395
AL- 93	32,160	25,875	58,300	430	476
AL- 96	29,180	22,950	51,600	385	450
AL- 97	34,800	20,750	46,700	340	370
AL-100	27,200	26,000	58,500	480	520
AL-101	29,860	26,750	60,000	450	510
AL-102	31,690	25,375	57,000	430	480
AL-103	30,540	25,200	56,800	420	480

CYCLIC TESTS

Model	W/D	Run	Pressure		Stress		
			psi	ft	avg	local	
AL-104	0.38	1	13,333	30,000	196	285	Held 13,333 psi for 1 hr
		2	10,000	22,500	147	212	Cycled 5000 times
		3	26,850	60,400	395	575	Returned to NSRDC and collapsed
AL-107	0.38	1	13,333	30,000	194	245	Held 13,333 psi for 1 hr
		2	10,000	23,500	145	184	Cycled 5000 times
		3	26,875	60,500	390	495	Returned to NSRDC and collapsed

TABLE 11 - SUMMARY OF STATIC TESTS OF CHEMICALLY STRENGTHENED HERCULITE II (1080 Na^+) GLASS HEMISPHERES

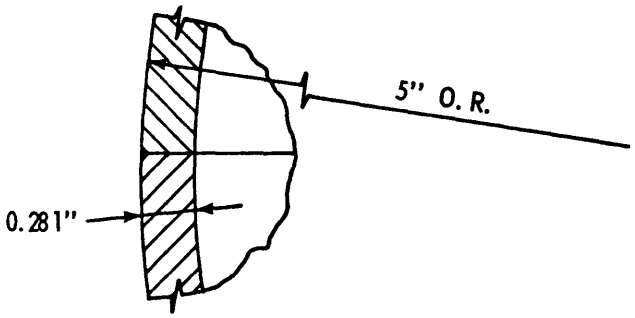

$\omega/D = 0.36$

Model No.	Collapse Pressure		Bearing Stress psi
	psi	ft	
HH-1	22,800	51,400	219,000
HH-2	18,800	42,400	175,000
HH-3	18,750	42,300	175,000
HH-4	17,300	39,000	161,000
HH-5	13,550	30,500	127,000

TABLE 12 - TEST RESULTS OF 10-INCH-DIAMETER 0.281 WALL ANNEALED PYREX GLASS HEMISPHERICAL SHELLS WITHOUT GASKETS

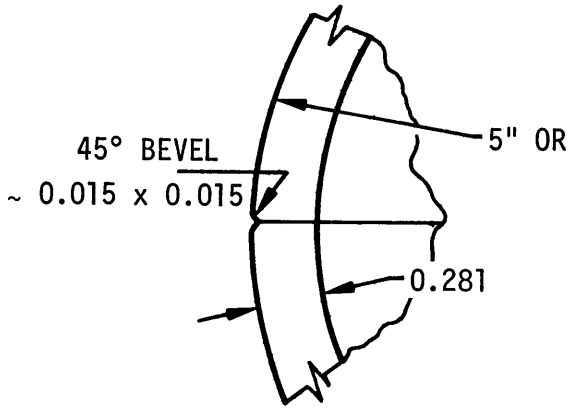

JOINT CONFIGURATION

Series 1 No. 150 Grit Diamond Wheel			Series 2 1200 Mesh Diamond Abrassive		
Test No.	Collapse Pressure - psi	Average Bearing Stress* ksi	Test No.	Collapse Pressure - psi	Average Bearing Stress* ksi
1	10,650	96	1	14,300	134
2	10,350	96	2	13,625	129
3	10,350	94	3	13,275	126
4	10,500	96	4	12,700	118
5	10,300	96	5	12,575	118
6	10,300	94	6	12,500	118
7	10,100	92	7	12,525	115
8	10,000	92	8	12,450	117
9	9,950	92	9	12,125	114
10	9,900	91	10	12,050	113
11	9,625	88	11	12,000	113
12	9,100	83	12	11,675	110
13	9,000	83	13	11,575	106
14	8,950	83	14	11,400	108
15	8,200	76	15	11,400	106
16	6,150	53	16	11,125	103
17	5,075	46			
No. of Tests - 17 Avg Collapse Pressure - 9323 psi Avg Collapse Stress - 85 ksi			No. of Tests - 16 Avg Collapse Pressure - 12,331 psi Avg Collapse Stress - 113 ksi		

*Based on measured thickness at joint. Reduction in thickness by bevelling edges not accounted for. Average bearing stress would be increased by about 10 percent if taken into account.

TABLE 13 - TEST RESULTS OF 10-INCH-DIAMETER 0.28 WALL ANNEALED PYREX GLASS HEMISPHERES WITH GASKETS

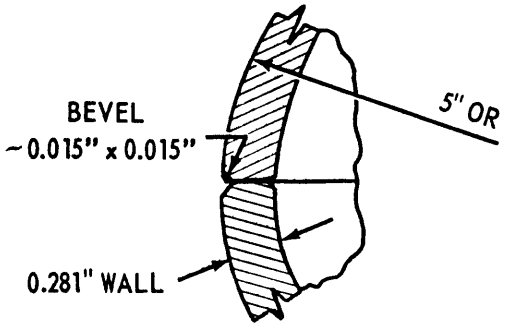

JOINT CONFIGURATION

Glass Fiber Cloth and Epoxy				Glass Fiber Cloth and Synthetic Rubber			
Test No.	Collapse Pressure		Collapse Stress	Test No.	Collapse Pressure		Collapse Stress
	psi	ft	psi		psi	ft	psi
1	21,475	48,300	196,600	1	22,740	51,200	208,100
2	19,350	43,500	177,100	2	21,200	47,700	194,000
3	18,350	41,300	168,000	3	20,825	46,900	190,600
4	12,800	28,800	117,200	4	18,400*	41,400	168,400
5	11,250	25,300	103,000	5	17,900*	40,300	163,800
6	9,375	21,100	85,800	6	17,000*	38,200	155,600
Avg Collapse Pressure = 15,433 psi Avg Collapse Stress = 141,200 psi				Avg Collapse Pressure = 19,678 psi Avg Collapse Stress = 180,100 psi			

*Tests terminated after drop in pressure noted. Edges of bearing surfaces spalled.

TABLE 14 - SUMMARY OF CYCLIC TESTS OF 10-INCH-DIAMETER 0.28 WALL ANNEALED PYREX GLASS HEMISPHERES

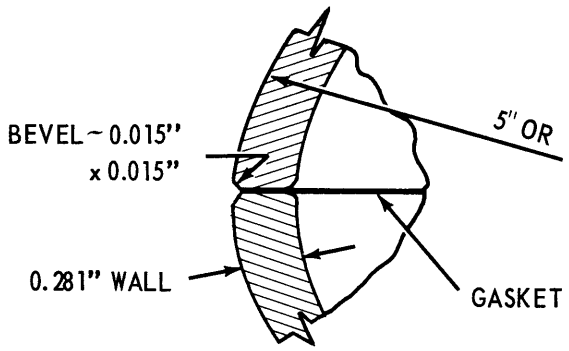

Model No.	Gasket Type	Proof Pressure		Cyclic Pressure		Stress psi	No. Cycles to Failure
		psi	ft	psi	ft		
C-1	0.003 in Glass Fiber Cloth and Epoxy	None	–	5,000	11,250	45,800	3,000*
C-2	0.003 in Glass Fiber Cloth and Epoxy	None	–	6,000	13,500	54,900	2,015
C-3	0.003 in Glass Fiber Cloth and Epoxy	None	–	7,000	15,750	64,000	197
C-4	0.003 in Glass Fiber Cloth and Epoxy	None	–	8,000	18,000	73,200	150
C-5	0.003 in Glass Fiber Cloth and Epoxy	13,333	30,000	10,000	22,500	91,500	706
H-1	0.003 in Glass Fiber Cloth and Hysol	13,333	30,000	10,000	22,500	91,500	1
H-2	0.003 in Glass Fiber Cloth and Hysol	None	–	10,000	22,500	91,500	4
H-3	0.003 in Glass Fiber Cloth and Hysol	None	–	7,500	16,900	68,6000	5

*Heavy damage to inner and outer surfaces of bearing joint observed after 3,000 cycles. No further testing attempted.

TABLE 15 - SUMMARY OF TEST RESULTS OF 10-INCH-DIAMETER 0.36 WALL PPG 1080 ANNEALED GLASS HEMISPHERICAL SHELLS

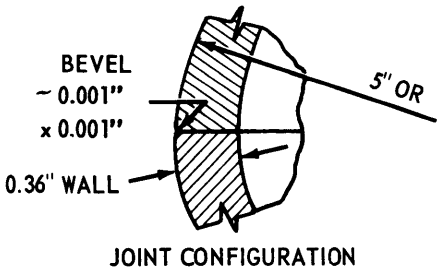

JOINT CONFIGURATION

1200 Mesh Diamond Abrasive Finish

Test No.	Collapse Pressure		Stress
	psi	ft	psi
1	17,950	40,400	131,000
2	17,600	39,600	129,000
3	16,950	38,100	126,000

No. 120 Grit Finish

Test No.	Collapse Pressure		Stress	Remarks
	psi	ft	psi	
1	21,475	48,300	158,000	Loaded at 18,000 psi/min
2	21,100	47,500	155,000	
3	19,175	43,100	145,000	
4	19,000	42,800	144,000	
5	18,075	40,700	137,000	Soaked in S. W. 20 days
6	17,100	38,500	128,000	
7	16,800	37,800	126,000	
8	16,700	37,600	126,000	Loaded at 20 psi/min
9	16,800	37,800	125,000	
10	16,800	37,800	123,000	
11	15,200	34,200	116,000	
12	15,150	34,100	112,000	2 Runs. 1st run to 15,000 held for 4 hrs. 2nd Run collapsed at 15,150 after 5 secs. Loaded at 18,000 psi/min
13	14,800	33,300	110,000	
14	14,800	33,300	110,000	
15	14,500	32,600	108,000	4 Runs. 1 hr. holds after 13,000, 13,500 and 14,000. Collapsed on 4th Run at 14,500 after 15 min. Loaded at 18,000 psi/min
16	14,000	31,500	105,000	2 Runs. 1 hr. hold at 13,500 on 1st Run. Collapsed on 2nd Run at 14,000 after 20 secs. Loaded at 18,000 psi/min.
17	14,000	31,500	105,000	2 Runs. 1 hr. hold at 13,500 on 1st Run. Collapsed on 2nd Run at 14,000 after 22 min. Loaded at 18,000 psi/min.
18	13,500	30,400	99,000	Collapsed at 13,500 after 48 min.
19	12,000	27,000	88,000	Hemisphere on hardened steel block
20	11,600	26,100	86,000	Hemisphere on hardened steel ring

TABLE 16 - SUMMARY OF STATIC TESTS OF CHEMCOR HEMISPHERES WITH REINFORCED BEARING SURFACES

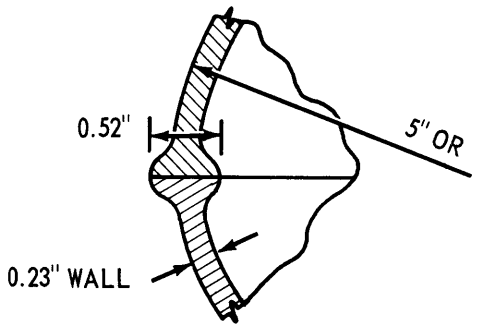

Loading Rate psi/min	Model Number	Collapse Pressure		Collapse Stress	
		psi	ft	Membrane psi	Avg Bearing psi
20	CH-1	19,500	43,900	217,000	100,000
	CH-2	17,625	39,700	196,000	90,000
	CH-3	16,500	37,100	183,000	83,000
	CH-4	12,125	27,300	135,000	65,000
	CH-5	11,125	25,000	124,000	60,000
15,000	CH-6	13,750	30,900	153,000	72,000
	CH-7	12,275	27,660	136,000	64,000
	CH-8	11,450	25,800	127,000	60,000
	CH-9	10,650	24,000	118,000	58,000
	CH-10	8,875	20,000	99,000	46,000

TABLE 17 - SUMMARY OF CYCLIC TESTS OF CHEMCOR 0312 HEMISPHERES WITH REINFORCED BEARING SURFACES

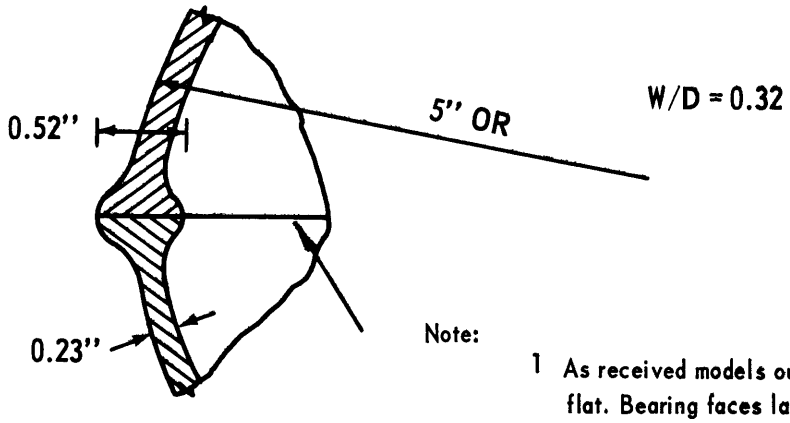

Note:

1 As received models out of flat. Bearing faces lapped with 1200 mesh diamond abrasive. About 0.002 to 0.003 in of surface compressed layer removed. No attemt made to restrengthen model.

2 Model glued together with glass reinforced plastic

TEST NUMBER	PROOF PRESSURE psi	CYCLIC PRESSURE psi		NUMBER CYCLES	REMARKS
		MAX	MIN		
1	NONE	10,000	200	5000	
2	NONE	10,000	200	5000	
3	NONE	10,000	200	5000	
4	13,333	10,000	200	4000	CYCLIC TESTS STOPPED AFTER 4000 CYCLES. MODEL STATICALLY COLLAPSED AT 13,800 PSI
5	NONE	10,000	200	3300	COLLAPSED
6	NONE	10,000	200	86	COLLAPSED
7	NONE	10,000	200	110	COLLAPSED

REFERENCES

1. Kiernan, T.J., "An Exploratory Study of the Feasibility of Glass and Ceramic Pressure Vessels for Naval Applications," NSRDC Report 2243 (Sep 1966).

2. Coffman, W.B. et al., "Feasibility Study of Plastic-Clad Glass Capsules for Deep Diving Submersibles," NOL TR 65-76 (Jun 1965).

3. Heathcote, T.B., "The Resistance of Hollow Glass Models to Underwater Explosions at Great Depths III Spheres with Overlays," NOL TR 66-78 (May 1966).

4. Perry, H.A., "Surface Compression Strengthened Glasses: Some Properties," NOL TR 71-21 (Mar 1971).

5. Gray, K.D. and J.D. Stachiw, "Light Housings for Deep Submergence Applications--Part III. Glass Pipes with Conical Flanged Ends," NCEL Technical Report R618 (Mar 1969).

6. Foreman, W. and R. DeHart, "Submersible Deep View Pioneers Glass/Metal Bending," Undersea Technology, pp. 24-27 (Dec 1967).

7. Murphy, D.W., "Development and Testing of a 56-In.-Dia. Jointed Glass Pressure Hull," ASME Paper No. 69-WA/UnT-2 presented at Winter Annual Winter, L.A. Calif (Nov 16-20, 1969).

8. Zilliacus, S. and H. Hashmall, "Impact Strength and Response of Protected Brittle Models of Deep Submergence Structures," David Taylor Model Basin Report 2314 (Dec 1966).

9. Lilliston, R.R., "Calculations on the Collapse of a Spherical Gas-Filled Cavity in a Compressible Liquid," David Taylor Model Basin Report 2223 (Aug 1966).

10. Moreno, D.H. and M.L. Salive, "The Effects of Size and Environment on the Uniaxial Compressive Breaking Strength of Glass, Alumina, and Pyroceram," NSRDC Report 3315 (May 1970).

11. Gifford, L.N. and R.F. Jones, "Structural Analysis of Deep Submergence Pressure Hulls," SNAME Paper No. 12 presented at Spring Meeting, Honolulu, Hawaii (May 25-28 1971).

12. Gifford, L.N., "Finite Element Analysis for Arbitrary Axisymmetric Structures," NSRDC Report 2641 (Mar 1968).

13. Rockwell, R.D. and D.S. Pincus, "Computer Aided Input/Output for Use with Finite Element Method of Structural Analysis," NSRDC Report 3402 (Aug 1970).

14. "Material Configuration Procedures and Criteria Manual for Manned Noncombatant Submersibles," NAVSHIPS 0900-028-2010 (Sep 1968).

15. Nishida, K., "Static and Cyclic Fatigue Tests of Fusion Sealed Pyrex Glass Spheres," David Taylor Model Basin Report 2246 (Sep 1966).

16. Nishida, K., "Structural Studies of Massive Glass: Sep 1968-May 1969," NSRDC Report 3180 (Aug 1969).

17. Reardon, E.F., "Exploratory Tests of Alumina Spheres Under External Pressure," NSRDC Report 3013 (Apr 1969).

18. Benecke, M.W., "Electron Beam and Laser Welding of Aluminum Oxide Hemispheres," Prepared by Boeing Company for U.S. Navy under Contract N00600-69-C-0370 (May 1967).

19. Krenzke, M.A. and R.M. Charles, "The Elastic Buckling Strength of Spherical Glass Shells," David Taylor Model Basin Report 1759 (Sep 1963).

20. National Materials Advisory Board, "Massive Glass as a Naval Structural Material," NMAB-262 (Apr 1970).

INITIAL DISTRIBUTION

Copies	
1	CHONR (Code 419)
1	CO, USNRL (Code 8430)
3	NAVMAT 1 MAT 034 1 MAT 03412 1 MAT 03422
7	NAVSHIPS 1 SHIPS 034 2 SHIPS 03424 1 SHIPS 03421 1 SHIPS 03423 1 PMS 381 1 PMS 395
1	NAVAIR 5-2032A
1	NAVFAC 04B4
1	NAVORD 1 ORD 03A
1	CO, NCEL
2	CO, USNOL 1 2302 1 211
3	CDR, NURDC 1 0651 1 6505 1 6523
1	CO & DIR, USNUSC
1	USNA
1	CO, PGSCHOL, Monterey
1	CO, USNROTC & NAVADMINU MIT
1	NAVWARCOLLEGE
12	DDC
2	National BUSTAND Attn: Mr. G. Cleek
1	Brown Univ School of Engr Providence, R.I. 02912 Attn: Prof P. Marcal

Copies	
1	IIT Research Institute 10 West 35th St Chicago, Ill. 60616 Attn: Dr. R. Cornish
1	Rutgers Univ New Brunswick, N.J. 08903 Attn: Prof. C. Phillips
1	Southwest Research Institute 8506 Culebra Rd San Antonio, Texas 78206 Attn: Dr. R. DeHart
1	Stanford Research Institute Menlow Park, Calif. 94025 Attn: Dr. R. Sedlacek
1	Woodshole Oceanographic Institute, Falmouth, Mass. 02543 Attn: Mr. J. Mavor
1	American Glass Research Butler, Pa. 16001 Attn: Dr. R. Mould
1	Boeing Co., Space Div. Seattle, Wash. 98124 Attn: Mr. H. Benecke
1	Coors Porcelain Co. Golden, Colorado Attn: Mr. M. Simmons
1	Corning Glass Works Corning, N.Y. 14830 Attn: Mr. E. Loytty
1	General Dynamics Corp. Electric Boat Div. Groton, Conn. 06340 Attn: Dr. R. McGratten
1	General Electric Co. Re-Entry & Environmental Systems Div. Philadelphia, Pa. 19101 Attn: Mr. T.E. Hess
1	Lockheed Missiles & Spacecraft Sunnyvale, Calif. 94088 Attn: Mr. L. Breidenbach

Copies	
1	MRR Associates 1140 Connecticut Ave., N.W. Wash., D.C. Attn: Mr. R. Ward
1	National Materials Advisory Board, 2101 Constitution Ave., N.W. Wash., D.C. 20418 Attn: Mr. D. Grooves
1	Penberthy Electromelt Co. Seattle, Wash. 98108 Attn: Mr. L. Penberthy
2	PPG Industries 1 Gateway Center Pittsburgh, Pa. 15220 Attn: Mr. C.R. Frownfelter
1	Westinghouse Electric Ocean Research & Engr Ctr Annapolis, Md. 21404 Attn: Mr. D. Manning

CENTER DISTRIBUTION

Copies	Code
1	172
5	1727

UNCLASSIFIED

Security Classification

DOCUMENT CONTROL DATA - R & D

(Security classification of title, body of abstract and indexing annotation must be entered when the overall report is classified)

1. ORIGINATING ACTIVITY *(Corporate author)*

Naval Ship Research and Development Center
Bethesda, Maryland 20034

2a. REPORT SECURITY CLASSIFICATION

UNCLASSIFIED

2b. GROUP

3. REPORT TITLE

THE STRUCTURAL BEHAVIOR OF GLASS PRESSURE HULLS

4. DESCRIPTIVE NOTES *(Type of report and inclusive dates)*

Final

5. AUTHOR(S) *(First name, middle initial, last name)*

Kanehiro Nishida

6. REPORT DATE	7a. TOTAL NO. OF PAGES	7b. NO. OF REFS
June 1972	111	20

8a. CONTRACT OR GRANT NO.	9a. ORIGINATOR'S REPORT NUMBER(S)
b. PROJECT NO. Task Area S 4636	3863
c. Task 12326	9b. OTHER REPORT NO(S) *(Any other numbers that may be assigned this report)* AD 746 878
d.	

10. DISTRIBUTION STATEMENT

Approved for public release: Distribution unlimited.

11. SUPPLEMENTARY NOTES	12. SPONSORING MILITARY ACTIVITY
	Naval Ship Systems Command

13. ABSTRACT

A report on glass pressure vessels for deep submergence is presented. Emphasis is on the structural response of spherical and hemispherical glass shells under external hydrostatic and cyclic pressure. Results of earlier programs are reviewed. A computerized analysis trading off the variables in the joint problem is presented. Final joint geometries are discussed and data on chemically strengthened glass hemispherical shells with equatorial joint rings under fatigue conditions are presented. The results indicate relatively efficient (W/D = 0.5), small pressure vessels of chemically strengthened glass are practical for unmanned noncritical applications to 20,000 ft. Nine 10-inch diameter chemically strengthened glass hemispherical shells of PPG 1080 glass with overall weight to displacement ratios of 0.5 survived at least 3000 cycles to 20,000 ft. Each hemisphere was then subjected to a proof test to 30,000 ft. Although this data is encouraging, substantial effort is necessary before glass structures can be applied in critical conditions even on the present small scale.

14. KEY WORDS	LINK A		LINK B		LINK C	
	ROLE	WT	ROLE	WT	ROLE	WT
Glass Structures						
Pressure Vessels						
Collapse Strength						
Cyclic Strength						
Stress Analysis						